Hydrogeochemical and Water Quality Evaluation of Groundwater Resource in Lake Tana Sub-basin

BY TSEHAY AMARE AGEGNEHU
ENSCHEDE, THE NETHERLANDS, MARCH 2015

SUPERVISORS:
Dr.Ir.Chris Mannaerts
Drs.J.B. (Boudewijn) de Smeth

Hydrogeochemical and Water Quality Evaluation of Groundwater Resource in Lake Tana Sub-basin

BY TSEHAY AMARE AGEGNEHU
ENSCHEDE, THE NETHERLANDS, MARCH 2015

Thesis submitted to the Faculty of Geo-Information Science and Earth Observation of the University of Twente in partial fulfilment of the requirements for the degree of Master of Science in Geo-information Science and Earth Observation.
Specialization: Water Resource and Environmental Managemen]

THESIS ASSESSMENT BOARD:
Dr. M.C. Lubczynski (Chair)
Dr. P. Gurwin, External Examiner, University of Wroclaw
Dr. Ir.C.M.M. Mannaerts
Drs. J.B. de Smeth

ABSTRACT

Lake Tana basin is located in northern Ethiopia in the Upper Blue Nile Basin. The main objective of the study was to determine the hydrogeochemical processes, evolution, source rock deduction, origin, age and surface water interaction as well as the determination of the suitability of the groundwater for domestic and agricultural purposes using GIS, Aquachem, PHREEQC geochemical modelling and different statistical approaches.

Secondary and primary new chemical and isotope data of water samples were used for hydrochemical interpretation of the Lake Tana sub-basins. The main contribution of ions to the groundwater is deducted from source rocks weathering processes on, silicate, plagioclase and carbonate weathering. A total of 15 different water types existed in the study area. The most water types are Ca-Mg-HCO_3, Na-Ca –HCO_3, Ca-HCO_3, Ca-Na-HCO_3, Ca-Mg-Na-HCO_3 and Na-HCO_3. Saline water points were observed in lower of Megech and Ribb River basins. The main factors that contribute to salinity development in the study area are the dissolution of salt through the process of evaporation and leaching of carbonate rocks.
The concentration of different mineral species in the water solution and their saturation index were identified by using PHREEQC hydrochemical model. The equilibrium with pure solid mineral phase was applied to determine the thermodynamic stability and the solubility of the minerals in six water samples between temperatures range 25 -75 Degree Celsius. From the results, except calcite in the water sample CSP-3 the mineral phases in the rest of water samples were not equilibrated. Calcite and Aragonite and Fluorite in the sample DW-2 and CO_2 in DW-1 close to zero but they were not equilibrated completely. Inverse hydrogeochemical modelling was also applied to determine the groundwater chemistry evolution along the flow path. The outcome indicates that dissolution and loss of water (evaporation), dissolution of CO_2, H_2 and O_2 dissolution and precipitation of different minerals phases are the main hydrochemical processes that occurred during groundwater evolution along the flow path.
The isotope signatures in all sampled natural water resources in the basin show a high depletion in of Oxygen-18 and Deuterium as well as a medium to high Oxygen-18 and Deuterium enrichment. Surface groundwater interaction is only observed between Megech River and boreholes samples and dug well's samples within Megech basin as proofed by isotope data.
The drinking water quality was ranked using Deininger for the National Sanitation Foundation (1975) water quality index (WQI) and irrigation water quality also determined by different irrigation water quality indices. The results show that except for a few water points in the Megech and Ribb basins, most of the water points are suitable for domestic and irrigation use.

In generally, the groundwater quality in the study area is mainly influenced by dissolved solutes, evaporation, leaching of carbonate rocks, the geomorphological setup, soil type as well as agricultural and anthropogenic effects.

Key words: - Groundwater quality, Hydrogeochemical processes, evolution, equilibrium saturation indices, inverse modelling, isotopes signature.

ACKNOWLEDGEMENTS

I would like to thank the Royal Government of Netherlands and International Institute of Geo-information and Earth Observation (University of Twente) for accepting my application and gave me the opportunity to purse my Master program.

I would like to express my deepest thanks to my two supervisors; Dr.Ir.Chris Mannaerts and Drs.J.B. (Boudewijn) de Smeth for their guidance, patience, comments and encouragement during laboratory and throughout the thesis work. I would like to thank Mrs. Josip Zarrky for his supporting and guiding me during field work preparation and laboratory work.

The fulfilment of this research work is supported by different individuals and organizations. At first I highly like to acknowledge Geological Survey of Ethiopia, especially Ato Mhudden Abdela; Director of the Groundwater Resources Assessment Directorate Ato Sileshi Mamo for their constructive comments unlimited support in providing the necessary materials in order to facilitate the field work. I would like to acknowledge regional, zonal, district and local people of North and South Gonder of Amhara regional State for their cooperation and necessary information.

I would like to thank all the WREM staff members and my entire classmate especially my friend Sonam from Bhutan for friendship, socialization and support during my stay in ITC.

I would like to thank my amazing family especially my husband Abebe and my son Yafet Abebe, Miche, Gashe and my friend Geni, for their love, day-to-day support and encouragement.

Finally, my special thanks go to all Habesha community, students at ITC for the friendship I had during my stay in Enschede.

TABLE OF CONTENTS

LIST OF FIGURES

LIST OF TABLES

LIST OF ABBREVATIONS

Abbreviations	Descriptions
FAO	Food and Agricultural Organization
USGS	United States Geological Survey
WHO	World Health Organization
US	United States
SMOW	Standard Mean Ocean Water
GIS	Global Information System
GLOVIS.USGS	USGS Global Visualization Viewer
GMWL	Global Meteoric Water Line
LWML	Local Meteoric Water Lin
IAEA	International Atomic Energy Agency
ICP-AES	Inductive Coupled Plasma Emission Spectrometry
Log	Logarithm
Meq/L	Mili equivalent per Litter
Mg/L	Mili gram per Litter
SAR	Sodium Absorption Ratio
SRTM	Shuttle Radar Topography Mission
WQI	Water Quality Index
TH	Total Hardness
TM	Thematic Mapper
Ksp	Equilibrium constant
IAP	Ion activity product
SPSS	Statistical Package for the Social Sciences
IBM	International Business Machines
M.A.S.L	Above Mean Sea Level
N/A	Not Applicable
AQ-1	Aqua-1
HCA	Hierarchal Cluster Analysis
T-BH/H-BH/G-BH/BH	Borehole sample
T-DW/H-DW/G-DW/DW	Dug well sample
T-CSP/H-CSP/G-CSP/CSP	Spring sample
T-RV/H-RV/G-RV/RV	River sample

1. INTRODUCTION

1.1. Background and Significance

Since earliest times groundwater has been exploited for domestic use, livestock and irrigation purpose; exploration often overlooked by people however, assessing its quality also important to know what the water is intended to be used for (Deborha Chapman, 1996);good chemical state water benefits the socio-economic development of a country. Many factors control the chemical composition of the groundwater such as composition of rainfall, geological processes within the aquifer, geologic structure and mineralogy of the watershed (K.Srinivasamoorthy,M.Vasanthavigar,S.Chidambaram, P.Anandhan, R.Manivannan, R.Manivannan, 2012). However, in addition to that the main external factors such as increasing population, intensive agricultural activities, various types of pollution and groundwater extraction also affect the groundwater chemistry (Rao & Nageswararao, 2013). Groundwater contamination is a serious problem faced by developing countries due to industrial effluents and rapid urbanization (Jerome & Pius, 2010), hence, a continuous groundwater quality assessment and monitoring is necessary to ensure a long-term sustainability of the resource (Rao & Nageswararao, 2013) The Government of Ethiopia has planned to utilize water resources in Nile River Basin for multipurpose. Lake Tana Basin is one of the sub-basins identified by government for agricultural development which should help to stimulate economic growth and to reduce poverty (Matthew McCartney, Tadesse Alemayehu & Awulachew, 2010). Shallow groundwater and surface waters are the main water supply sources of drinking and agricultural activities. Large and small scale irrigation activities, construction of power plants, urbanization and development of industries have increased water demand in the basin. Extensive modern irrigation schemes are developing in the Ribb, Gumara, and Koga and Megech River catchments. In addition, groundwater investigation and Tana-Beles hydroelectric power are among the activities carried out in the basin (Getachew Zewde, 2010). The present study aims to assess the hydrogeochemical processes in the basin which are crucial for every socio –economic developments in the basin.

1.2. Research Problem

Hydrogeochemical and isotopic studies in Lake Tana basin are fragmentary and have up to be now a very limited impact on the way, water is used. Additional detailed study is suggested to understand the presence of different geochemical characteristics than the previous anticipation. In general, detailed investigation should be done to determine hydrogeochemical processes, evolution, interaction between the different ground waters and between groundwater and surface waters, as well as the origin of ground waters. Currently, contamination threatens groundwater resources due to extensive and improper irrigation activities, rapid increase of population and urbanization. As result, high nitrate concentration and salinity development in the groundwater described in the previous study especially wetlands in Rib, Megech, Denmbia and Fogera plain (Girum dmassu Nadew, 2010). The author recommended for further investigation to understand the process of salinization. Teshale Tadesse Danbara, 2014)indicated increasing of suspended and dissolved matter in Lake Tana which also will affect the groundwater chemistry through interaction with groundwater. According to Zenaw, (2009)when the Tana Lake level is high, the lake is acting as a hydraulic barrier which reverses the flow of groundwater into the lake. This condition leads the groundwater movement to become slow and water level is raised to the surface which results in direct evaporation. Poor quality and drying-up of wells and springs had been reported after prolonged drought in the regional hydrogeochemical and isotope study in the source region of Blue Nile River, Ethiopia(Kebede, Travi, Alemayehu, & Ayenew, 2005). However, spatial pollutant distribution related with land use and land cove, comprehensive study on hydrogeochemical process, evolution and source-rock deduction and specifically general groundwater quality evaluation has not been carried out in the region. This research is attempted to do detailed hydrogeochemical and water quality evaluation of groundwater resources in the Lake Tana Sub-basin. It aims to identify the hydrogeochemical processes, evolution and age of the groundwater, source rock deduction and chemical composition as well as the determination of the suitability of the groundwater for domestic and agricultural purposes using GIS and PHREEQC geochemical modelling and different statistical approaches.

1.3. General Research Objective

The main objective of the proposed study is to gain insight into hydrochemical processes and evolution and to map the spatial distribution patterns of water quality data and relate these to geology and land use using GIS, Aquachem, PHREEQC geochemical modelling and different statistical approaches. Isotopic approaches also applied to determine the surface-groundwater interaction and the age of the groundwater.

1.4. Specific Objectives

The research was aimed at achieving the following specific objectives:

- To assess and interpret groundwater quality parameters of existing water points
- To map the spatial distribution of groundwater quality data in relation to salinization problems and land use.
- To determine factors influencing the chemical composition of the groundwater.
- To evaluate the chemical speciation in water solution and saturation indices and source rock deduction.
- To determine groundwater chemical evolution along the flow path.
- To rank the water quality using Water Quality Index (WQI) approach.
- To evaluate the groundwater quality and suitability for different uses (irrigation and drinking water) by comparing to different standards.
- To provide scientific information to better solutions for water use and to establish management strategies of the area.

1.5. Research Questions

1. What are the major issues and problems related to groundwater quality?
2. What are the factors influencing the chemical composition of groundwater?
3. What is the spatial distribution of groundwater quality in the study area?
4. How do geology, geological structure and land use related to water quality parameters?
5. What are mineral types in the ground water?
6. What are the sources of groundwater?
7. What is the level of the groundwater chemistry compared to standards?

2. LITERATURE REVIEW

2.1. Previous Groundwater Chemistry Studies and Findings

Few regional hydrogeochemical and isotopic studies conducted by different authors. However, they are fragmentary and have very limited inputs.
Findings:

- Kebede et al., (2005), studied the first regional groundwater recharge, circulation and evolution and used hydrogeochemical and isotope data in the Upper Blue Nile Basin; the study determined two chemically distinct water type high TDS, Na-HCO_3 and low TDS Ca-Mg-HCO3. The author described problems like poor water quality, drying-up of wells and springs after prolonged drought.
- Hydrochemical database flow separation and groundwater recharge estimation was used by (Getachew Hadush Asmerom, 2008). In this study chloride and electrical conductivity were used to estimate groundwater recharge. The author described about increasing of phosphates in surface water and nitrate in all natural waters.
- Another author Nadew, (2010), used geochemical and isotope data to determine the interaction between groundwater and surface water; in some water samples the measured electrical conductivity reached up to 10660μS/cm and nitrate concentration from 30-128mg/l.

2.2. Chemical Characteristics of Groundwater

Groundwater is usually associated with geology, geologic structure and soils which determine the chemical property of groundwater (Chapman, 1996). In addition, external forces such as human activities, industrial effluents and agricultural activities often influence groundwater chemistry. Hydrochemically groundwater may classified in to three groups such as meteoric, juvenile and connate(Chapman, 1996). The most abundant portion of groundwater is meteoric water derived from precipitation (rain and snow). It includes water from rivers, ice melt and lakes which are indirectly derived from precipitation.
Connate waters are called that fossil water, which were accumulated or entrapped in the sedimentary rocks at the time of deposition. They are two types distinguished epigenetic and syngeneic connate water. Connate waters usually are not developed for any water supplies because of their high salt concentration. The third type of groundwater is called juvenile, usually known as magmatic water; when magma cooling, it contains water vapour and gases etc. Water vapour separates from magma and moves upwards the earth's surface from high temperature and then it condensed into superheated water.

2.3. Groundwater Quality

Groundwater characterized by chemical, physical and biological qualities. Odour, colour, turbidity and temperature are physical properties of groundwater. Large concentration of dissolved minerals may be harmful to plants and animals. For example, high sodium concentration in the water may be harmful to people who have heart trouble. Very hard water, which is enriched with calcium and magnesium, is not suitable for domestic use and it may cause scale effects on the inside of the pipelines and boilers. Monitoring the quality of the groundwater for multi- purpose by considering many parameters directed towards a whole range of quality issues. Another monitoring category may be only single quality monitoring or specifically may concentrate on industrial spill, saline intrusion and agricultural pesticides etc.

Nowadays, the growth of population, technology, rapid increase of urbanization, industrial effluents and agricultural activities increased the stress upon water resources especially in developing countries. Hence, continuous groundwater quality assessment and monitoring is mandatory in order to prevent or control the groundwater pollution (Rao & Nageswararao, 2013).

2.4. Water Sampling Method

Sampling method must be taken account in order to get accurate analytical results. The number of samples must be considered economically and also how samples are to be taken for water quality investigation. Some most important water quality parameters such as pH, Temperature, Conductivity, Turbidity, Alkalinity and Dissolved Oxygen must be determined immediately after sampling. The reason for field measurements is these parameters which are considered as standard for basic water quality testing may change their level substantiality if not measured in the field. The types of field sampling containers and preservation methods can also affect samples in analysed later in a laboratory. After sampling the samples must be appropriately labelled, sealed and shipped to a laboratory as soon as possible preferably dark and cool condition.

3. STUDY AREA

3.1. Location and accessibility

The study area located in Northern Ethiopia; Amhara Regional State, at about 560 km North of Addis Ababa. Geographically, the area is bounded by 1282800 to 1412600mN latitude and 307500 to 428500mE longitude. It covers an area of 6235 km2. The national highway that runs from Addis Ababa to Bahirdar and, Woreta_ Gonder towns are the main routes to the study area. There are many all-weather roads to access the study area.

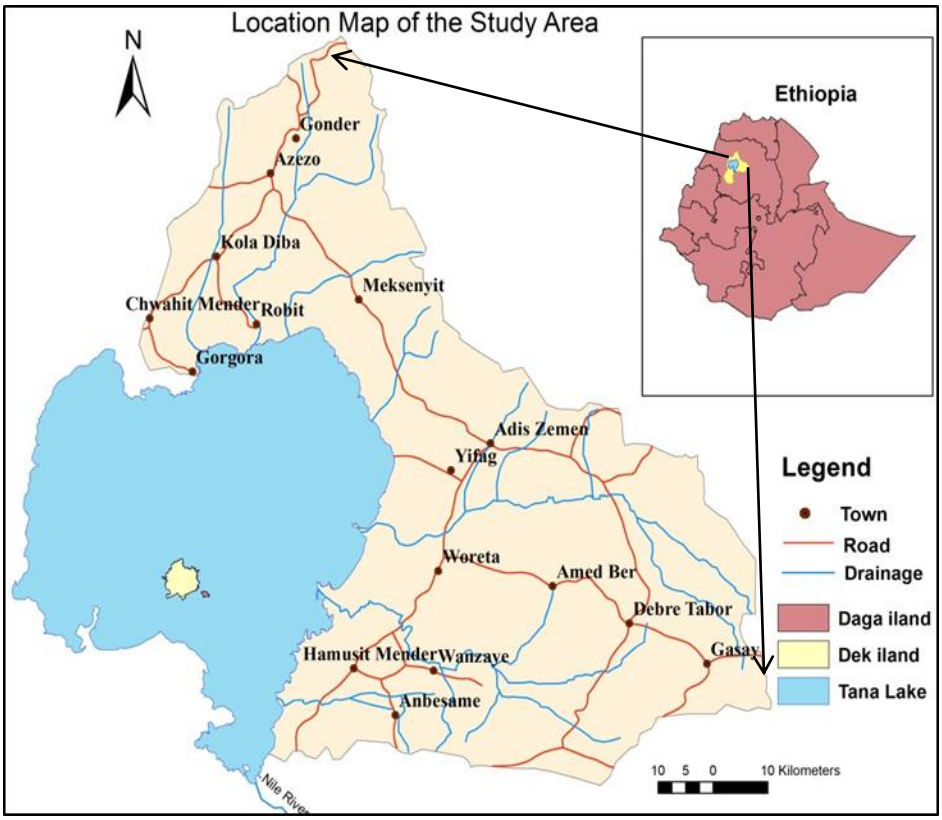

Figure 1: Location map of the study area

3.2. Settlement

According to 2007 Ethiopian Central Statistical Agency report Amahara region population is the second largest portion of the country's population. The Lake Tana basin is one of places of the country with high population density which lays Amhara Region. The population distribution in the study area is variable. Dense population can be observed in the urban area than rural. However, the rural population is in larger numbers comparing to urban populations. The dominant ethnic group in the study area is Amhara and their language is Amharic. There are also other ethnic groups like Gurage and Tigray especially around the urban areas. The people's income in the study area generally depends on agriculture and animal husbandry.

3.3. Physiography

Topographically approximately 35% of the total area is flat land; most of Gumara, Rib and Megech River catchments are topographically flat. The altitude of the area varies from highest 4135 m.a.s.l at Guna Mountain to the lowest flat Palins about 1077 m.a.s.l. High altitude chain mountains extended from Northern part of the study area towards South East to the way Guna mountain.

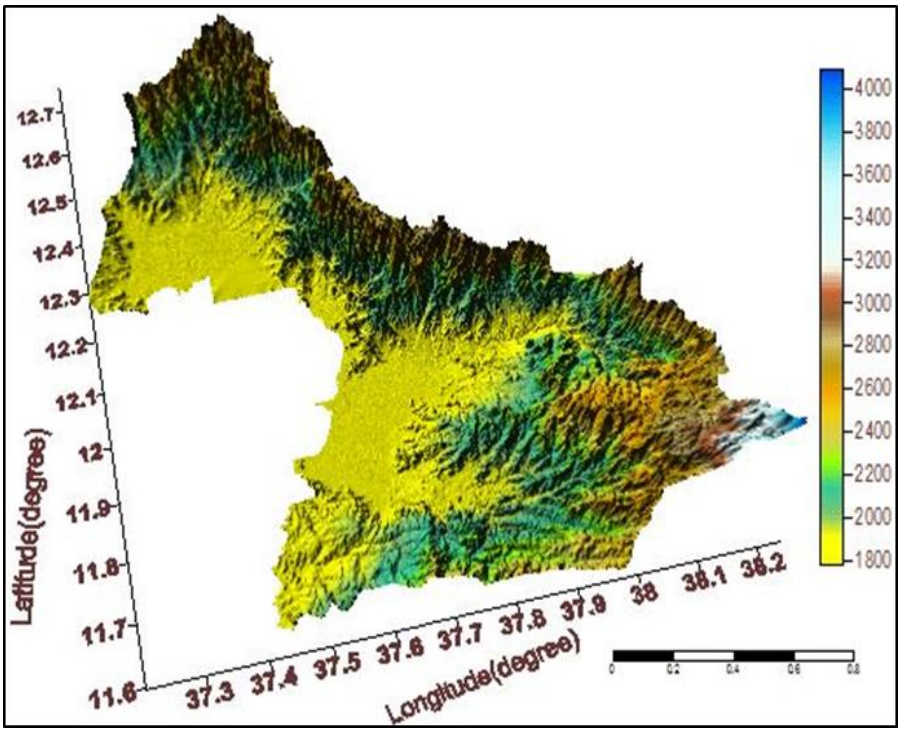

Figure 2: Three dimensional surface models generated from 90m resolution of SRTM data

3.4. Climate

As many places in Ethiopia the climate condition in the study influenced by altitudes. There are four climatic zones in the study area. The tropical climate zone is found in the flat land area and the highest elevated area is found toward Guna Mountain which is represented by Alpine (Kur) climatic zone. In the following table the climatic zones of the study area are classified based on the Ethiopia climatic classification after Tesfaye chernet (1993), Javier Goza'Ibez and Dulce Cebria'n (2006).

Table 1 : Climate zones of the study area

Climatic Regions	Altitude of the Regions (m.a.s.l)	Mean Annual Temperature (0C)	Presence in the study area
Alpine (Kure)	3300 and above	10 and above	present
Temperate (Dega)	2300-3300	10-15	present
Subtropical (Weina Dega)	1500-2300	15-20	present
Tropical (Qolla)	800-1500	>30	present

3.5. Rainfall

Meteorological data were obtained from the Geological Survey of Ethiopia. The main rainfall season in the study area is during summer (June – September) due to massive moist air driven from the Atlantic and Indian Ocean; very short rainfall period starting from March and Mid of May. Dry season is during winter October to February which characterized by with little rainfall or no rainfall. The mean monthly rainfall distribution indicated below in the graph which recorded in those four stations from 1993-2006.

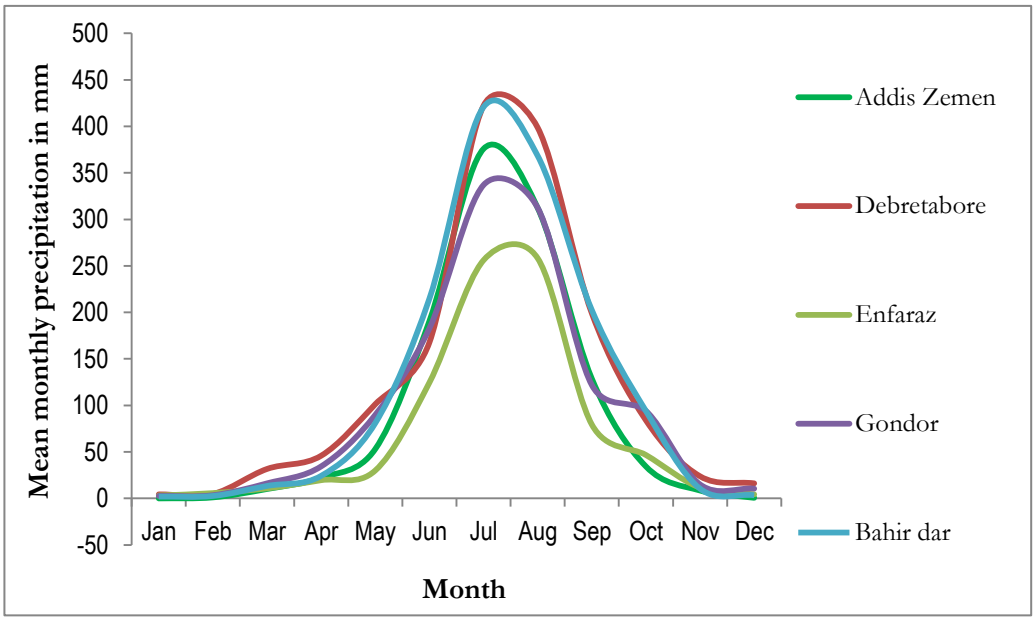

Figure 3: Mean monthly rainfall distribution pattern for stations within the study area

As indicated above in (figure. 3) all stations received maximum peak rain in July and August. For all stations, maximum rainfall recorded at Debretabore 422mm, Bhairdar 420mm, Gondor 337mm, Addis Zemen 376mm and Enfaraz 258mm. The lowest mean monthly rainfall recorded at all stations during January with values 0-4mm. As many place in Ethiopia the rainfall in the rainy season in the study area is a major source of water for agricultures.

3.6. Potential Evapotranspiration (PET/ETo)

Potential evapotranspiration is the sum of evaporation and transpiration which is released from vegetated surface. It is one factor that influences the hydrological cycle of a given area. Evapotranspiration is variable from one place to another depends on the vegetation distribution, type and also root type of vegetation. There are different method used to estimate evapotranspiration namely Penman-Monteith and Thornthwaite methods. For this study used data obtained from the Geological Survey of Ethiopia from different hydrogeological reports. The value of potential evapotranspiration calculated using FAO-Penman-Month method which obtained from the Climate meteorological database.

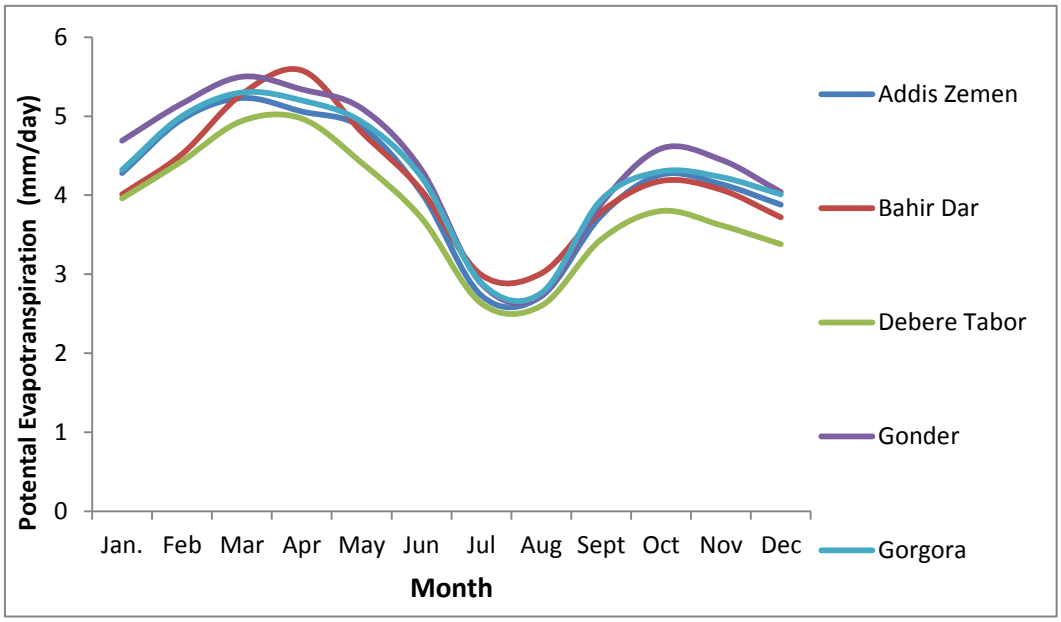

Figure 4: Monthly Mean Potential Evapotranspiration (PET/ETo)

Potential Evaporation as shown in the figure above the highest value recorded at all stations during February to May. The lowest rate occurred during a rainy season in June and September which is typically the rainy season. Relatively, greater evaporation rate observed in months October to January.Here, based on the Penma-Monteith methods, annual average potential evapotrnspiration rate of Addis Zemen, Bahirdar, Debretabore, Gonder, Gorgora stations are estimated as 4.16mm/day, 4.17 mm/day, 3.82 mm/day, 4.39 mm/day, 4.26 mm/day respectively.

3.7. Geology and hydrogeology

3.7.1. Geology

The geology of the area has been mapped by different researchers; and their geological interpretation varies over the years. Geological, hydrogeological and dam site investigations are the main studies carried out in the basin.

The basin is entirely covered by volcanic formations, unconsolidated lacustrine sediments, Quaternary basalt, Tertiary Taramber basalt and alluvial sediments cover the area (Mengesh et al, 1996).

Mesozoic and Tertiary sediments surrounded Lake Tana and thick Eocene Oligocene flood basalt covers depressed area in the basin (Hautot, Whaler, Gebru, & Desissa, 2006).

The geological and hydrogeological studies were carried out by Geological Survey of Ethiopia. Hautot et al., 2006) mapped different geological units on the Debretabore and Bahirdar map sheets, at 1:250,000 scale. Some of the geological units are Aiba formation which consists of flood basalts with rare basic tuffs, plateau basalt, Quaternary basalt; Alajie formation consists of interlayered silicic rocks (peralkaline rhyolite and transitional basalts), Guna basalt, Guna phonolite and tuff. For the most dominant outcrops in the study area, a further description is given here below.

3.7.2. Upper Basalt and Trachyte (TV4)

These volcanic rocks are the dominant outcrops in the basin, and are exposed on the northern and eastern parts of the study area, especially along highlands around Debretabore, Gonder and Addis Zemen. The basalt mineral crystals are not visible (aphanitic), dark grey, and mostly very slightly weathered. The formation is characterized by fractured, spheroidal weathering, mainly massive and rarely columnar jointing. These basalts are usually associated with ignimbrite, tuffs, trachyte and Boulder tuffs(Workneh

Haro, Degene Hailemariam, Iaysu Getachew, Thomas Kassahun, Shimelis Ashenafi, Getachew Burisa, 2010).

Figure 5: Columnar jointed basalt and Trachyte plug left side along Gonder- Woreta road.

3.7.3. Quaternary Lacustrine Sediments (QIS)

These sediments are extensively exposed in the flat plains surrounding Lake Tana, mainly in Megech, Dembia and Fogera plains. The unit is characterized by various bedded and reworked tuff. The sediments frequently interbedded with gravely to cobbled mud rocks. Lake sediments such as loose tuffs, pebbly tuffs and loose reworked tuff occur to South of (Haro et al., 2010).

3.7.4. Quaternary Basalt (QV1)

The Quaternary is basalt exposed in the south-western part of the study area. This unit is variable in nature. It formed as fine-grained basalt, amygdaloidal scoriaceous basalt, scoria cones overlain by layered fine-grained basalt, young fresh basalt, mixed with pyroclastic flow, vesicular basalt enriched secondary minerals(Haro et al., 2010). It is probably exposed under Quaternary sediments in the Tana Graben. The thickness of the unit ranges from 100m to 300m(Zenaw Tessema , 2009).

3.7.5. The Middle Basalt Flows (TV2)

This unit is exposed in the southern part of the study area. It shows sharp topographic changes forming distinct cliff, from underlying lower basalt. These basalts are also stratified and form continuous basalt layers with rare pyroclastic intercalation. Estimated lava layer's thickness ranges from 7-10m, but in different places one layer can measure from 40 -50 meters (Haro et al., 2010).

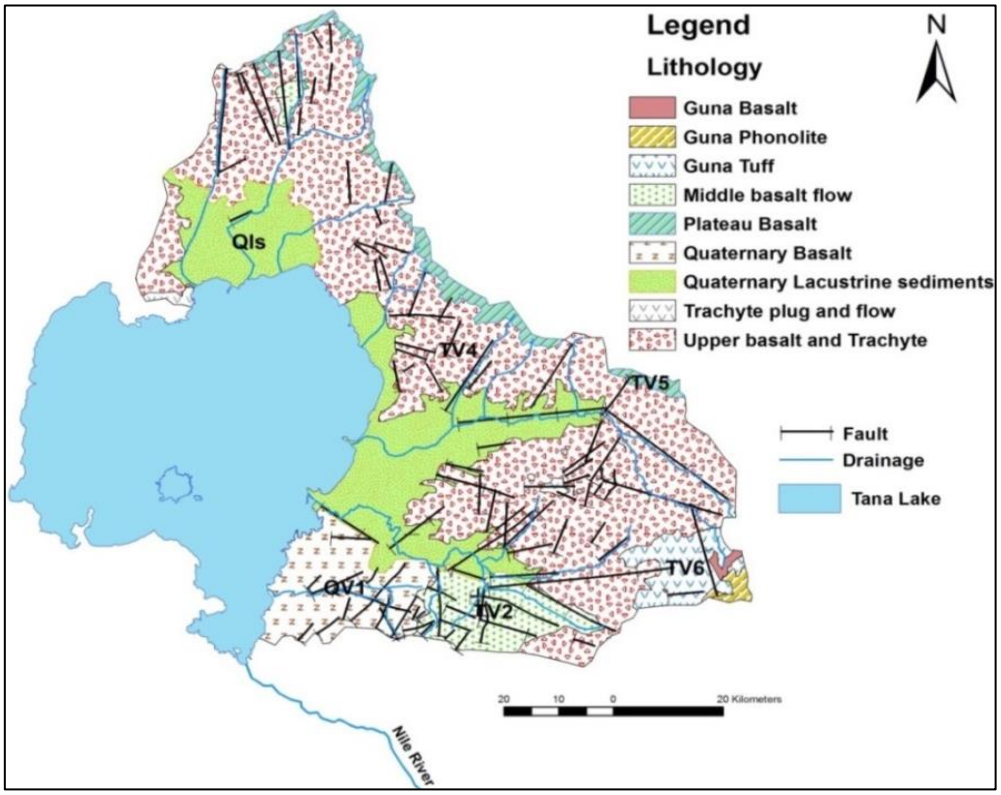

Figure 6: Geological map of the study area.

Hydrogeological setup of the study was classified in many studies based on hydrogeological characteristics of the different water bearing and permeability dynamics of geological formation as well as water points inventory data (yields of spring and hydraulic characteristics of the borehole) etc. Based on data obtained from different hydrogeological studies it is known that there are four major aquifers existing in the study. These are the Tertiary Upper Basalts and Trachyte aquifers, Quaternary sediment aquifers, the Quaternary Basalt aquifer and the Mesozoic sediment's aquifer.

3.7.6. Tertiary Upper Basalt and Trachyte aquifer

This aquifer unit covers a large part of the study area and one of the major water-bearing formations in the study area. Hydraulic conductivity, groundwater storage and yields of springs of this aquifer varies from place to place due to the presence of fractures and joints (fault and lineaments) (Yonas Mulugeta, Aschalew Gurmu, 2013).

3.7.7. Quaternary Lacustrine Sediments aquifer

This aquifer unit covers the wide extensive flat lowlands around Lake Tana. It is one of most promising hydrological units of the water supply from shallow wells and dug wells in the study area.

According to (Bereket Fentaw, 2013) in their hydrogeological report of Debretabore map sheet, the unit with grain size sandy and silt has better permeability and productivity whereas very fine ash interbedded with massive tuffs have low permeability and productivity. The quality of groundwater is variable in this unit. It hosts shallow fresh groundwater and but also lenses of brackish(Zenaw, 2009).

3.7.8. Quaternary Basalt aquifer

Quaternary basalt is in one of the most productive aquifers in volcanic rocks in Ethiopia. It is characterized by fractures, joints and vesiculated surfaces, which will facilitate the permeability and productivity of the rock. The vesicles are interconnected with each other, and in some places filled with secondary materials. There is hot springs around the Wanzaye locality within this unit, which associated with deep-seated faults and fractures. This indicates neotectonic activity in the area. During a dry season, the yield of spring ranges from 10-20 l/sec and the yield of a nearby borehole were reported to be the range from 2-10 l/s (Bereket Fentaw, Alemayehu Tadesse, 2013).

3.7.9. Mesozoic Sediments aquifers

Mesozoic sediments are expected in the Tana basin to reach up to a depth of 300-400m. According to (Zenaw, 2009)from a Magneto telluric Survey, very thick (1.5-2km) Mesozoic sediments occur, which overlain by 250m thick basalt. The Mesozoic sediment aquifers are a highly productive, particularly when in sandstone and limestone. In the future, these aquifers can be used for development activities depending on the quality and quality and cost of pumping.

3.8. Soil

Most of the soils of the area are derived from various volcanic and undifferentiated rocks (Nadew, 2010). Soil type and its distribution depend on the variation of parent rocks or lithology, slope gradients, climate conditions and geomorphology. The major soil groups, as classified by Food and Agricultural Organization of the United Nations (FAO) and Ministry of Agriculture Ethiopia, are Lithosols, Chromic vertisols, Euteric Nitosols, Chromic Luvisols, Euteric Cambisols and Orthic Luvisols. The soils are identified by brown, reddish brown and yellowish- brown colour.

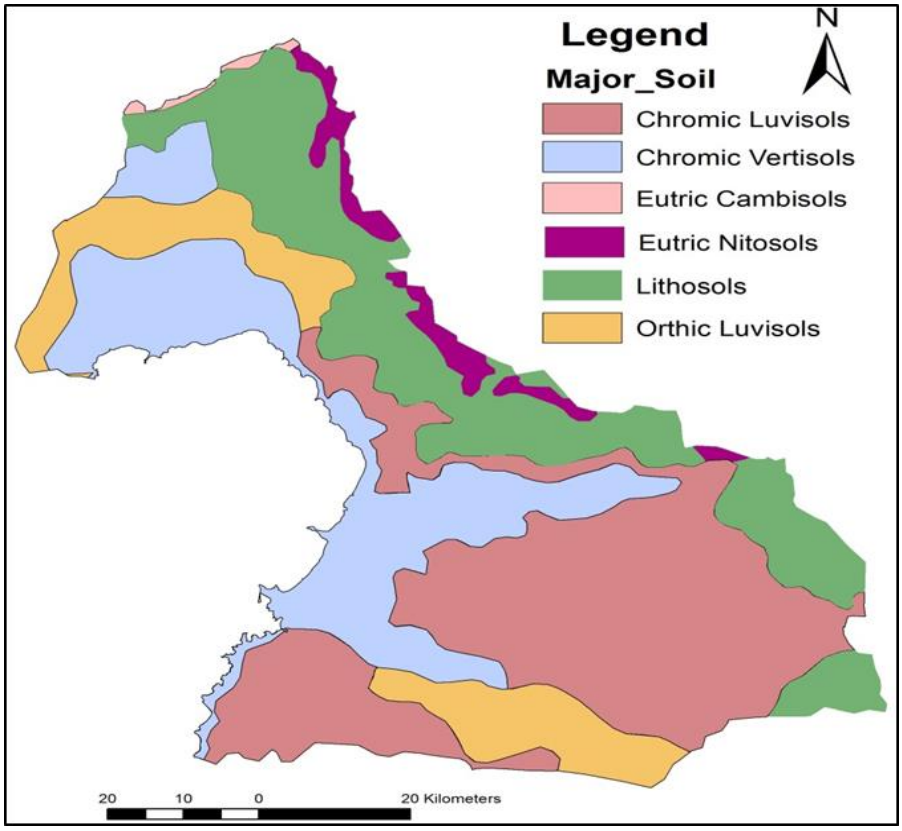

Figure 7: Soil map of the study area

3.9. Land Use

Land-use changes over time due to human activities. Updated land use information is necessary for any developmental activities, particularly water resource management. Land use and land cover vary from place to place depending on population density, climate conditions and agricultural activities. Intensive agricultural activities are practicing in the lowland and moderately cultivated topographically rugged area. Shrubs and crops cover the area. Large and small-scale irrigation schemes have been developed in the region. Rice, maize, oat, wheat, sorghum and vegetables are the main agricultural products in the area.

Land use/ land cover map is produced by classifying November 2013 Landsat 4-Present images (path 170, row 52 & 51) and (path 169, row 52) which were downloaded from http://glovis.usgs.gov (USGS Global Visualization Viewer). The Erdas imagine a tool for supervised classification methods was used to classify the images. A total of 80 ground truth points was collected to verify the accuracy of the classified image. The result of the classified image shows 80% of the total area is covered by crops.

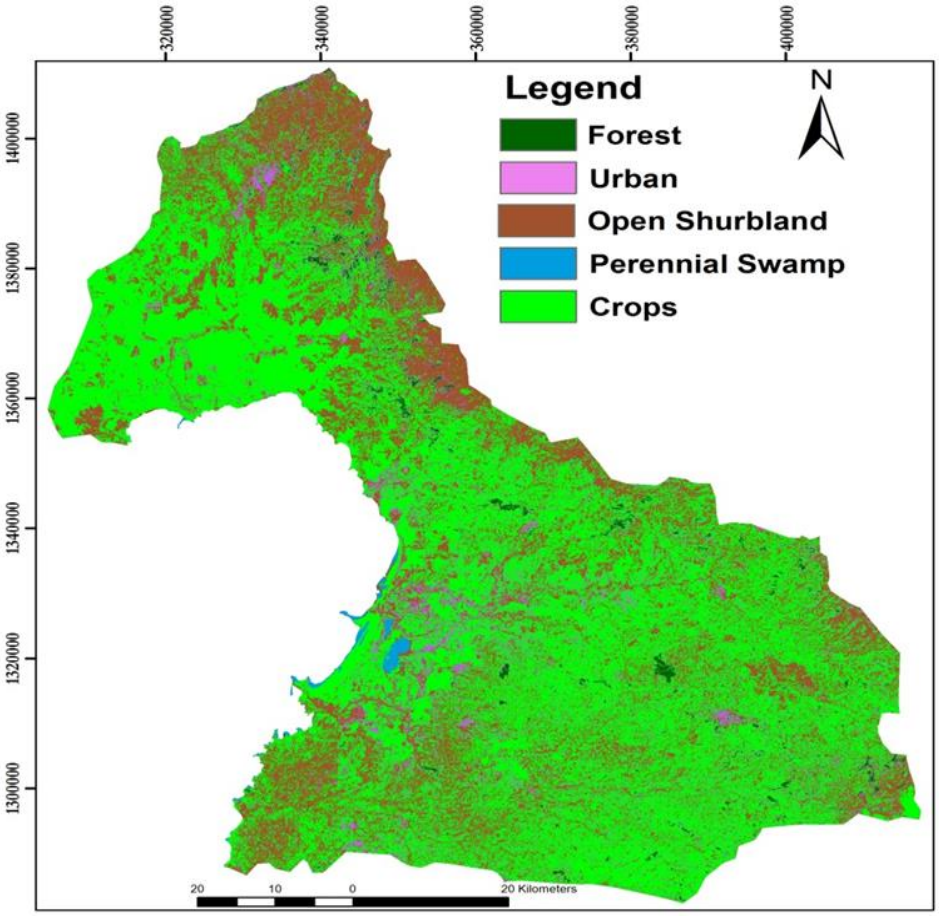

Figure 8: Land use/Land cover map of the study area.

Using the pivot table tool from ArcGIS and Excel, the accuracy of classified image was calculated. The overall accuracy is 85% and Kappa coefficient 75.5%, which proves an acceptable classification.

Table 2: Accuracy result of land use classification.

Ground points	Forest	Urban	Open Shrub land	Perennial Swamp	Crops
Forest	7	0	0	0	0
Urban	0	9	0	0	6
Open Shurbland	0	2	5	0	11
Perennial Swamp	0	0	0	4	0
Cultivated land	1	4	4	0	25

Overall accuracy = 85% Kappa coefficient = 77.6%

Figure 9: Land Cover pictures

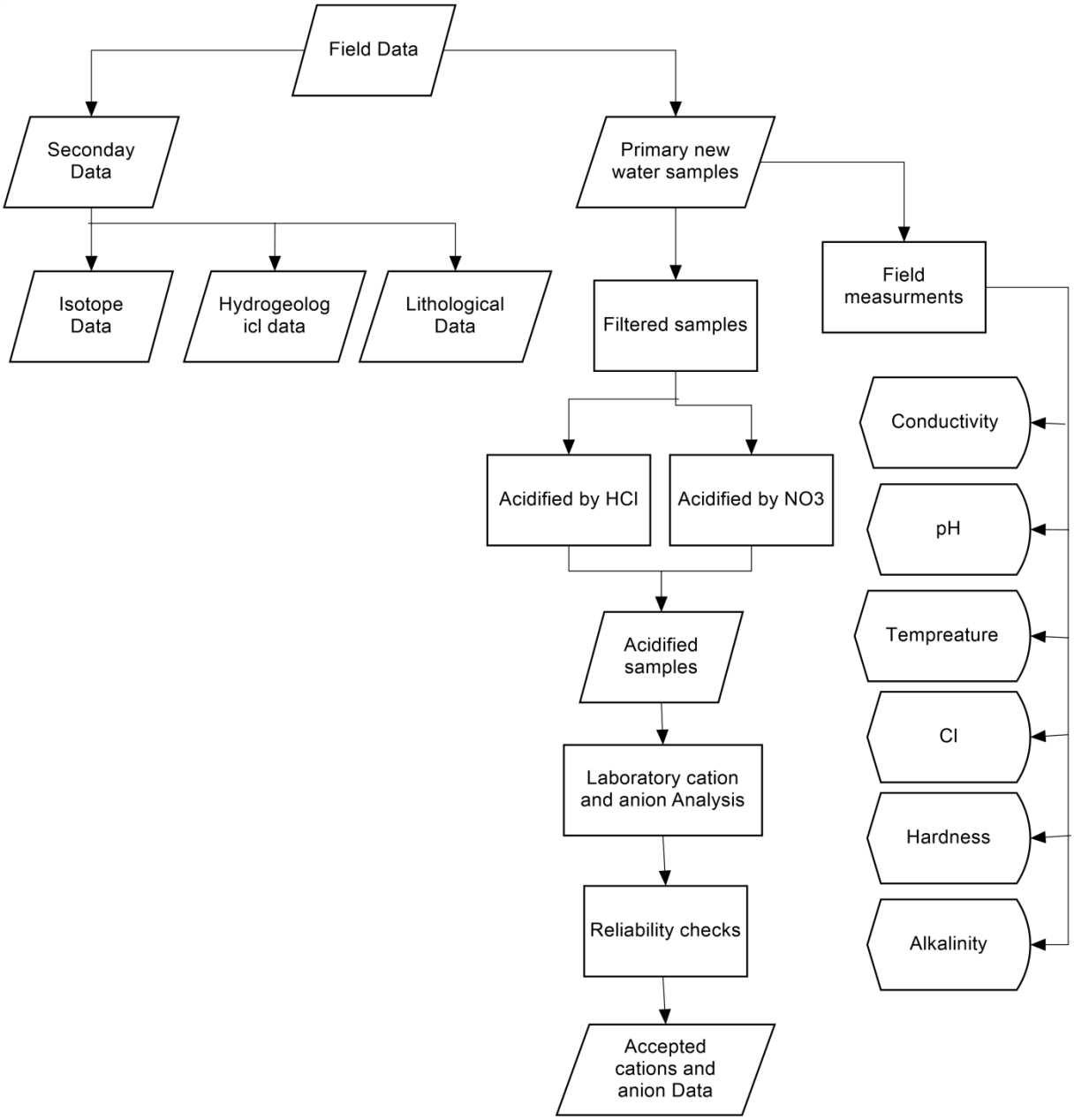

Figure 10: Field data collection and laboratory analysis flow chart

4. APPROACHES AND METHODS

4.1. Primary Data Collection

During field study water samples collected from different water points. A total of 37 representative water points was collected for laboratory analysis by taking account into lithological, flow direction and topographical setting of the area. Out of the 37 water samples, 13 samples were collected from Boreholes, 20 samples from dug wells and 2 samples from surface waters. For all water points, pumping was carried out before sampling for a few minutes to get fresh water.

The 37 water samples collected using 50ml and 100ml plastic pre-rinsed sample bottles. The 50ml samples were acidified with nitric acid for cation analysis and 100ml samples acidified with hydrochloric acid for anion analysis. Cellulose acetate membrane filter paper 0.45μm in size was used to filter all samples. Immediate field measurements were taken for Alkalinity, Chlorine, Hardness, Electrical Conductivity, pH and Temperature.

Table 3: Summary of field hydrochemical measurements

Parameters	Mean	Median	Mode	Minimum	Maximum
EC μs/cm	546.3	457	457	110.7	2310
PH	7.2	7.2	7.2	5.97	9.09
Temp oC	23.7	24.4	24.9	16.7	28.8
Oxygen (mg/L)	3.2	2.85	2.92	1.6	6.79
Hardness (mg/L)	252.7	260	260	60	1110
Alkalinity (mg/L)	330.6	335.5	427	54.9	896.7
Cl (mg/)	24	11	12	3	319

4.2. Secondary Data

Addition hydrogeological and geological information was obtained from the Geological Survey of Ethiopia, Ministry of Water, Irrigation & Energy of Ethiopia and Amhara Water Resources Bureau. Additional chemical data were obtained from a recent MSc thesis submitted to Addis Ababa University; Girum Admasu Nadew from his thesis "Groundwater and Surface water interaction in Lake Tana Sub-basin". It was analyzed in the Water Works Design and Supervision Enterprise Laboratory. One exceptional sample was excluded with an EC 10660 μ S/cm.

Table 4: Summary of secondary hydrochemical data

Parameters		Mean	Median	Mode	Minimum	Maximum
EC	µs/cm	598.9	496.9	N/A	54.7	2490
PH		7.4	7.3	8.2	5.0	10.0
TDS	mg/L	348.2	310	493	47.5	1398
NH_4	mg/L	0.5	0.3	0.1	0.0	5.0
Na	mg/L	56.8	29.5	44.0	5.8	390.0
K	mg/L	2.6	1.7	0.7	0.2	13.4
Ca	mg/L	56.5	41.9	15.2	4.8	211.3
Mg	mg/L	16.3	10.1	6.9	1.0	90.6
F	mg/l	0.63	0.4	0.4	0.0	0.9
Cl	mg/L	20.7	10.5	10.5	1.0	319.2
NO_2	mg/L	0.03	0.01	0.01	0.001	0.54
NO_3	mg/L	15.1	6.6	0.6	0.6	128.6
HCO_3	mg/L	330.3	281.6	176.2	74.2	1390.8
SO_4	mg/L	20.3	2.7	0.4	0.1	325.2
PO_4	mg/L	0.3	0.2	0.3	0.0	4.2

4.3. Laboratory Analysis

Primary new water samples were collected from seven Lake Tana sub-basins such as Gelda, Gumara, Ribb, Megech, Garno, Gemera and Drima. A total of 37 samples were collected from boreholes, dug wells, springs and surface water. Many samples couldn't be collected because of difficulties with access. The road was muddy, and the vehicles couldn't cross to the Wanzaye and Robit localities. All collected samples were analysed using different analytical instruments in the ITC Geo Science Laboratory. Inductive Coupled Plasma Emission Spectrometry (ICP_OES) was used to analyse major cation concentrations. Ammonia and phosphate concentrations were determined using SEAL AQ-1 Discrete Multi-Chemistry Analyser. A HACH Spectrometer was used to analyse nitrite, nitrate, and chloride and fluorine concentration. The accuracy of HACH instrument assessed before running the test by using chlorine standard concentration and blanks. Comparison of the standard samples with the HACH instrument readings showed a good correlation with a very slight difference. The sample measurements were adjusted according to the correlation result. For others water quality variables field measurements were taken such as EC, pH, Temperature, Oxygen, Cl, Alkalinity and Hardness.

Table 5: Summary of laboratory hydrochemical measurements

Parameters		Mean	Median	Mode	Minimum	Maximum
NH4	mg/L	0.64	0.59	0.21	0.03	2.82
Na	mg/L	37.55	27.12	N/A	3.43	173.76
K	mg/L	3.33	1.60	1.60	0.35	24.20
Ca	mg/L	59.30	48.49	N/A	12.23	241.25
Mg	mg/L	21.16	15.88	N/A	2.04	119.18
Fe	mg/L	1.14	0.14	0.04	0.01	34.91
F	mg/L	0.15	0.08	0.01	0.00	0.82
Cl	mg/L	20.3	7.85	N/A	2.70	247.50
NO2	mg/L	0.02	0.01	0.01	0.00	0.09
NO3	mg/L	14	10.30	10.50	1.20	105.60
SO4	mg/L	15.5	3	1.23	1	230
PO4	mg/L	0.12	0.10	0.12	0.03	0.43
TDS	mg/L	378.6	304.2	306.2	74.2	1547.7

4.3.1. Checking charge balance of water quality analysis

Charge balance error calculation helps to determine the accuracy of the analytical result. Based on the principle of electro neutrality the sum number of equivalents for positive cation must be equal to negative anion in solution.

$$\sum \text{cation} = \sum \text{anion}$$

After water samples, analysis completed in ITC Geo-Water Science Laboratory the result of all cation and anion were tested for charge balance error. The percent difference calculated using the following formula.

$$\text{Percent difference (\%)} = \frac{\sum \text{cation} - \sum \text{anion x100}}{\sum \text{cation} + \sum \text{anion}}$$

where the sum of anions and cations are in milliequivalent per liter The Percent difference between out of 37 primary water samples 3 samples show 10% which indicates the unacceptable analysis.

Totally, out of 92 secondary and primary water samples 3 samples show percent difference above 10%.

4.4. Geochemical Modelling

Geochemical modelling is important to identify the processes that are likely to be controlling the behaviour of a geochemical system.

4.4.1. Aquachem 2014.1

Aquachem is a fully-integrated software package developed for numerical and graphical analysis of geochemical data sets. It frequently used for the interpretation, analysis, and comparison of aqueous geochemical data. Aquachem is able to plot simultaneously multiple plots such as Piper and Stiff diagram, which used to plot different water types and rock deduction respectively.

4.4.2. Hierarchical cluster analysis (HCA)

Hierarchical cluster analysis is a semi-statistical technique in which similar objects grouped together or is close one to another. Water chemistry data can be grouped with similar aquifer lithology and storage time(Asmelash Gebreyohanns Abreha, 2014). In addition to that it can be grouped with similar water physical properties, isotopic and chemical composition (Kebede et al., 2005). In this study, water samples with similar chemical characteristics were grouped based on distance from observations.

4.4.3. PHREEQC Model

PHREEQC model is a computer program designed to simulate chemical reaction and transport process in natural or polluted water. The method used to assess different geochemical parameters speciation under the influence of redox conditions and mineral concentration in groundwater(Kumar et al., 2011). Using the model, various reactive mineral phases and their saturation indices can be identified in the groundwater. Moreover, it has a capability for the reaction path, advection transport, precipitation-dissolution and kinetic reaction calculation (Kumar et al., 2011).

4.4.4. Inverse modelling

Inverse geochemical modelling is one of the capabilities of PHREEQC model, which used to determine the groundwater chemistry along the flow path (Federico et al., 2008). Groundwater chemistry varies due to the reaction between mineral compositions in the aquifer along flow path; their geochemical evolution can be identified using inverse modelling from one point in the aquifer to another point along the groundwater the flow path (Sharif et al., 2008).

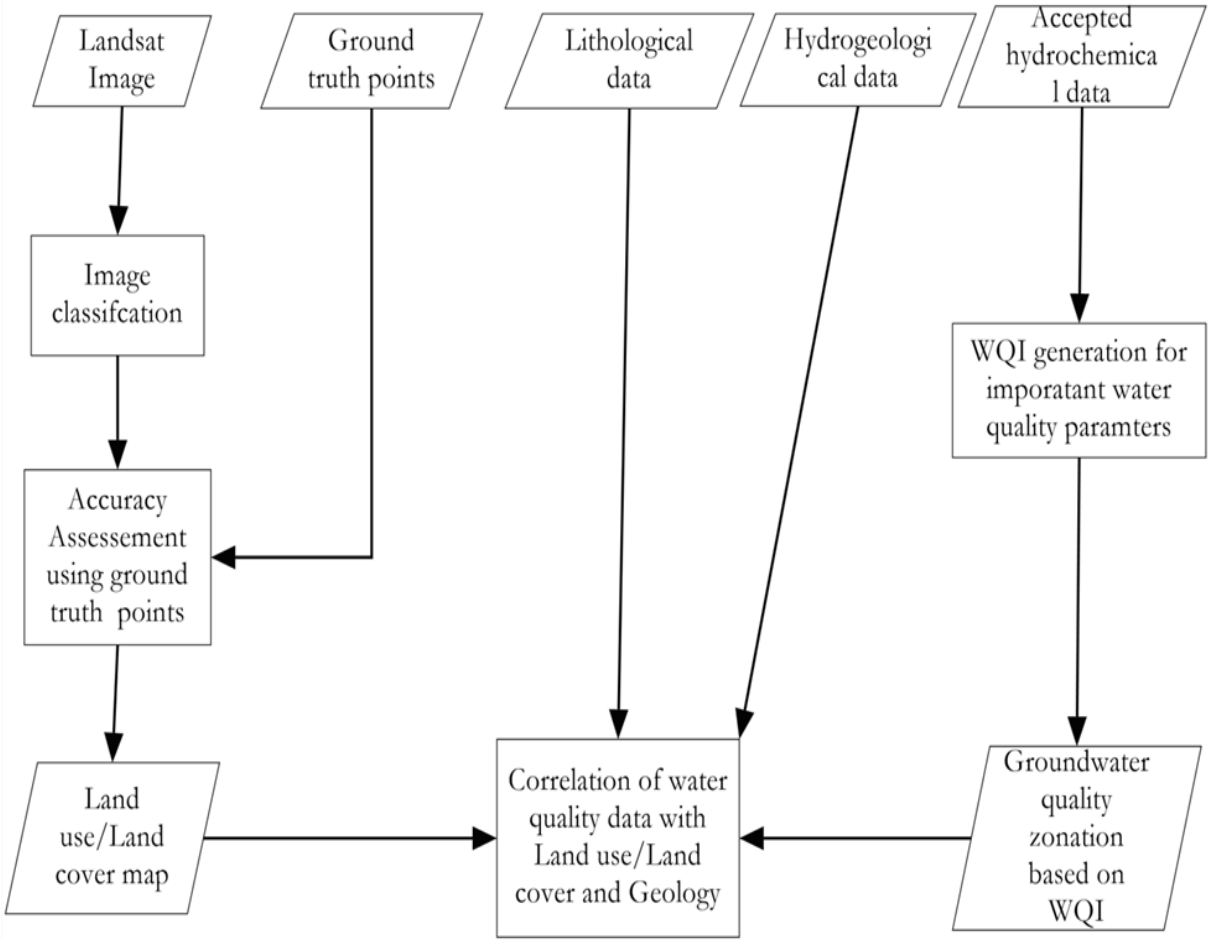

Figure 11: Flow diagram to determine the correlation of water quality index with land use/cover.

5. RESULTS AND DISCUSSION

5.1. Hydrochemistry

Groundwater is usually associated with geology, geologic structure and soils, which determine the chemical property of groundwater. In addition to that external forces such as human activities, industrial effluents and agricultural activities often influence groundwater chemistry. Hence, continuous groundwater quality assessment and monitoring are mandatory in order to prevent or control the groundwater pollution.

A total of 87 secondary and primary water samples were used for hydrochemical interpretation of the sub-basins; among them 46 samples taken from dug well, 32 samples from Borehole,4 river samples, 4 springs and one sample taken from Lake Tana. The water quality in the study area mainly influenced by the occurrence of basic and acidic volcanic rocks, agricultural, anthropogenic effect, major tectonic structures, topographic setup and soil type. There are different chemical characteristics of groundwater along the flow path that can be related to the reaction between mineral compositions in the aquifer. The most dominant dissolved cation in water samples area Ca^{+}, Mg^{+}, $NH4^{+}$, Na^{+} and K^{+}. Among anions HCO_3^{-}, Cl^{-}, SO_4^{2-} and NO_3^{-} are main dominant dissolved ions. HCO_3^{-} is the most dominant anion. According to Demlie, Wohnlich, & Ayenew, (2008) high HCO_3^{-} content of water is common characteristics of Ethiopian highland water. The temperature of the water samples varies from the lowest 14.60c to the highest 28.80c. The pH value of the water samples ranges from 5 to 9.09. A plot of field measured Electrical Conductivity (EC) values ranges from lowest EC 54.7 μS/ borehole around Gorgora area to the highest 10660μS/cm Serbia Mariam holy spring. Serbia Mariam holy spring has highest electrical conductivity in the study area with values 10660μS/cm, which associated with carbonate rocks related to deep process(Nadew, 2010). Another high EC was measured in lower of the Megech river basin around Robit village with value 2490 μS/cm. In general, Megech and lower of Ribb river basins fall into high salinity area.

According to WHO (2011) standard 95.6% TDS concentration of all water samples shows that within the allowable range. However, the remaining TDS concentrations are above the WHO standard which are greater than 1000mg/l and indicates the unacceptable range.

Ca-Mg-HCO_3 is most the dominant hydrochemical type; it shows 34.52% from total water samples and Na-Ca –HCO_3 the second dominant water type represents 14.29% from out of 87 samples.

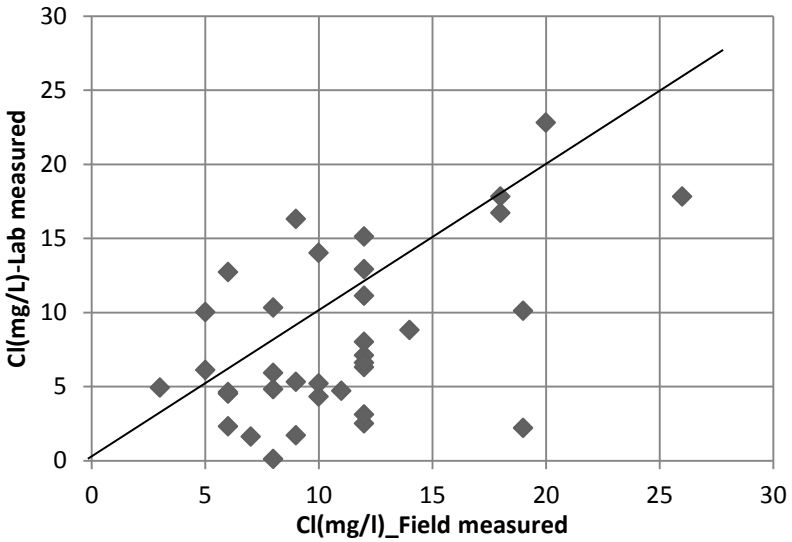

Figure 12: Correlation of chlorine field measured vs Lab measured

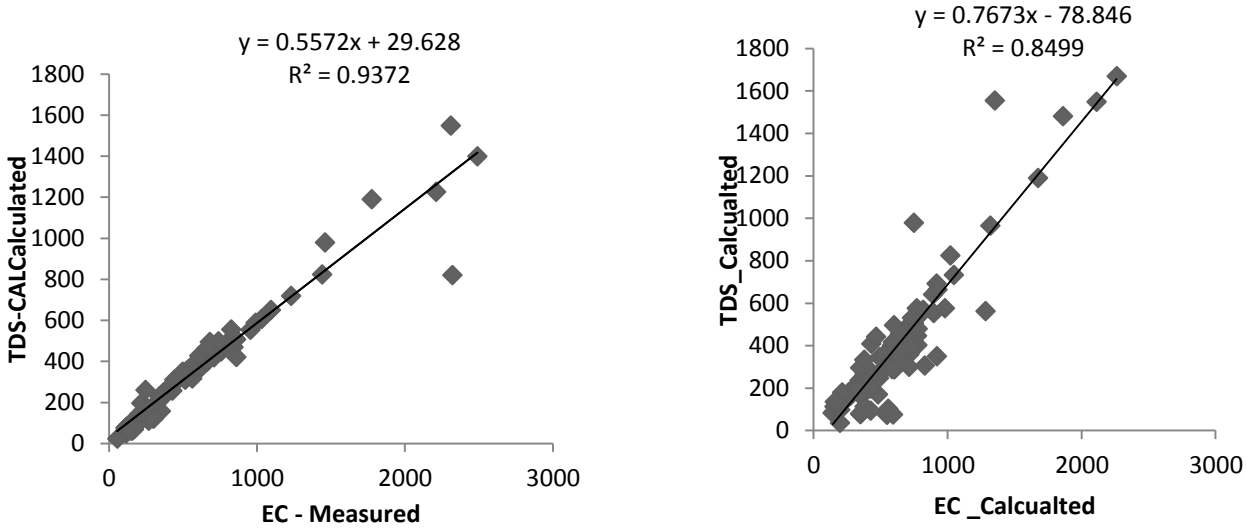

Figure 13: Direct relationship between TDS and EC

There is good correlation between calculated TDS versus measured EC and calculated TDS versus calculated EC.

For the above correlation EC calculated from the ionic composition using the following equation

EC = K*y2. Where K is infinite dilution conductivity

y is monovalent ion activity coefficient

The above formula can be used for ionic strength (IS) less than 0.5 and temperature of the water between 20 and 300.

Table 6: Correlation matrix of variables of the hydrochemical data sets

	EC	NH4	Na	K	Ca	Mg	F	Cl	NO3	HCO3	SO4	TDS
EC	1											
NH_4	0.10	1										
Na	0.97	-0.01	1									
K	0.91	-0.06	0.95	1								
Ca	0.38	0.42	0.15	0.12	1							
Mg	0.20	0.50	-0.04	-0.03	0.83	1						
F	0.82	-0.03	0.86	0.85	0.12	-0.10	1					
Cl	0.97	0.17	0.93	0.91	0.39	0.25	0.80	1				
NO_3	0.05	0.10	-0.06	-0.04	0.45	0.38	0.04	0.15	1			
HCO_3	0.98	0.08	0.98	0.92	0.32	0.11	0.83	0.93	-0.03	1		
SO_4	0.91	0.18	0.82	0.80	0.45	0.39	0.68	0.93	0.13	0.82	1	
TDS	0.99	0.12	0.95	0.89	0.43	0.25	0.80	0.97	0.09	0.98	0.90	1

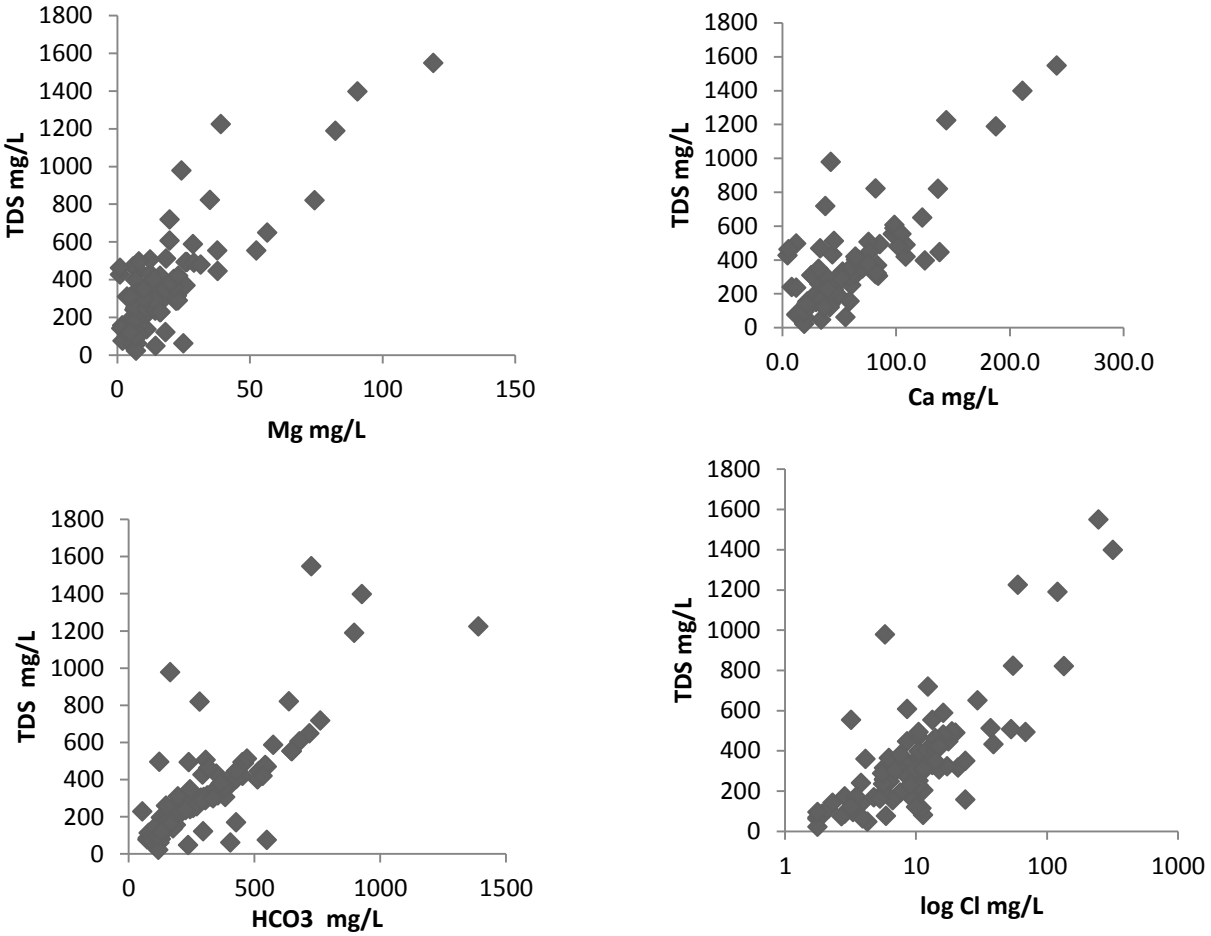

Figure 14: Major ions concentration relationship with TDS.

Total dissolved solid (TDS) refers to any minerals, cations, anions, salts and metals that are dissolved in the water. The interrelationships in the figures above show that the major ions contribution to TDS.

5.2. Water Quality Index for drinking water quality assessment

A water-quality index developed by Brown et al (1970) and then later improved by Deininger for the National Sanitation Foundation (1975). WQI is an algorithm that expresses a measure of the qualitative state of water (Poonam, Tanushree, & Sukalyan, 2013). It has been successfully applied by many researchers in the recent years to assess overall water quality for drinking purpose (Verma, Thakur, Katiyar, Singh, & Rai, 2013). For example, Jerome & Pius, (2010) used Brown et al., (1972) weighted arithmetic index method to calculated WQI for important parameters, which are considered to determining the suitability of groundwater for drinking purpose such as temperature, pH, Electrical Conductivity (EC), Magnesium (Mg^{2+}), Chloride (Cl^{-}), Nitrate (NO_3^{-}), Total hardness (TH), Calcium (Ca^{2+}), Dissolved oxygen (DO), Total dissolved solids (TDS) and Alkalinity (A). The number of parameters depends on the intended use of water; WQI can be widened if various parameters are used or for few parameters, the technique can be used. For example, Chowdhury, Muntasir, & Hossain, (2007) used weighted arithmetic index method to calculate water quality for drinking water purpose for parameters namely EC, PH, DO, TDS and BOD. A WQI arithmetic mean method developed by Brown et al calculating in the following way: Three steps are followed to calculate:

The weight assigned to each parameter (WI)

Relative weight calculated (wi)

Rating scale assigned to each parameters by dividing each parameter concentration by its respective standard.

$$W_i = \frac{wi}{\sum_{i=1}^{n} wi}$$ where; W_i is relative weight

wi is the weight of each parameter

n is the number of the parameters

Rating scale calculates by using the following expression

$$qi = (Ci - C_{io} / Si - C_{io}) x100$$

Where; Ci is each parameters concentration
Cio is the ideal value of the parameters in the pure water
Si is the standard permissible value of nth parameters according to WHO or any country standard in mg/l

Cio value PH=7 and for other parameters usually considered as zero.

For calculate WQI first sub-index (SI) determined for each parameter and then WQI calculating in the following equation

$$SI = W_i \times qi$$

$$WQI = \sum_{i}^{n} SI$$

After the WQI applied the result of the water quality is a combination of numeric and alphanumeric variables. The spatial distribution of the water quality can be mapped based on numerical classification.

Using the above equation, WQI computed for parameter's pH, NH_4^+, Na^+, Ca^+, Mg^+, F^-, NO_2^-, NO_3^-, SO_4^{2-}, TDS, and O_2^-. World Health Organization (WHO) standard for drinking water quality was used to compute the relative weight.

As Pius, Jerome, & Sharma, (2012) WQI classification, the computed WQI value ranges from 2.45 to 597.4. Based on the values water quality was categorized as Excellent, Good, Poor, Very poor and Unfit for drinking purpose. In the following table, the relative weight of each chemical parameter is presented.

Table 7: The relative weight for each water parameter

Chemical parameters	WHO standard	Weight	Relative weight $W_i = \frac{wi}{\sum_{i=1}^{n} wi}$
PH	6.5-8.5	4	0.10256
NH_4	1.5	3	0.0769
Na	200	4	0.1026
Ca	200	3	0.0769
Mg	50	3	0.0769
F	1.5	2	0.0528
Cl	5	3	0.0769
NO_2	3	2	0.0513
NO_3	50	5	0.1282
SO_4	250	4	0.1026
TDS	1000	5	0.1282
O_2	5	2	0.0513

The computed WQI out of 87 groundwater's samples 72.25% represents "Excellent," 13.75% shows "Good water," 5% of samples indicate "Poor water," 2.5% indicate "Very poor" and 3.75% shows Unfit for drinking purpose.

The main factors influencing water quality are both natural and human such as precipitation and dissolution of dissolved solute, evaporation, leaching of carbonate rocks, agricultural activities or improper use of fertilizer and pesticide and anthropogenic effect. As an example, poor water quality in near to Gonder town and intensive agricultural activity area at lower of the Megech river basin are clear indications of the anthropogenic creation pollution and the leaching of fertilizer effect respectively. The computation included only ground water samples. WQI classification indicated in the following table.

Table 8: WQI classification

Range	Types of water	% of classification
<50	Excellent	72.5
50-100	Good	13.75
100-200	Poor	5
300-300	Very poor	2.5
>300	Unfit for drinking	3.75

The spatial distribution of WQI, nitrate NO_3, total dissolved solids (TDS) and pH maps indicated below

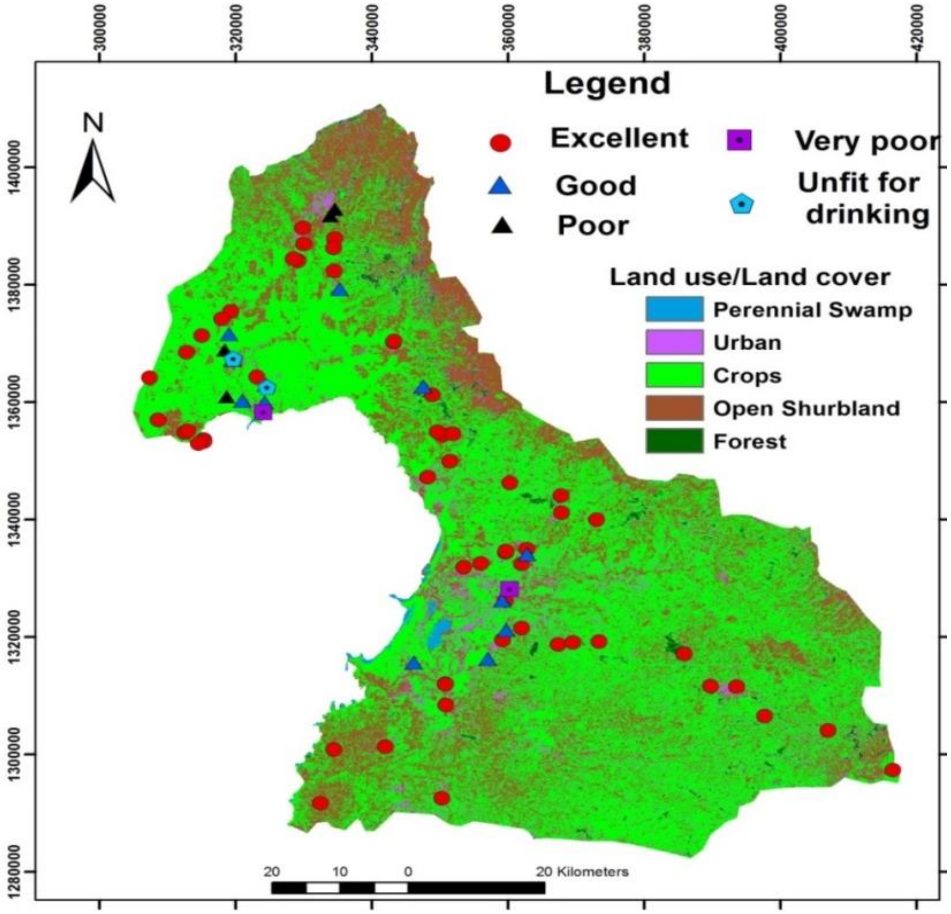

Figure 15: Water Quality Index Map versus Land use/Land cover

Table 9: Quality criteria of water samples compared to drinking standards of Ethiopia and WHO (mg/L)

	Highest Desirable Level			Number of Exceeding Value	
Parameters	Ethiopian standard	WHO standard	Range	Ethiopia	WHO
PH	6.5-8.5	6.5-8.5	5-9.95	4	4
TDS	1500	1000	68-6410	1	4
Na	358	200	3.43-3750	2	5
Mg	150	-	1-119.18	0	-
NH_4	-	1.5	0.004-4.9	-	6
Ca	200	-	4.8-241.3	2	-
F	3	1.5	0.01-3.8	1	1
Cl	533	250	0.95-1007	1	2
NO_3	50	50	0.62-128.6	5	5
SO_4	483	250	0.1-675.9	1	1

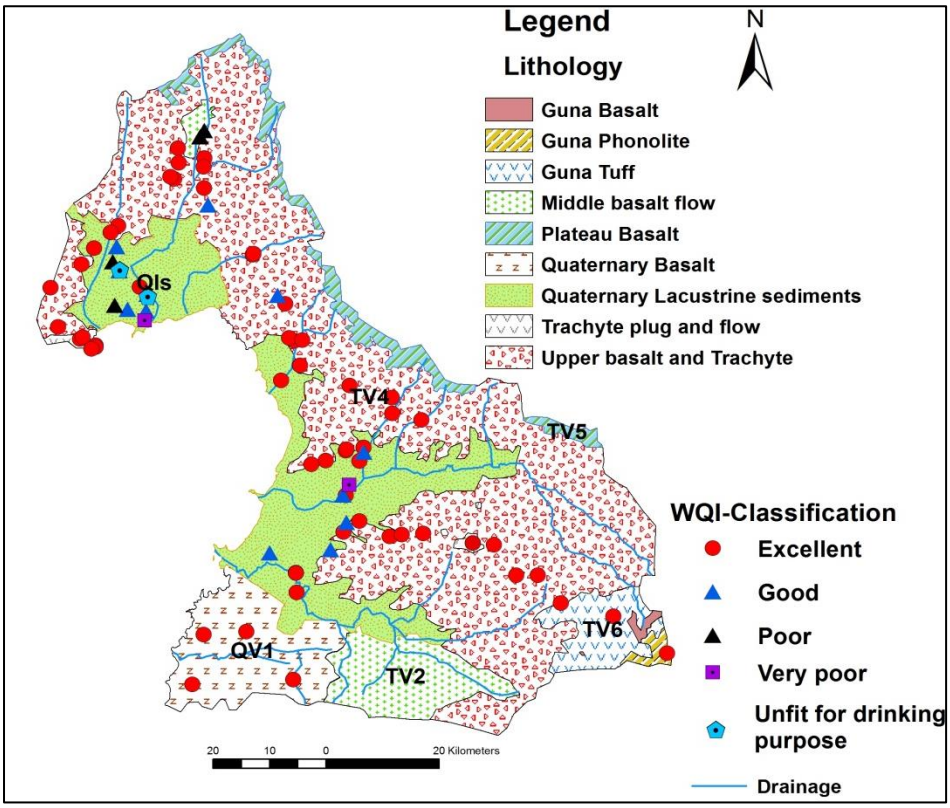

Figure 16: Water Quality Index Map versus Geology

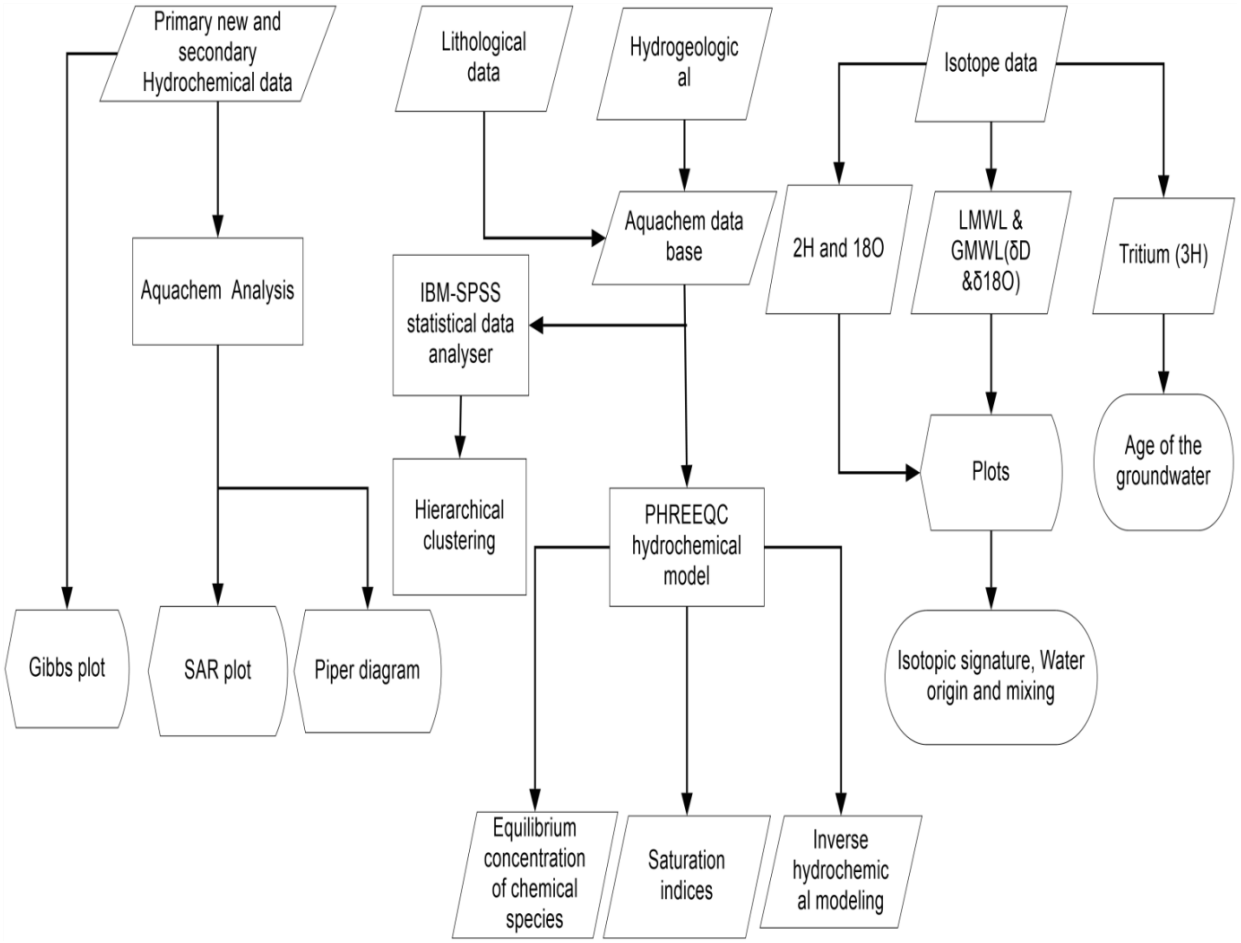

Figure 17: Flow chart of Aquachem Analysis, Geochemical modelling and Isotopes signature

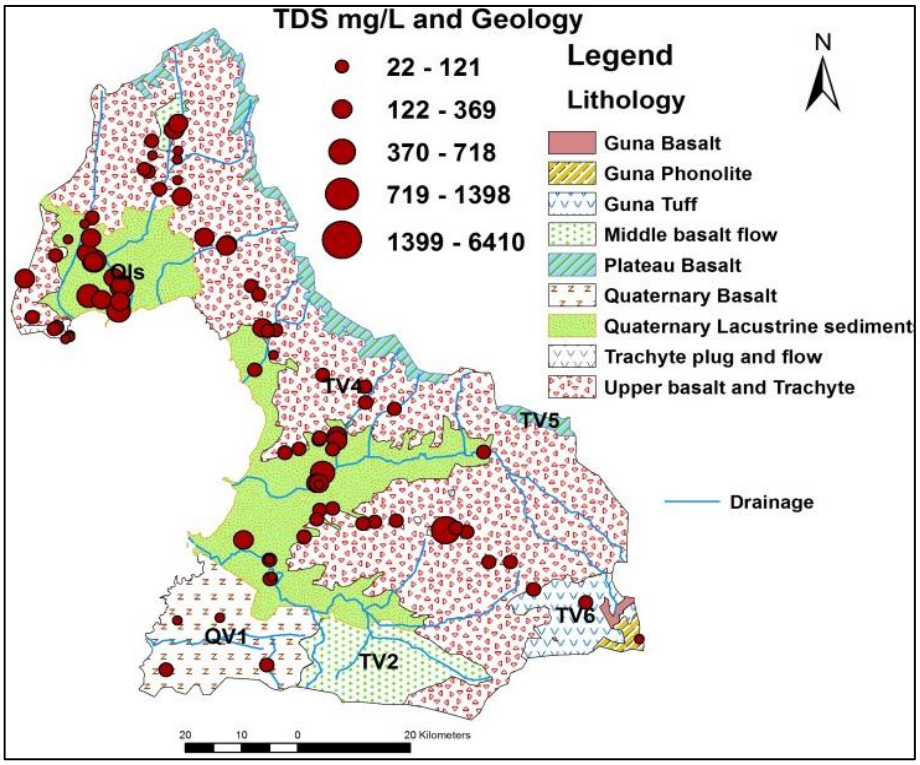

Figure 18: Spatial distribution of TDS versus Geology.

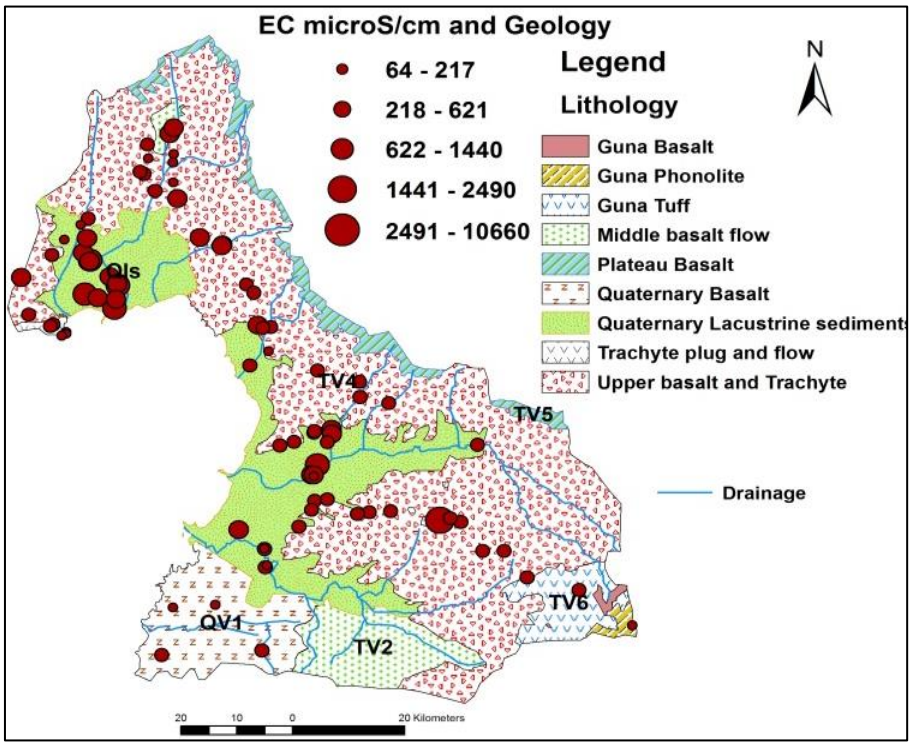

Figure 19: Spatial distribution of EC versus Geology

5.3. Major ions Signature and water types

Piper's diagram displays the relative concentration of the major anion and cation into two separate trilinear plots. It facilitates the visualization of all chemical character of the water types. The AquaChem 2014.1 version was used to classify the water types. After checking the reliability of all hydrochemical data; different water types were identified based on the dominant anions and cations. In this classification, fifteen major chemical facies were identified from the Piper diagram. These include all natural water such as boreholes, springs, river and lake water.

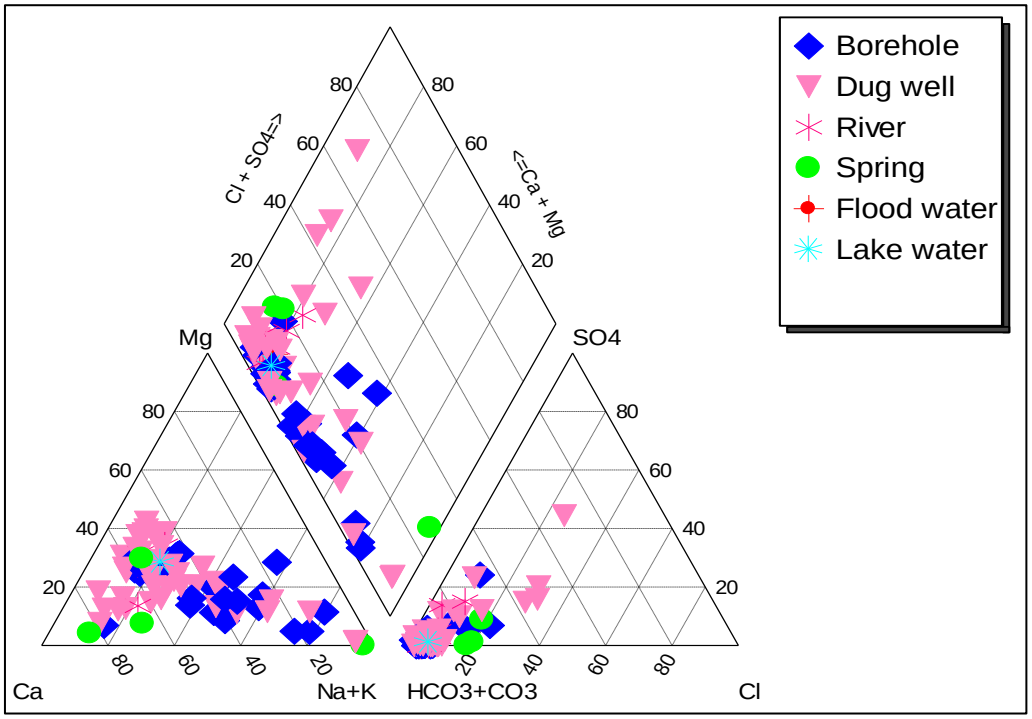

Figure 20: Piper diagram representing hydrochemical facies.

The most dominant hydrochemical types are Ca-Mg-HCO_3; it is about 34.52% or 29 samples. 14.29% show Na-Ca –HCO_3, 9.52% represent Ca-HCO_3, Ca-Na-HCO_3 and Ca-Mg-Na-HCO_3 each represents 8.33% and 7.14% of the samples show Na-HCO_3 from out of 87 samples. All water types presented in table 10. According to Demlie et al., (2008) water types indicated by Ca-Mg-HCO_3 and Ca-Mg-Na-HCO_3 associated with weakly mineralized water and circulate in the scoriaceous and basaltic aquifers. Samples having water types Na-Ca-HCO_3 and Ca-Na-HCO_3 drains in the intermediate and fractured acidic rocks such as ignimbrite, rhyolite, tuff and trachyte. Ca-Na-Mg-HCO_3, Na-Mg-Ca-HCO_3, and Na-Mg-HCO_3 water types are the mixture of the above two. Na- HCO_3 water type is highly mineralized water type. It shows that the contribution of major ion to the groundwater salinity.

Some water types represented by Na-HCO_3, Ca-Mg-HCO_3-Cl, Ca-Mg-SO_4-HCO_3-Cl, Ca-Na-Mg-HCO_3-Cl and Na-Ca-HCO_3-SO_4 are highly mineralized water in the study area. For these water types, Electrical Conductivity range is from 600- 2490µS/cm and also TDS ranges between 400-1547.7mg/l. There is hot springs in Wanzaye locality. According to Kebede et al., (2005) the thermal groundwater in the Tana Graben influenced by a silicate hydrolysis accompanied by the carbon dioxide influx from a deep source. It has high TDS with Na-HCO3 water type.

Table 10: A general overview of all natural water types of the study area

Hydrochemical type	Percentage
Na-HCO_3	7.14
Na-Ca-HCO_3	14.29
Na-Ca-Mg-HCO_3	3.57
Ca-Mg-HCO_3	34.52
Ca-HCO_3	9.52
Ca-Na-HCO_3	8.33
Ca-Mg-Na-HCO_3	8.33
Ca-Mg-HCO_3-NO_3-Cl	1.19
Ca-Mg-HCO_3-NO_3	1.19
Ca-Na-Mg-HCO_3-Cl	1.19
Ca-Na-Mg-HCO_3-SO_4	1.19
Ca-Mg-HCO_3-Cl	1.19
Ca-Mg-SO_4-HCO_3-Cl	1.19
Na-Ca-HCO_3-SO_4	1.19
Na-Mg-HCO_3	1.19

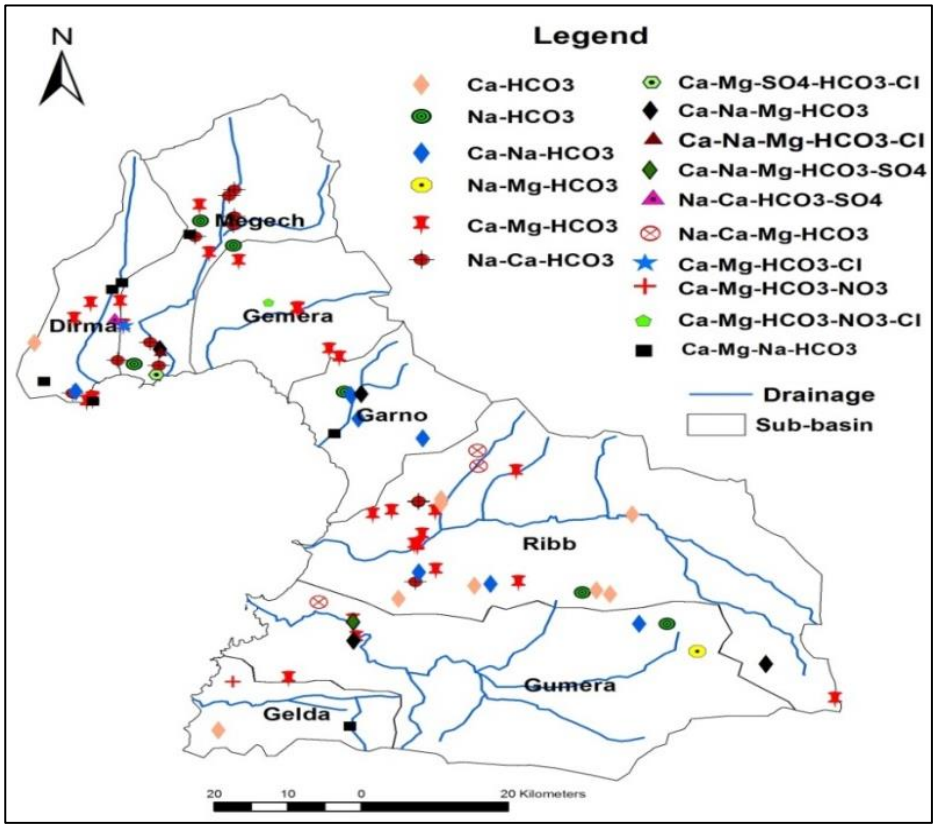

Figure 21: Spatial distribution hydrochemical water of all nature
Note: The names in the map are the names of the rivers

5.4. Water Quality Criteria for Irrigation

Shallow groundwater plays an important role for water supply sources of drinking, irrigation and livestock development. Most of the private owned shallow hand dug wells used for irrigation whereas drinking water supply wells used by community. Currently, two big irrigation projects are developing in Megeach and Ribb River basins, which help to improve food security and water scarcity in the region. According to Ministry of Water, Irrigation and Energy of Ethiopia, the irrigation and drainage projects cover 62,457 hectares in the Lake Tana sub-basin.

There are a number of empirical indices, which are used to examine the water quality for irrigation purpose. These indices were used to determine the chemistry of the groundwater and the suitability of the water for crop growth. Further explanation has given below for the main parameters considered in evaluating the quality of irrigation water.

5.4.1. Salinity Hazard

Salt concentration in soil reduces water availability for crop growth. It usually measured as electrical conductivity (EC). High EC value indicates salinity hazard. There is many water points ranged from fresh to brackish in the study area. Water points located in the Fogera plain and lower of Megech river basin have been moderate to high salinity. The source of the salinity is according to (Zenaw, 2009) associated with evaporation of shallow groundwater and lack of the drainage system.

The United States Salinity Laboratory has established guide in 1954 based on salinity and SAR Criteria as shown below.

Table 11: Water quality analysis result based on the US salinity criteria.

EC (μS/cm)	Class	Remarks
<250	Low salinity (C1)	Good for most of the crops
250-750	Moderate (C2)	Moderate, salt tolerance plants can grow
750-2250	Medium to high (C3)	Satisfactory for moderately salt tolerant crops
2250-4000	High (C4)	Unfair for irrigation
>4000	Very high (C5)	Unfit for irrigation

5.4.2. Sodium Hazard

The high concentration of sodium in the soil relates to the total salt content, which reduces infiltration or permeability of water flow as well as reduce soil aeration by sealing the pores of a soil.

The effect of excess sodium can be related to the relative proportions of sodium ions and calcium plus magnesium ions and expressed in a Sodium Adsorption Ratio (SAR)-

$$SAR = \frac{Na}{\frac{\sqrt{Ca + Mg}}{2}}$$; expressed in mill equivalents per litter.

Table 12: Irrigation water classification based on sodium content (after Wilcox, 1954)

Classification	SAR	Water class	Comments
S1	0-10	Excellent	Good for almost all type soils
S2	10-18	Good	The water can be used on coarse-grained permeable soil unsatisfactory for highly clay soils
S3	18-26	Fair	Good drainage and high leaching or organic matter may require additionally for the soil. This helps to protect the effect of excess exchangeable sodium.
S4	>26	Poor	Unsatisfactory for irrigation purposes

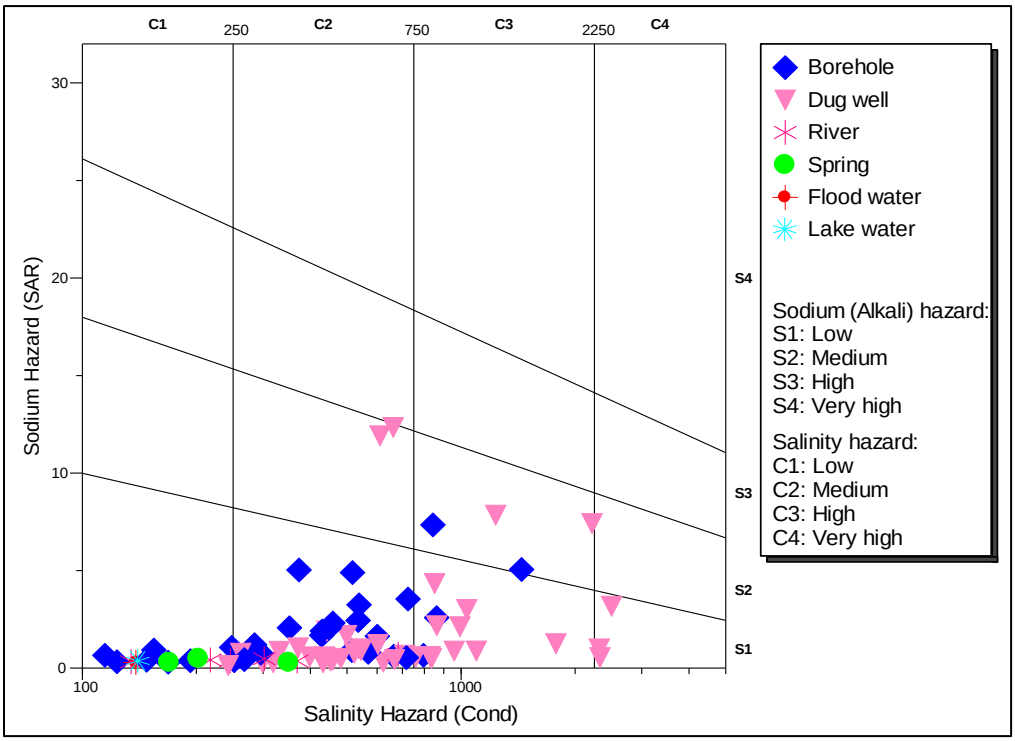

Figure 22: Wilcox diagram showing suitability limits of water for irrigation.

Groundwater with the medium, to low sodium (alkalinity) and medium to high salinity can be used for irrigation purpose almost the soil with little danger. Generally, the value of the water compared to US SAR and EC criteria most of the water is suitable for irrigation.

Three dug wells such as G-DW18, H-DW43 and T-DW35 in lower of Megech River have very high salinity hazard, which range from 2250-4000μS/cm or C4 salinity hazard group, which are unsuitable for irrigation purpose comparable to the above criteria. However, the sodium hazard or SAR hazard ranges from excellent to fair or from S1 to S3 water class. Thus, the sodium hazard could not be a major concern in all study areas.

5.4.3. Magnesium Hazard

Magnesium is one of the important qualitative criteria for irrigation water quality. High concentration of Mg affects the physical properties of soil; Mg >50 mill equivalents per litter considered as harmful and expressed in the following way:

$$\textbf{Mg Adsorption Ratio} = \frac{Mg}{Ca+Mg} x100;\ \text{the units are in mill equivalents per litter}$$

There is no water sample in the study area with Mg Adsorption Ratio greater than 50 mill equivalent per litter. Therefore, Magnesium hazard is not concerned as a major hazard to agricultural development.

5.4.4. Permeability Index (PI)

Permeability Index (PI) equation was used to determine the effect of water quality parameters on soil permeability. The high concentration of sodium, magnesium, calcium, carbon trioxide and bicarbonate in soil can reduce the soil permeability. The soil permeability is also influenced by long-term use of irrigation water. If the PI value greater than 75meq/l indicates good quality of water for irrigation and also PI values between 25 and 75 meq/l indicates the water suitability for irrigation. However, PI values less than 25meq/l indicates water quality unsuitable for irrigation purpose. Permeability Index (PI) is expressed by the following equation.

$$\textbf{PI} = \frac{Na+\sqrt{HCO3}}{Ca+Mg+Na}\ \textbf{X100}$$ Where, all the values are in meq/l

There are four samples which do unsuitable for irrigation based on computed permeability index (PI) values. These samples are G-DW18, 23.6%, T-DW35, 16.9%, T-BH20, 21.6% and H-DW43, 16.2%. These samples are located in Robit village, Gura Amba and Farat. Generally, most of the water samples ranged from 30%-60%, they are suitable for irrigation. There are fourteen water points with PI value greater than 75 %, which are excellent water points for irrigation purpose.

The chemistry of surface water analyzed except for the Rivers Gelda and Garno. For all surface waters such as Megech, Ribb, Gumera, Dirma, Gemera River and Lake Tana, the calculated criteria for irrigation purpose show moderate to excellent water for irrigation. The Electrical Conductivity ranges for all surface water from 134-680μS/cm and TDS between 85-493mg/L. Generally, all surface waters are suitable for irrigation.

5.5. Nitrate

Some water points highly polluted by nitrate, which is located close to the urban area. Naturally nitrate occurring at the low level in the ground water. High concentration clearly indicates anthropogenic effects. According to WHO guideline the nitrate level in drinking water is 50mg/L. The nitrate level as indicated in the table below ranges from 64.8-128mg/L in five different water sources in study area. Excess amount nitrate concentration in drinking water can cause blue baby syndrome (methemoglobinemia) in infants

(Esmaeili, Moore, & Keshavarzi, 2014). These water wells are used by population in the area. Therefore, protection should be taken to reduce the nitrate level.

Table 13: Water wells with high nitrate concentration.

Water Source	Location	Longitude	Latitude UTM	EC µS/cm	TDS mg/	NO3 mg/L	Cl mg/L	HCO3 mg/L	NO2 mg/L
Dug well	Bahr Gimb	33924	137180	833	493.0	128.6	68.4	238.8	0.01
Borehole	Gondar town	334541	1392929	722	432.0	81.6	39.0	347.7	0.01
Borehole	Gonder town	333851	1391781	859	506.0	82.6	53.2	306.1	0.01
Dug well	Robit school	324574	1362610	2490	1398.0	64.8	319.2	927.2	0.01
Dug well	Robit	319614	1367450	2310	1547.7	105.6	247.5	725.9	0.0

5.6. Hierarchical cluster analysis

Hierarchical cluster analysis is a semi-statistical technique in which similar objects grouped together or is close one to another. Hierarchical cluster analysis is carried out to determine water samples those have similar chemistry. Surface water points were not included in the classification. A total of 80 groundwater samples classified using IBM-SPSS statistical data analyzer. Euclidean distance method was used to combine or split cluster between sets of observations. Hydrochemical variables which were included in the classification are EC, pH, NH_4^+, Na+, K^+, Ca^{2+}, Mg^{2+}, F^-, Cl^-, NO_2^-, NO_3^-, $SO4_2$-, $PO_4^{3-}$and TDS. The hierarchical clustering resulted in three main groups and five subgroups and presented in Dendrogram.

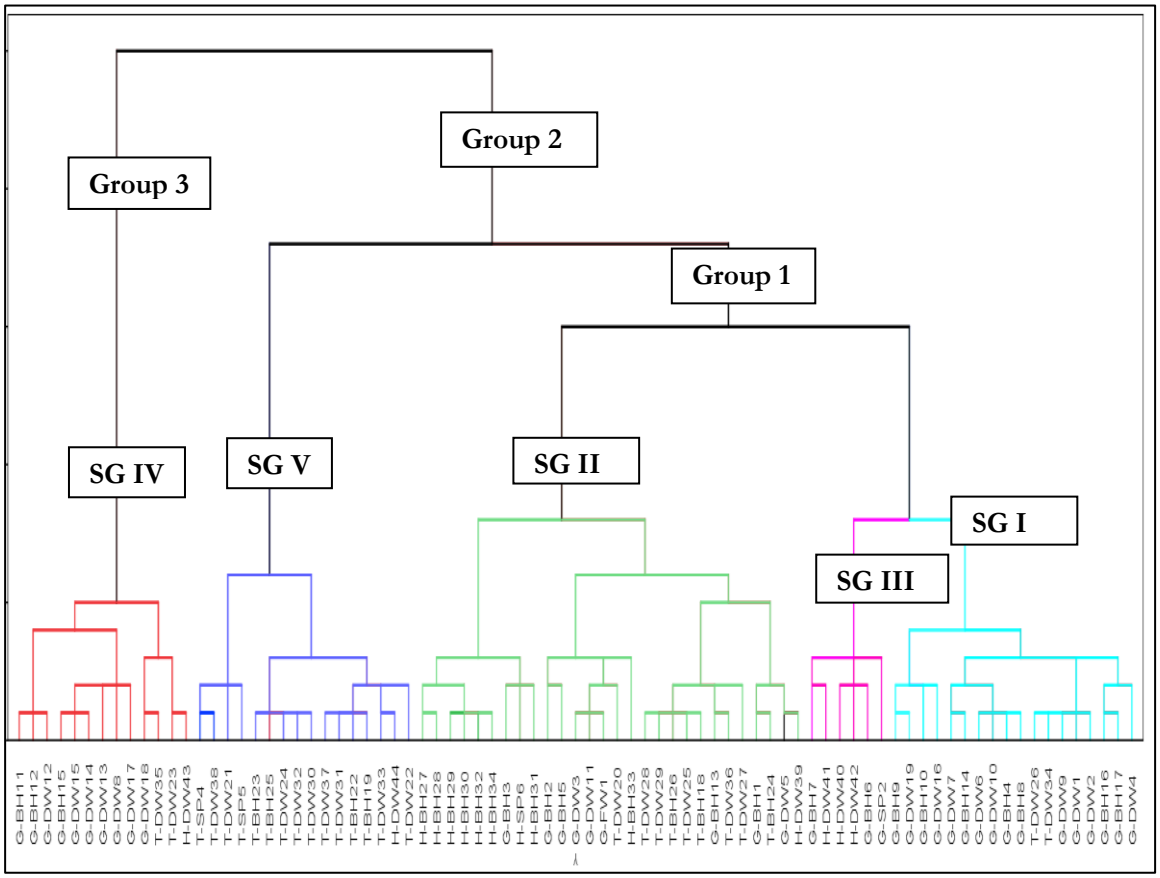

Figure 23: Dendrogram of the hydrochemical data.

Table 14: Mean hydrochemical composition of groundwater sub-groups and groups.

Cluster Sub-group	EC	pH	TDS	NH_4	Na	Mg	K	Ca	Cl	NO3	HCO_3	SO_4	PO_4
SG I (G1-n=18)	645	7.1	387.5	0.49	58.3	17	1.8	71.9	10.4	19.4	649	0.62	0.35
SG II (G1-n=26)	329.6	7.1	197.4	0.48	23	12	3.6	39.6	6.7	7.6	233.5	6.7	0.12
SG III(G1-n=6)	500	7.1	324	0.16	77.1	4	1.8	22.6	13.3	1.9	268.3	0.24	0.09
SG IV(G3-n=13)	1435	7.3	817	1.09	119	46	2.8	125.7	91.4	39.6	617.9	103.9	0.65
SG V (G2-n=18)	524.8	7.2	338.6	0.66	33.4	20	2.6	60.4	10.8	11.2	367	4.87	0.00

5.6.1. Interpretation of hydrochemical composition of hierarchical cluster subgroups

Subgroup SGI water types have electrical conductivity from 284-1230μS/cm and also bicarbonate (HCO_3) ranges from 401mg/L to 761mg/L. This subgroup water kind of distributed many places excluding Gemera and Gelda sub-basins. It contains various water types. Ca-HCO_3 is the most dominating water type. Generally, this subgroup water types have TDS range from 173-718 mg/L.

Subgroup SGII distributed in all sub-basins. Electrical conductivity ranges from 54.7-956 μS/cm and TDS ranges 220-553 mg/L. Most of the water sources are boreholes, and each one is fresh water.

Subgroup SGIII water types distributed toward the north of Gonder, lover of Ribb River and upper part of Gumera River basin. The water types are Na-HCO_3, Na-Ca-HCO_3 and Ca-HCO_3 types. The Electrical Conductivity ranges from 350-659.91μS/cm and TDS ranges 157-462mg/L. Generally, this group water type is believed to be a moderately diluted groundwater type.

Subgroup IV water types moderately to high saline water types. Almost the water types distributed to lower of Megech and Ribb river basin. The rest distributed to North Gonder and Makesegnt towns. The Electrical Conductivity ranges from 722-2490μS/cm. Ca-Mg-SO_4-HCO_3-Cl, Ca-Na-Mg-HCO_3-Cl, Na-Ca-HCO_3, Ca-Mg-HCO_3, Ca-Mg- HCO_3-Cl and Na-Ca-HCO_3-SO_4 are some of the water types in this group with high Electrical Conductivity (1440-2490μS/cm).

Some water points in the Subgroup SGV moderately diluted dug wells, boreholes and springs. This subgroup's water points were distributed along Woreta-Gonder Road. The Electrical Conductivity of the water ranges from 169.2-860μS/cm and TDS ranges 113-553mg/L.

5.7. Source- rock deduction

The source rock deduction carried out for hydrochemical composition of six water points with the help of AQUACHEM software. The initial condition of the groundwater originates from rainfall and then through time the water composition altered by rock weathering, evaporation and aeration(Hounslow, 1995). During weathering, the ions and cation added to the water.

The technique helps to determine the origin of the water sample's analysis (Hounslow, 1995). The used data for source deduction and geochemical modeling was different from other's analysis above. This analytical data contains silicon oxide parameter that was obtained from the Geological Survey of Ethiopia. Silicon oxide is necessary for the source rock deduction and geochemical modeling since the area lies within volcanic terrain.

Table 15: Hydrochemical composition of water points for source deduction and geochemical modelling (parameters in mg/L except pH and EC μS/cm)

Parameters	Na^+	K^+	Ca^{2+}	Mg^{2+}	HCO_3^-	Cl^-	F^-	$SO2^-$	NO_3^-	$SiO2^{+2}$	pH	EC	TDS
CSP-2	4.9	0.13	23.1	7.6	109.8	0.4	0.1	4.3	9.732.	96	7.23	214	143.4
DW-2	220	1.6	211.3	90.6	927.2	319.2	0.58	220.6	64.79	80	6.45	2390	1601.3
CSP-3	3.6	0.9	19.4	4.6	85	2.5	0.17	7	10.2	40.2	8.12	171	114.6
BH-1	15.7	0.66	148.4	36.1	200.5	122.7	0.19	44.6	66.5 3	0.4	7.73	1196	801.3
CSP-1	5	0.01	15	4	78	1	0.28	2	0.4	35	7.68	143	95.81
DW-1	2.36	0.47	25.2	8.95	127	5.2	0.16	2.36	18.6	24.6	6.55	244	163.5

Based on the rock source deductions result of six water samples from Aquachem software, a summarized result of different ionic comparisons and their values are given in table 16 below. The result of all water points values and conclusion also given in appendix 3. The source rock deduction analysis indicates the following process and presence of the minerals. The result the processes and presented minerals of Csp-2, Csp-3 and BH- 1 show similar results as indicate in (appendix.3), mainly volcanic glass and ferromagnesian were presented minerals from the source rock deduction analysis. In addition to that, weathering processes such as silicate weathering, plagioclase and carbonate weathering or brine halite-albite and ion exchange were observed from the source rock's analysis. For example, plagioclase weathering and carbonate weathering or brine are main processes in the water Csp-1. The ratios of HCO_3^-/SiO_2 and Mg/ (Ca+Mg) for this water point is ambiguous. DW-1 results showed that ion ratios of SiO_2 (mmol/L), HCO_3^-/SiO_2 and Mg/ (Ca+Mg) are ambiguous. However, the processes of SiO2/(Na+K-Cl), (Na+K-Cl)/(Na+K-Cl+Ca) Cl-/Sum Anions and HCO_3^-/Sum Anions ratio shows that cation exchange, plagioclase weathering, rock weathering and silicate or carbonate weathering respectively. For the water points DW-2 the resulted processes are, carbonate weathering or brine, albite weathering, plagioclase weathering, limestone- dolomite weathering, ion exchange and rock weathering. In addition, volcanic glass is the mineral presented in this water sample from the analysis.

Table 16: Ions ratios value (source rock deduction)

	VALUE					
Parameter	DW-2	DW-1	BH-1	CSP-1	CSP-2	CSP-3
HCO_3-/SiO_2	11.413	5.084	2.19	6.497	3.28	2.082
SiO_2/(Na+K-Cl)	1.642	-9.891	2.99	-0.183	2.657	7.427
(Na+K-Cl)/(Na+K-Cl+Ca)	0.071	-0.034	0.207	-0.594	0.152	0.085
(Na/(Na+Cl)	0.515	0.412	0.885	0.165	0.946	0.69
Mg/ (Ca+Mg)	11.41	5.08	2.2	6.5	3.28	2.08
Cl-/Sum Anions	0.327	0.057	0.02	0.417	0.006	0.041
HCO_3-/Sum Anions	0.551	0.813	0.95	0.396	0.892	0.815

Table 17: Volcanic rocks chemical composition data in Lake Tana basin (in wt %)

Rock type	SiO_2	Al_2O_3	Fe_2O_3	CaO	MgO	Na_2O	K_2O	TiO_2	P_2O_5	MnO
Aphanitic basalt	37.8	14.2	14.58	14.12	5.16	3.81	1.86	5.01	2.146	0.177
Aphanitic basalt	40.8	14.6	14.06	9.59	5.25	4.86	1.89	4.22	4.245	0.157
Guna lava flow	61.2	17.26	3.43	1.09	0.28	9.73	6.22	0.74	0.082	0.27
Glassy basalt	38.7	19.77	22.02	0.89	0.92	0.01	0.81	3.753	0.272	0.374
Welded crystal tuff	56	13.1	7.19	3.45	1.88	0.99	1.14	1.43	0.35	0.13
Olivine basalt	43.2	13.3	16.7	8.89	5.8	2.59	0.79	3.72	0.31	0.19
Porphyritic basalt	62.4	14.4	5.7	3.42	0.87	2.91	1.06	1.04	0.4	0.14

Note: Volcanic rocks chemical composition was obtained from Journal of Africa Earth Sciences and Geological Survey of Ethiopia from different geological reports.
Stiff plots constructed by plotting the mill equivalents per liter of three or more cations and three or more anions which show the main chemical compositions in the groundwater. A method of graphically comparing the concentration of selected anions and cations for selescted samples. The shape formed by the Stiff diagrams shows to identify samples that have similar or differetnt chemical compositions .

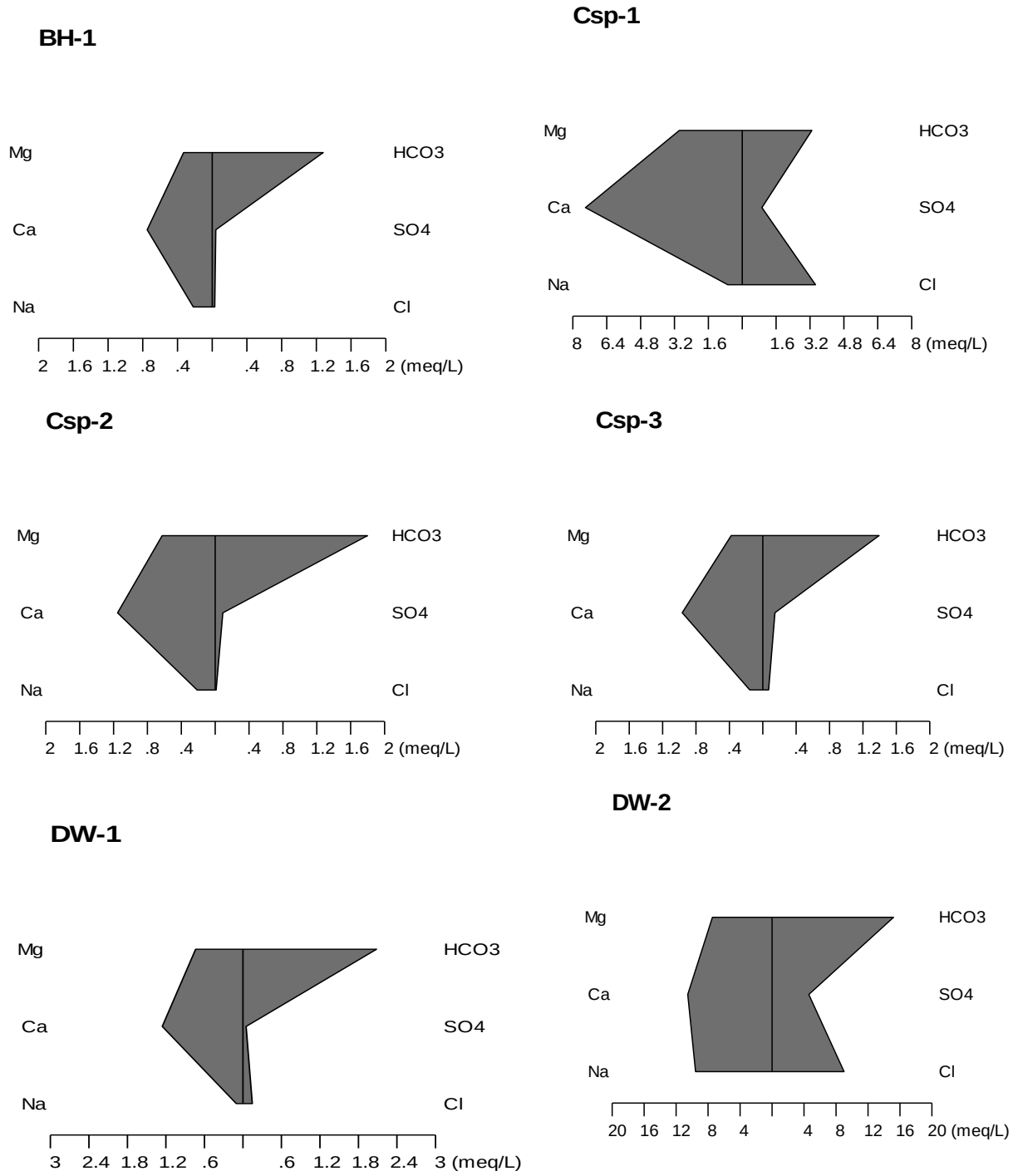

Figure 24: Stiff diagrams show source-rocks deduction of subgroups of water samples

Understanding the relationship of anions and cations and the binding characteristics of ions in the groundwater reaction medium gives some insight into the geochemical characteristics of the aquifer (Arunprakash, Giridharan, Krishnamurthy, & Jayaprakash, 2013). Calcium, Sodium and Magnesium are the most dominant cations in the study area. Similarly, between the anion's bicarbonate (HCO_3) and chlorine (Cl) and sulphate (SO_4) are the most dominant ions. As indicated in the plot of Ca + Mg versus HCO_3 + SO_4 (fig.25) most of the water points fall close to the equiline. This reflects that most of the anions almost balance the alkali earth metals in the groundwater samples. In addition to that, the ion might have resulted from weathering of sulphate and carbonate's minerals (anhydrite or gypsum)(Singh, Rina, Singh, & Mukherjee, 2013). The ratio among Ca +Mg vs HCO_3 (fig.25) varies from 0.067 to 3.716. About 85% of the samples are below the equiline. This indicates that bicarbonates (HCO_3) were being added to the groundwater at a greater rate than Ca +Mg (Glover, Akiti, & Osae, 2012). The relationship between Na + K vs Ca +Mg is another method to determine the dominant source rock. As observed in the (Fig. 27) most of the water points plotted along 1:1 trend line. However, few samples plotted above and below the equiline indicating that although silicate and carbonate weathering to contribute ions to the groundwater carbonate weathering is more dominant than silicates weathering.

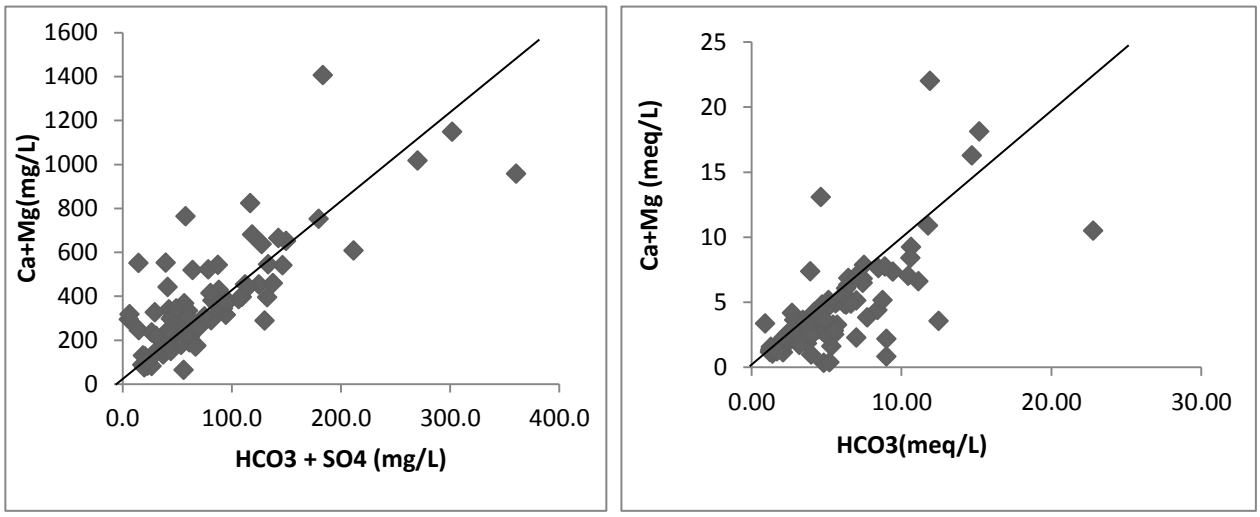

Figure 25: Scatter diagram of Ca + Mg vs HCO_3 + SO_4 and Ca +Mg vs HCO_3 at left side.

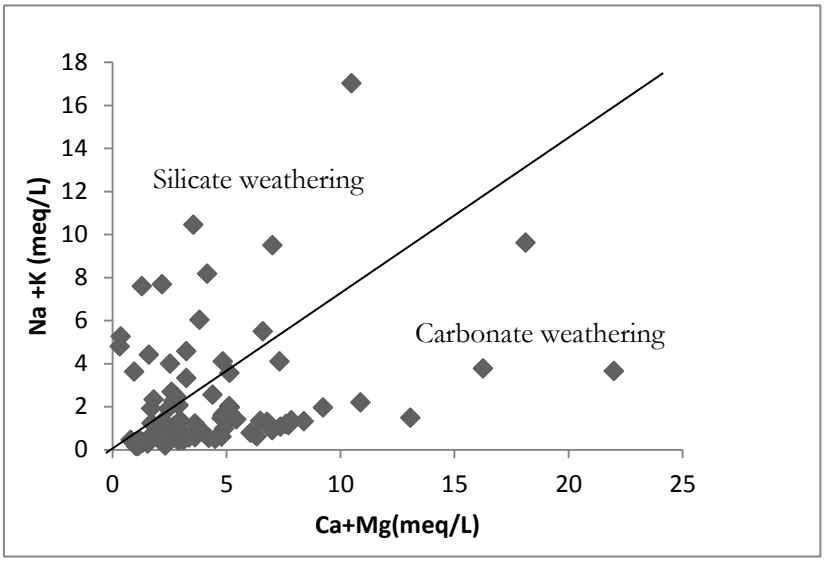

Figure 26: Relationship between Na + K vs Ca +Mg.

5.8. Geochemical Modelling

5.8.1. Equilibrium concentration of mineral species in the water solution and their saturation index

PHREEQC hydrochemical model was used to identify the equilibrium concentration of mineral species in the water solution and their saturation index. Using six water point's hydrochemical composition of groundwater the mineral's phases in the groundwater were identified. The groundwater samples were collected from three main sub-basins such as Megech, Ribb and Gumara. These samples can represent relatively the overall study area. The Initial solution calculation gave possible solid mineral phases and its saturation index, which indicated in table 18 below. And also the description of solution, distribution of species and solution composition were observed from calculation.

A Saturation Index shows whether the water will tend to precipitate or dissolve. It defined by

SI =log (IAP/KSP) where, Ksp = Equilibrium constant and IAP = Ion activity product

Saturation Index with zero values indicates that the water is just balanced or equilibrated. Positive value indicates that the water is over saturated this may build up scaling in the water pipes. The SI with the negative values indicates that the mineral phases in the water under saturation, this indicates that more minerals have to be dissolved. The water may form corrosive when react with metal fixtures or may increase metal content in water by deteriorating the pipes(Panthi, 2003). From the result, equilibrium of solutes with slight over saturated show towards Aragonite and Calcite. The rest mineral's phases show under saturation condition. Quartz, H_2, H_2O O_2 and, SiO_2 show very negative saturation index. These minerals and gases have to dissolve more to be saturated. The presence of carbon dioxide in the water shows an active organic (biodegradation) process. Many mineral phases expected in the groundwater as an example Aluminum and Iron bearing minerals. However, these minerals were not included in the analytical data.

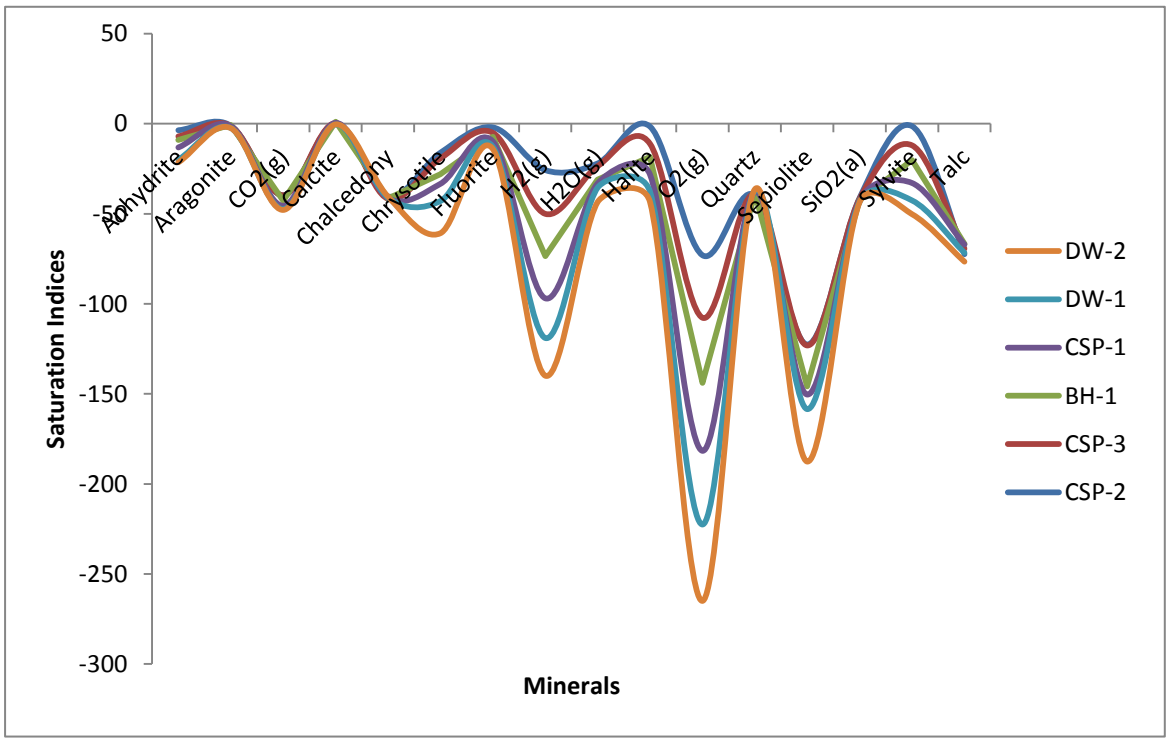

Figure 27: Solid mineral phase and their Saturation Index.

Table 18: Solid Mineral Phases and their Saturation Index in the water samples

Parameters	Molecular Formula	CSP-1	DW-1	Dw2	CSP3	BH-1
Anhydrite	$CaSO_4$	-4.05	-3.83	0.7	-3.41	-2.06
Aragonite	$CaCO_3$	-0.68	-1.42	2.23	-0.11	-0.12
Calcite	$CaCO_3$	-0.54	-1.28	2.38	0.03	0.02
Chalcedony	SiO_2	0.33	0.19	2.63	0.37	0.26
Chrysotile	$Mg_3Si2O5(OH)_4$	-4.35	-10.59	-2.47	-1.34	-5.96
$CO_2(g)$	CO_2	-2.71	-1.38	1.04	-3.12	-1.65
Fluorite	CaF_2	-2.62	-2.92	1.52	-2.98	-2.22
H2(g)	H_2	-23.41	-21.15	-20.95	-24.29	-22.05
H2O(g)	H_2O	-1.53	-1.55	-1.57	-1.5	-1.5
Halite	NaCl	-9.82	-9.45	-3.17	-9.58	-7.3
O2(g)	O_2	-36.81	-41.67	-42.1	-34.71	-39.19
Quartz	SiO_2	0.76	0.62	3.06	0.8	0.69
Sepiolite	$Mg_2Si3O_7.5OH:3H_2O$	-2.53	-6.88	2.56	-0.49	-3.76
SiO_2	SiO_2	-0.52	-0.66	1.78	-0.47	-0.58
Sylvite	KCl	-12.08	-9.7	-4.68	-9.74	-8.24
Talc	$Mg_3Si4O10(OH)_2$	-0.01	-6.54	6.47	3.1	-1.75

5.9. Equilibrium with pure phase

Equilibrium phase indicates the state of balance. It can be defined as the amounts of mineral assemblage that dissolved or precipitated in water when heated by a given temperature and second as a function of pressure. Pure mineral phase will precipitate or dissolve to achieve equilibrium in the aqueous solution. PHREEQC a computer program allows determining mineral conditions in the solution phases. In this study, the initial solid phase's concentration of each mineral phase was determined from the saturation index in table 18, and then it was used to calculate the equilibrium condition in solution phase to determine the thermodynamic stability and the solubility of the minerals. The used temperature for this calculation was ranging between 25 -75 Degree Celsius. Some minerals with less SI value were omitted for the calculation from each water sample. The result of equilibrium saturation indices presented below in table 19 and using user graphs (figure.28). It also includes initial and final mineral's concentration in mole. From saturation index results as indicated in table 19 and figure.28, except Calcite in the water sample CSP-3, the rest mineral's phases in all samples were not equilibrated over the temperature range. CSP-3 equilibrated or stabilized between the temperatures 60-75 Degree Celsius. Calcite, Aragonite and Fluorite in the sample DW-2 and CO_2 in DW-1 close to 0 as indicate in the plot, however, they not equilibrate completely. The plots also indicate the solubility of different minerals in each water sample. For example, Anhydrite, Aragonite, Chalcedony and SiO_2 are in the water sample CSp-3 precipitated or under saturated condition, but Quartz and Sepiolite over saturated.

As a second example, Calcite, Aragonite, Chalcedony and Quartz are over saturated in the water sample BH-1, the rest of the minerals were under saturated condition. Sepiolite is less soluble than the rest of the minerals in this sample. The rest sample's minerals were under saturated and over saturated condition.

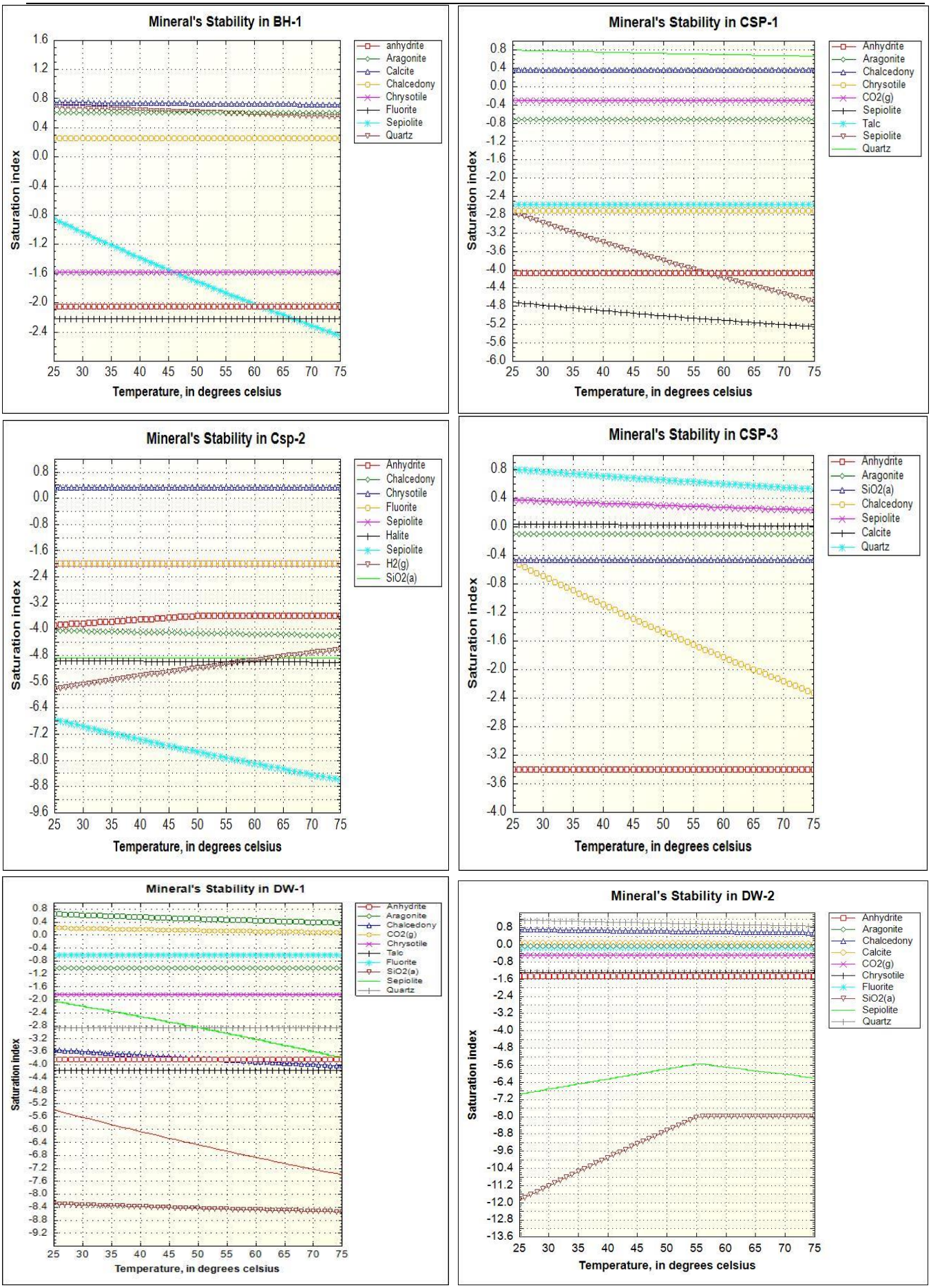

Figure 28: Saturation indices of the minerals in water that have equilibrated over the temperature range

Table 19: Saturation Indices and initial and final mineral concentration in various solutions

	CSP-2			CSP-3			BH-1			CSP-1			DW-1			DW-2		
Parameters	SI	Initial	Final	SI	Initial	Final	SI	Initial	Final	SI	Initial	Final	SI	Initial	Final	SI	Initial	Final
Anhydrite	-3.59	0.00	0.00	-3.41	0.00	0.00	-2.06	0.01	0.03	-4.08	0.00	0.00	-6.79	0.00	0.00	-1.48	0.03	0.10
Aragonite	-1.0	0.09	0.08	-0.11	0.78	1.85	0.60	3.98	9.47	-0.72	0.19	0.00	-1.02	0.10	0.23	-0.06	0.87	2.10
CO_2 (g)	-39.7	0.00	0.00	-3.72	0.00	0.00	-3.01	0.00	0.00	-2.82	0.00	0.00	-1.84	0.01	0.02	-0.48	0.33	0.35
Calcite	-	-	-	0.03	1.07	0.00	0.71	5.50	0.00	-0.58	0.26	0.45	-0.88	0.13	0.00	0.05	1.23	0.00
Chalcedony	-40.3	0.12	0.00	0.22	2.34	0.00	0.10	1.78	0.00	0.34	2.29	0.00	0.21	1.66	0.00	0.56	5.25	0.00
Chrysotile	-16.1	2.04	0.00	-8.63	0.05	0.00	-8.9	0.03	0.00	-5.27	0.00	0.00	-9.57	0.00	0.00	-17.9	0.00	0.00
Fluorite	-2.0	0.01	0.01	-2.98	0.00	0.00	-2.2	0.01	0.01	-2.59	0.00	0.00	-2.88	0.00	0.00	-1.28	0.05	0.05
H_2(g)	-25.7	0.00	0.00	-24.3	0.00	56.5	-23.5	0.00	56.0	-23.4	0.00	55.5	-22.1	0.00	55.5	-20.9	0.00	55.7
H_2O(g)	-22.	0.00	28.55	-7.5	0.03	0.00	-7.7	0.03	0.00	-2.10	0.03	0.00	-2.36	0.02	0.00	-7.97	0.03	0.00
Halite	-1.55	0.03	0.02	-9.6	0.00	0.00	-7.3	0.00	0.00	-9.8	0.00	0.00	-9.44	0.00	0.00	-5.79	0.00	0.01
Quartz	-39.9	0.00	21.07	0.5	6.31	0.00	0.4	4.79	0.00	0.77	6.31	0.00	0.64	4.68	0.00	0.86	14.1	0.00
Sepiolite	-122.6	5.62	0.00	-22.5	0.32	0.00	-22.8	0.14	0.00	-4.4	0.00	0.00	-8.09	0.00	0.00	-29.1	0.00	0.00
SiO2	-41.14	0.00	0.00	-0.5	0.34	9.01	-0.6	0.26	6.83	-0.50	0.32	8.92	-0.63	0.23	6.57	-0.13	0.74	20.12
Sylvite	-1.32	0.30	0.00	-10.7	0.00	0.00	-8.3	0.00	0.00	-12.7	0.00	0.00	-9.68	0.00	0.00	-7.64	0.00	0.00
Talc	-72.44	0.00	0.00	3.10	1259	1259	2.62	416.9	417	-0.30	0.50	0.50	-4.60	0.00	0.00	-4.94	0.00	0.00

5.10. Inverse Geochemical Modeling with Evaporation

Inverse geochemical modelling is one of the capabilities of PHREEQC model, which is used to determine the groundwater chemical evolution along the flow path (Federico et al., 2008). It attempted to determine sets of mole transfers of phases that account for changes in water chemistry between one or a mixture of initial waters and a final water(D. L. Parkhurst & Appelo, 2013). The mole of low mineralized water in the initial solution changes due to water gained or lost by precipitation, dissolution and through redox reaction, and it must be equal to the mole of water in the final solution or highly mineralized water during chemical evolution along the flow path. According to Parkhurst & Appelo, (1999) including phases of the composition water (H_2O), is necessary to model evaporation or dilution. The initial and final solutions were selected for six water chemistry data. The selection was made for this study based on a logical assumption that the solution relatively high TDS value considered as the discharge area and solution with less TDS value considered as recharge area. The most difficult part in inverse modeling is a selection the composition and identifies the reactive phase. The selection made for the most suitable reactant phases which are existed in the host rocks (volcanic rocks) in the study area. In addition, some mineral phases were taken from the equilibrium concentration of mineral species and their saturation index. For the study area, three flow paths were selected for inverse modeling.

Table 20: Hydrochemical composition of groundwater points for inverse modelling

Water points		Na^+	K^+	Ca^{2+}	Mg^{2+}	HCO_3^-	Cl^-	F^-	SO_4^{-2}	NO_3^-	SiO_2^{+2}	pH	TDS
CSP-3	Initial	3.6	0.9	19.4	4.6	85	2.5	0.17	7	10.2	40.2	8.12	114.6
BH-1	Final	15.7	0.7	148.4	36.1	200.5	122.7	0.19	44.6	66.5	30.4	7.73	801.3
CSP-1	Initial	5	0.01	15	4	78	1	0.28	2	0.4	35	7.68	95.81
DW-1	Final	2.36	0.47	25.2	8.95	127	5.2	0.16	2.36	18.6	24.6	6.55	163.5
CSP-2	Initial	4.9	0.13	23.1	7.6	109.8	0.43	0.1	4.3	9.7	32.96	7.23	143.4
DW-2	Final	220	1.6	211.3	90.6	927.2	319.2	0.58	220.6	64.79	80	6.45	1601.3

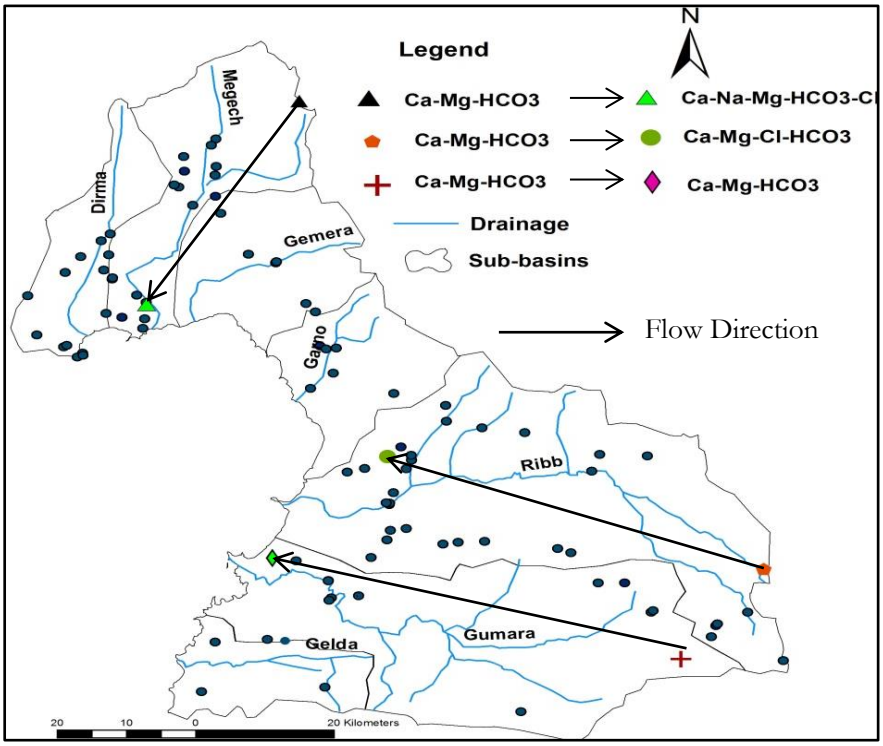

Figure 29: Flow paths for inverse geochemical modeling.

5.10.1. Inverse Modelling One

The first inverse modeling was conducted between Kidane Mhiret spring (CSP-2) which located plateau zone in Megech river basin in North Gonder and (DW-2) which located lower of Megech basin. CSP-2 has TDS value 143.4 mg/L with weathered and fractured upper basalt aquifer and Ca-Mg-HCO3 water types. It was used as the initial solution in the modeling. DW-2 dug well has TDS value 1601.3 mg/L with lacustrine sediment aquifer, and Ca-Na-Mg-HCO3-Cl water type taken as the final solution in the modeling. 0.9 uncertainty limit for initial solution and 1.2 was used for the final modelling.

Table 21: Result of inverse modelling flow path one

	Solution fractions	Minimum	Maximum	
Solution 1	5.81E+00	9.82E-01	1.28E+02	
Solution 2	1.00E+00	1.00E+00	1.00E+00	
Phase	Mole transfers	Minimum	Maximum	Molecular Formula
$CO_2(g)$	1.51E-02	0.00E+00	1.78E-01	CO_2
$H_2O(g)$	-2.68E+02	-1.00E+03	0.00E+00	H_2O
Ca-Montmorillon	-9.31E-06	-3.86E-05	0.00E+00	$Ca0.165Al2.33Si3.67O10(OH)_2$
K-feldspar	-6.18E-04	-2.73E-03	8.99E-05	$KAlSi_3O_8$
Biotite	6.40E-04	0.00E+00	2.73E-03	$KMg3AlSi3O10(OH)_2$
Calcite	1.93E-03	-1.40E-01	1.16E-02	$CaCO_3$
Quartz	-1.90E-02	-1.71E-01	0.00E+00	SiO_2
Kaolinite	-9.69E-03	-2.51E-02	0.00E+00	$Al2Si2O5(OH)_4$
K-feldspar	2.17E-05	-8.08E-04	8.99E-05	$KAlSi3O_8$
Illite	6.06E-05	0.00E+00	1.50E-04	K0.6Mg0.25Al2.3Si3.5O10(OH)2
Plagioclase	1.35E-02	0.00E+00	3.40E-02	$Na0.62Ca0.38Al1.38Si2.62O_8$
Chlorite	3.84E-04	-1.52E-02	1.64E-03	$Mg5Al2Si3O10(OH)_8$
Chalcedony	-1.88E-02	-1.71E-01	0.00E+00	SiO_2
$H_2(g)$	3.78E+01	0.00E+00	5.65E+01	H_2
$O_2(g)$	1.89E+01	0.00E+00	2.83E+01	O_2

The model result indicates that the optimized transfer in CSP-2 (solution 1) was concentrated 5.81-fold to produce solution 2, Therefore, approximately 5.81 kg of water in solution 1 is reduced to 1 kg of water in solution 2 as shown by a solution fraction above in Table 21. The mole transfer with positive value shows that dilution is simulated and negative values indicate precipitation of minerals or evaporation is simulated. The main hydrochemical process occurred along the flow path are dissolving of carbon dioxide H_2, O_2, Biotite , K-feldspar, Gypsum, Plagioclase, Illite and Chlorite. In addition to that, Evaporation (loss of water (H_2O) 268 mole or 4.824kg) and precipitation of the rest mineral's phases with negative values are the main processes occurred during the chemical evolution. Small amounts of dissolution of Illite and precipitation of Ca-Montmorillon and K-feldspar are required in the models.

5.10.2. Inverse Modelling Two

The second inverse modeling was conducted between Dobo/farta spring (CSP-3) which located plateau zone in Ribb river basin and Shehoch, South Gonder (BH-1) which located lower of Ribb basin. CSP-3 has TDS value 114.57 mg/L with weathered and fractured upper basalt aquifer and Ca-Mg-HCO_3 water types. It was used as the initial solution in the modeling. BH-1 borehole well has TDS value 801.32 mg/L and lacustrine deposit and gravel deposit aquifer with Ca-Mg-Cl-HCO_3 water type taken as the final solution in the modeling. The uncertainty limits 0.65 for initial solution and 1.25 for final solution were used for the modelling.

Table 22: Result of inverse modelling flow path two.

	Solution fractions	Minimum	Maximum	
Solution 1	1.12E+00	1.00E+00	7.19E+00	
Solution 2	1.00E+00	1.00E+00	1.00E+00	
Phase	Mole transfes	Minimum	Maximum	Molecular Formula
$CO_2(g)$	2.10E-03	0.00E+00	1.05E-02	CO_2
Kaolinite	-5.59E-03	-3.22E+02	0.00E+00	Al2Si2O5(OH)4
Illite	4.72E+01	0.00E+00	8.86E-03	$K0.6Mg0.25Al2.3Si3.5O10(OH)_2$
K-mica	-3.19E+01	-5.29E-03	0.00E+00	$KAl_3Si_3O10(OH)_2$
Chalcedony	-2.24E-04	-7.90E-03	0.00E+00	SiO2
Biotite	5.52E-04	0.00E+00	1.77E-03	KMg3AlSi3O10(OH)2
Chlorite	-4.52E+00	-9.64E-04	6.55E-04	$Mg5Al2Si_3O10(OH)_8$
Quartz	-4.14E-02	-9.14E-02	0.00E+00	SiO_2
Calcite	1.01E-04	-1.82E-03	4.54E-03	$CaCO_3$
Ca-Montmorillon	-1.62E-02	-6.82E-03	0.00E+00	$Ca0.165Al2.33Si3.67O10(OH)_2$
H_2O	-6.55E+00	-3.44E+02	0.00E+00	H_2O
K-feldspar	-1.12E+01	-5.87E+02	-2.02E-02	$KAlSi3O_8$
$H_2(g)$	9.36E-02	0.00E+00	1.00E+03	H_2
$O_2(g)$	4.68E-02	0.00E+00	1.00E+03	O_2
Fluorite	5.287e-07	0.000e+00	9.698e-06	CaF2
Plagioclase	8.20E-04	0.00E+00	2.39E-03	$Na0.62Ca0.38Al1.38Si2.62O_8$
Chrysotile	4.247e-04	-7.482e-04	1.092e-03	$Mg3Si2O5(OH)_4$

The model result indicates that CSP-3 (solution 1) was concentrated 1.12 -fold to produce solution 2. Therefore, approximately 1.12 kg of water in BH-1 is reduced to one kg of water in solution 2 as shown by the solution fraction above in Table 22. The mole transfer with positive value shows that dilution is simulated and negative values indicate evaporation. As indicated in the table dissolution of H_2, O_2, CO_2, Illlite, Biotite, Calcite Fluorite, Plagioclase and Chrysotile occurred along the flow path. The rest mineral's phases with negative values were precipitated. In addition to that, 6.55 mole or 0.1179 kg of water was evaporated. Plagioclase, Chrysotile and Fluorite are required in small amounts for dissolution and Chalcedony and Biotite precipitated in fewer amounts in the model.

5.10.3. Inverse Modelling Three

The second inverse geochemical modeling was conducted between Konga spring (CSP-1) from the recharge zone in Gumara River basin, and Waktra-01or Fogera dug well (DW-1) in lower of Gumara basin. Konga spring (CSP-1) has TDS value 95. 81mg/l and Ca-Mg-HCO_3 water type. It has a weathered and fractured basalt aquifer, taken as an initial solution in the modeling. DW-1is dug well located in lower of the Megech basin with quaternary lacustrine sediment's aquifer. It has TDS value 163.48mg/l, and Ca-Mg-HCO_3, water type. It was used as a final solution in the modeling. The uncertainty limit of the initial solution was 0.8 and final solution 1.2 for the modelling.

Table 23: Result of inverse modelling flow path three.

	Solution fractions	Minimum	Maximum	
Solution 1	5.72E-01	7.39E-10	1.00E+00	
Solution 2	1.00E+00	1.00E+00	1.00E+00	
Phase	Mole transfers	Minimum	Maximum	Molecular Formula
CO_2(g)	3.43E-03	0.00E+00	9.22E-03	CO_2
Fluorite	7.33E-07	0.00E+00	9.27E-06	CaF_2
H_2O(g)	2.93E+01	0.00E+00	5.55E+01	H_2O
Illite	5.81E-05	-6.64E-04	5.30E-04	$KMgAl2.3SiO10(OH)_2$
K-mica	-5.54E-05	-4.51E-04	5.51E-04	$KAl_3Si_3O10(OH)_2$
K-feldspar	-5.96E-05	-4.65E-04	1.61E-04	$KAlSi3O_8$
Biotite	9.20E-05	0.00E+00	3.14E-04	$K0.6Mg0.253Al2.5Si3.5O10(OH)_2$
Kaolinite	-3.15E-04	-1.00E+03	0.00E+00	$Al_2Si_2O5(OH)_4$
Chlorite	4.02E-05	-1.00E+03	2.07E-04	$Mg_5Al_2Si3O10(OH)_8$
Chalcedony	-1.02E-06	-1.26E-03	0.00E+00	SiO_2
Plagioclase	1.56E-05	0.00E+00	3.00E-04	$Na0.62Ca0.38Al1.38Si2.62O_8$
H_2(g)	3.558e-03	0.000e+00	5.552e+01	H_2
O_2(g)	1.779e-03	0.000e+00	2.776e+01	O_2
Ca-Montmorillon	-4.804e-04	-4.433e-03	0.000e+00	$Ca0.165Al2.33Si3.67O10(OH)_2$

The model result indicates that solution 1 was concentrated 0.572-fold to produce solution 2. Therefore, approximately 0.572 kg of water in solution 1 is added to 1 kg water in solution 2. As indicated in model 1 and 2 the mole transfer with positive value shows that dilution is simulated and the negative value indicates precipitation or evaporation. The main hydrochemical processes occurred along the flow path are precipitation of K-mica, K-feldspar, Ca-Montmorillon, Kaolinite and Chalcedony dissolution of H_2O, H_2, O_2 and CO_2 and dissolution of the rest of the minerals with positive value. As indicated in table above, 5.81E-05 moles of Illite, 9.20E-05 mole of Biotite, 4.02E-05 mole of Chlorite and also the rest mineral's phase with the positive values were dissolved along the flow direction.

In general, the dissolution and loss (evaporation) of water (H_2O), dissolution of H_2, O_2 and CO_2 and dissolution and precipitation of different mineral phases are main the hydrochemical process that occurred during groundwater evolution along the flow path. A small amount of Gypsum dissolution is required in the model.

5.11. Isotopic signature

5.11.1. Identifying Groundwater Recharge using Environmental Stable Isotopes

The use of isotope method is widely accepted technique among many hydrogeological professionals. Since several decades, the stable isotopes of hydrogen and oxygen have been applied for water resource's investigation. The technique was used to determine the origin, dynamic and groundwater interaction with surface and the atmosphere (Mook, 2000). The stable isotopes of (**δ**2H) and oxygen (**δ**18O) were used in this study. The isotopic concentration of water is expressed in comparison with the isotopic concentration of mean oceanic water (SMOW) and expressed in per mil (%0). The deviation of deuterium (**δ**2H) and oxygen (**δ**18O) expressing in the following way:

$$\boldsymbol{\delta}^{2}H\%_{0} = \frac{(^{2}H/^{1}H)\ \text{sample} - (^{2}H\text{-}^{1}H)}{(^{2}H/^{1}H)SMOW}$$

Where; $\boldsymbol{\delta}^{2}H\%_{0}$ = Deuterium in per mil, ^{1}H - hydrogen

Similarly for deviation of $\boldsymbol{\delta}^{18}O$;

$$\boldsymbol{\delta}^{18}O\%_{0} = \frac{(^{18}O/^{16}O)\ \text{sample} - (^{18}O/^{16}O)\ SMOW\ X\ 1000}{(^{18}O/^{16}O)SMOW}$$

Where; $\boldsymbol{\delta}^{18}O\%_{0}$ = Oxygen 18 in per mil and ^{16}O = Oxygen 16,

Isotope's fractionations represent variability of isotope's abundance in the aqua system. Isotopes separate into light and heavy fractions due to the geological process, evaporation, diffusion, condensation and heating. Much amount water vapor evaporate from oceanic region which causes most abundant isotopically light water molecules such as ^{1}H and ^{16}O to evaporates much higher than the remaining behind ^{2}H and ^{18}O C.W.FETTER, (1994). Water vapor in the atmosphere gradually becomes cooler to precipitate. Isotopically heavy isotopes (^{2}H and ^{18}O) rainfalls precipitate more rapidly than ^{1}H and ^{16}O. Isotopically positive values show enrichment of samples with ^{2}H and ^{18}O compared to SMOW and negative values indicate depletion.

The isotopes of water point's data for this study were used from secondary data and local meteoric water line (LMWL), which is represented by δD = 7.61 δ18O+13.72 equations, downloaded from the International Atomic Energy Agency (IAEA) web page. A total of 45 water points isotopes data were used such as 16 Boreholes, 18 Dug wells, 4 springs, 5 Rivers samples, 1 flood water sample and 1 Lake Tana water sample. Monthly precipitation isotopes data the year of 2002 obtained from three stations from IAEA website, such as Kombolcha, Woldiya and Kobo, which are located approximately 150-200 km from the study area. When LMWL comparing with Global Meteoric Water Line (GMWL, which represented by δD = 8δ18O+10 equation), the relation shows that most of LMWL fall above GMWL (Fig.30). High D-Excess observed in Ethiopian rainfall isotope comparing to GMWL. This means in practical term, the source of Ethiopian precipitation from Atlantic and Indian Ocean.

In general, precipitation isotopes show different values due to seasonal variation comparing to GMWL. For example, from the plot during spring the rainfall enriched in δ18O, however, during the winter season shows depletion.

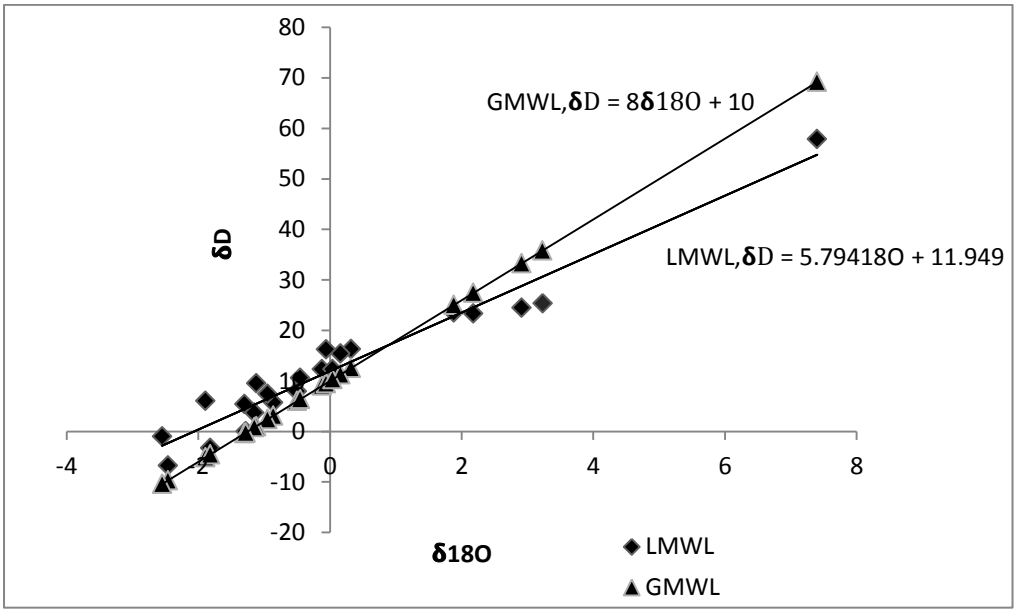

Figure 30: Plot of isotope signature of rainfall (LMWL versus GMWL).

The ^{2}H versus ^{18}O plot of different water sources in the study area revealed certain trends. It can be categorized into three water groups. Group A water types such as Lake Tana, Angoribit flood water (G-FW1) and Yifag Dikule (G-BH7) deep well showing both oxygen-18 and Deuterium enrichment. Especially one borehole at Yifag (G-BH7) is highly enriched by both oxygen-18 and Deuterium; this sample might be influenced by evaporation before percolating to the groundwater. Lake Tana as indicated on the plot recharged directly from precipitation. However, there is no groundwater point mixed with the Lake Tana.

Group B water types include boreholes, dug wells and springs and they are similar to precipitation and river water isotopic signature. This indicates the origin of the groundwater mainly from local rainwater or it might be recharged from river water during different seasons.

Group C water types such as Serbia Mariam spring, Gassy well; Debretabore (G-BH6) and Woreta (G-BH1) are highly depleted waters and have oxygen-18 less than -4 ‰ and Deuterium less than -20 ‰. The low D-excess is an indication of cold climate isotopic signal. Low isotopic signature in this group probably due to the cooler climate during recharge from high altitude or the water point's subjected to secondary evaporation prior to infiltration at the surface.

According to Mazor, (1991)the other reason can be that the water points originated from ancient water which existed in different climate regime or due to isotopic exchange with aquifer.

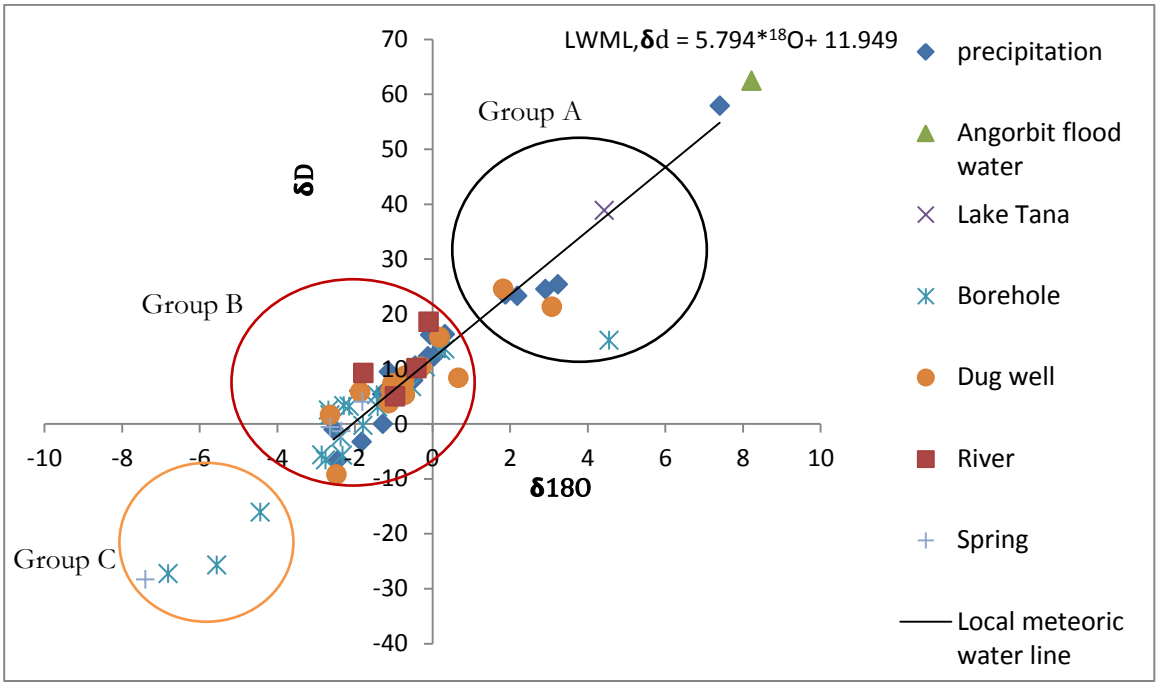

Figure 31: Isotopes of Oxygen-18 versus Deuterium of different water points

In short, it can be concluded that, except Yifag Dikule (G-BH7) well in Group A, the rest water points directly recharged from rainfall. Group B water points show a close correlation with the LWML. This indicates that the rainfall is the primary source of the rivers, boreholes, springs and dug wells. These Boreholes dug wells and springs might be interaction with the rivers in different seasons. Group C water points highly depleted water points; this might be due to isotopic exchange with aquifer or the water points originated from ancient water in different climate regime. Lake Tana water enriched by both oxygen-18 and Deuterium and it has a close correlation with LWML, thus indicating that the Lake directly recharged from rainfall. However, as indicated in the plot there is no interaction between groundwater points and Lake Tana.

Megech River has a mixed relationship with Borehole G-BH12 which located in Gonder, Adisgei Jara hand-dug well (G-DW16), Robit (T-DW 20), Acher Hana Mariam (G-DW16) and Robit school hand-dug well (G-DW 18). These groundwater points are enriched by both oxygen-18 and Deuterium and close to the river. Borehole (G-BH11) is more enriched by both oxygen-18 and Deuterium than Megech River. This borehole might be recharged from Andreb Dam, which located in Gonder. Water points on the Northern side of Rib basin highly depleted. These boreholes located around Debretoabore, Addis Zemen, Gassy well and Woreta. The boreholes might have been recharged by local rains.

Angrobit flood water located on the flat plain in Gumara river basin. It is highly enriched by both oxygen-18 and Deuterium; however, there is no correlation with Gumara and Ribb Rivers with groundwater. Generally, except Megech River basin there is no correlation with others surface water and groundwater points nearby.

According to Mebush Geyh, (2000), a plot of **δ**18O/Cl- used to detect highly mineralized groundwater, the source of salinization of brackish and thermal water and also the processes of leaching of salt, dissolution and mixing of fresh water with saline water and influence of evaporation can be identified. The isotope plot of **δ**18O versus chlorine indicates that water samples such as Lake Tana, Angoribit flood water and Yifag dikule deep well affected by evaporation process. These samples evaporation effect clearly observed on the plot of Deuterium versus oxygen -18(Fig.31).

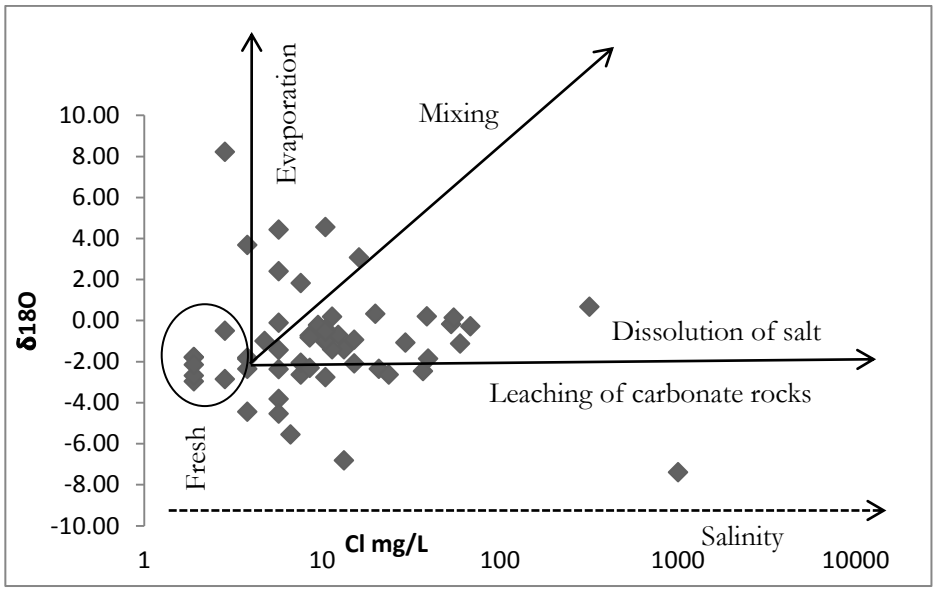

Figure 32: **δ** 18 O versus Cl mg/L for the identification of different salinization process

Water samples located in Tach chanqua (G-BH 14), Wonfera (G-BH 15) and Robit School (G-DW18) and Gura (T-DW35) hand dug wells occurring in the mixing zone

The leaching process or extracting minerals from a solid by dissolving them in a liquid observed in the Serbamariam spring (G-SP3) which associated with carbonate rocks.

Freshwater with low Cl (1.96 mg/L) concentration and low isotope signatures are observed in Gumara River, Hamusit (G-BH2) and Char Char dug well. According to Zenaw, (2009) shallow wells in the lower of Megech and Ribb sub-basins are subjected to evaporation process. The evaporation influence clearly confirmed in the plot of Oxygen-18 versus Deuterium in the water samples Yifag Dikule (G-BH7) deep well, Lake Tana, Angorbit, flood water, Ribb River, Robit School hand-dug well (G-DW 18). For example, Robit village school (G-DW18) hand dug well has 319. 2mg/L chloride content associated to dissolution of salt through the process of evaporation and leads to a development of groundwater salinity.

Another method which used to determine the influence of evaporation is Gibbs diagram. It also helps to determine the rock-water interaction and atmospheric precipitation. It represented by a simple plot of TDS versus a weight ratio of Cl/ (Cl +HCO_3) and Na +K/ (Na +K+Ca). All the cations and anions are expressed in millequivalents per liter. The result shows that the majority of the groundwater sample's weight ratio of Cl/ (Cl +HCO_3) and Na +K/ (Na +K+Ca) falls on the rock-water interaction and the remaining samples fall towards evaporation-dominance and precipitation. These suggest that the rock forming minerals and some extent evaporation and precipitation were the dominant factors that influencing the groundwater chemistry. Dug wells located lower on Megech and Ribb River basins such as Serba (G-DW17) Robit Village School (G-DW18), Guramba (G-DW13) and Shena Tsion (T-DW23) were highly influenced by evaporation process. Gibbs plot clearly shows the influence of evaporation in these

wells. For example, Robit village school (G-DW18) hand dug well has EC 2490 μS/cm and TDS 1398 mg/L (in Gibbs diagram) indicates the process of evaporation leads to a development of groundwater salinity.

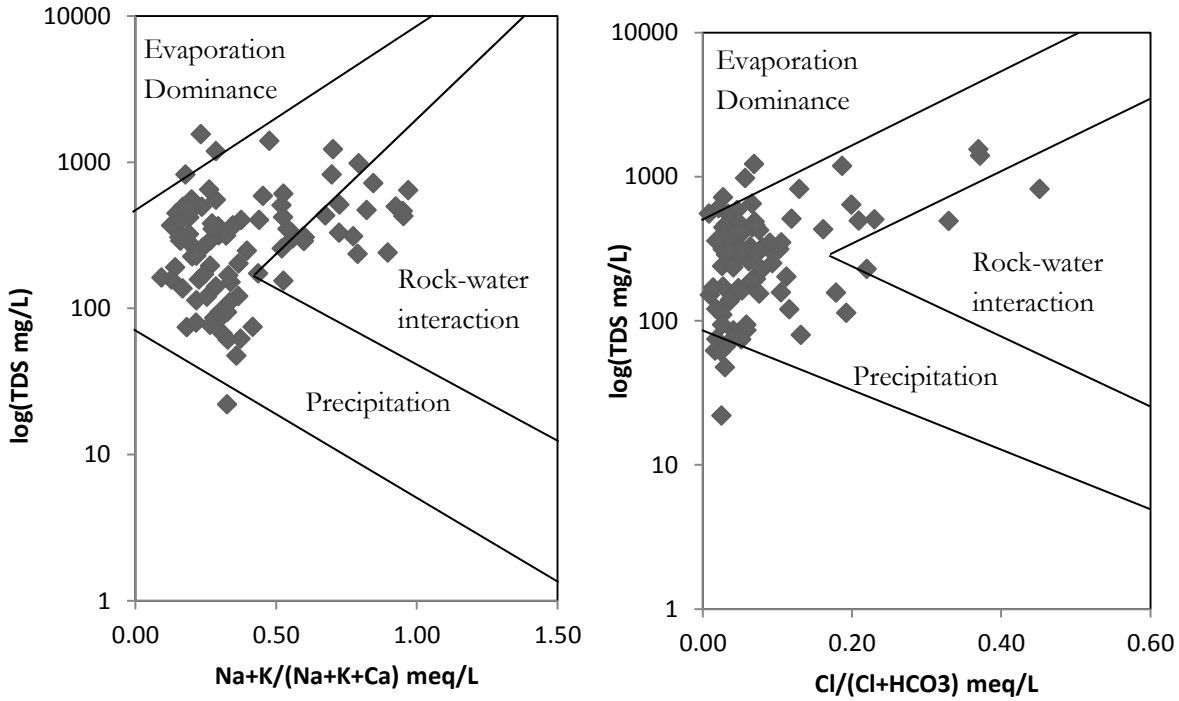

Figure 33: Groundwater chemistry controlling mechanism.

5.12. Dating Groundwater with Tritium (^3H)

Tritium is one of the trace elements used to determine the water age. It occurs in the waters of the hydrological cycle which arises from both man-made and natural sources. Cosmic- ray interaction in the atmosphere produces ^3H naturally. The radioactive hydrogen isotope (^3H) has a half-life of 12.43 years. In 1952, the initial tritium content test in the atmosphere ranges from 2-8 TU (Tritium Unit), this concentration produced by cosmic ray spallation. The composition of ^3H in water samples has been used in relative dating assuming that much of the ^3H entered into the hydrologic cycle after the year 1953 bombing, (R.Allan Freeze, Johan.A.Cherry,1979)..

A total of 33 secondary data of ^3H was collected from different sources to supplement the hydrogeochemical characterization of aquifer systems in the study area. Based on the guidelines which provided by (Ian D. Clark, Petter Frtiz, 1997)and assuming that piston flow system (no mixing or dispersion) is applicable the tritium concentration in the Tana basin categorized as:

I. The measured water tritium content of less than 0.8 TU is considered as pre-1952.
II. Water with the tritium content of 0.8-4TU is categorized as mixed water (components of pre and post-1952).
III. Water with tritium value ranged from 5-15TU may indicate recharge after 1987
IV. Water samples with tritium concentration 16-30TU are recharged since 1952 but no specific time for recharge.
V. Water to tritium values more than 30TU might be recharged in the year 1960s or 1970s.

Accordingly, based on the tritium content of different groundwater points in the study area, they might be recharged prior to 1952, before and after 1952 and recharged after 1987.

Table 24: Some of the tritium data for the study area

Site name	Type	X	Y	3H (TU)	Well depth (m)
Gorgora town supply/Kes Mender	borehole	312606	1355049	0.5	121
Dashen brewery /Lashka	borehole	328564	1383745	0.52	301
Arb gebeya town supply	borehole	363781	1285984	1.65	95.6
Debretabore town supply/Gafat	borehole	396407	1313342	0.51	109
Gassay town supply	borehole	407117	1304322	0.37	42
Addis Zemen town supply	borehole	367852	1341230	3.43	137
Robit Medihanealem tsebel	dug well	324540	1362647	0.92	10
Woreta town supply/Jicaa	borehole	359326	1319721	0.63	76

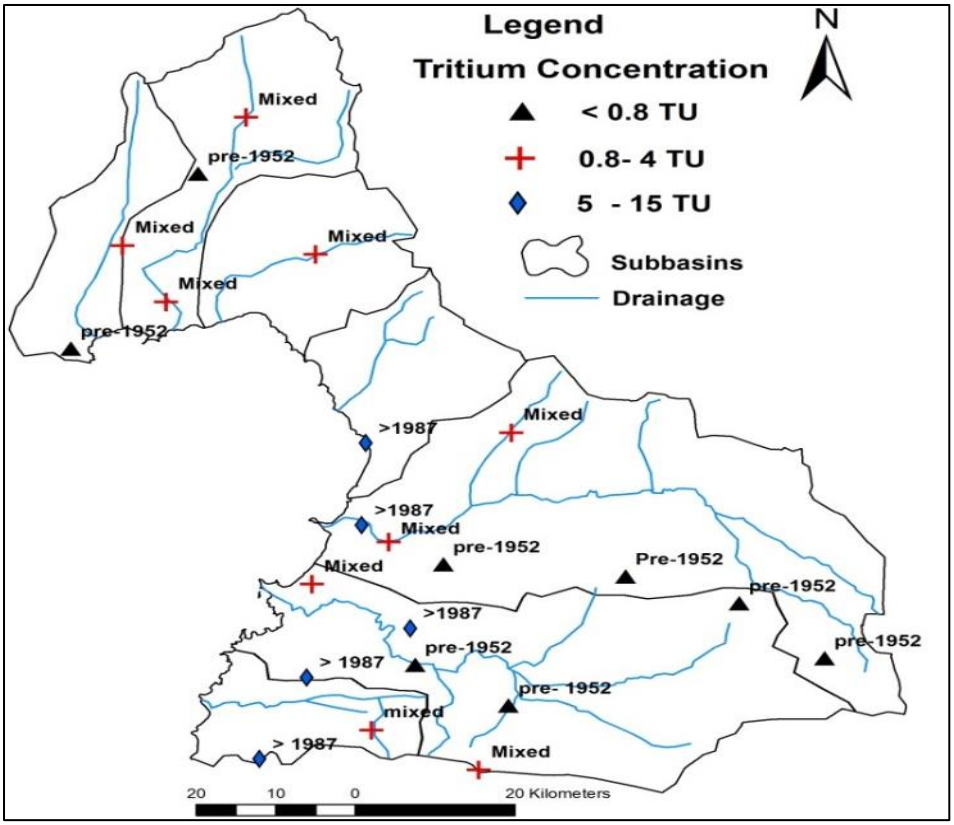

Figure 34: Groundwater ages determined from tritium data.

The lower tritium concentration (<0.8 TU) exhibited in Gorgora, Debretabore and Gassay towns water supply boreholes, Dashen brewery, spring of Serbamariam, Guramba Kidanemhiret and hot springs in wanzaye. These groundwater points might be recharged prior to 1952. Town water supply boreholes with tritium concentration (0.8-4 TU) are located in Maksegniet, Arbgebeya, Anbaseme, Addis Zemen, Koladiba and Angereb and dug wells in Wagtera School, Shaga/Gguaya and Robit dug wells. The tritium concentration of these boreholes suggested that mixed water classes or recharged before and after 1952. Groundwater samples with the tritium concentration ranges from 5-15 TU were collected from Zenzelma and Hamusit town's boreholes, Ager Kirigna Mariam and Rike dug wells and cold spring in Tanku Gerbriel/Medenhaleam tsebel. These groundwater samples must have recharged after about 1987.

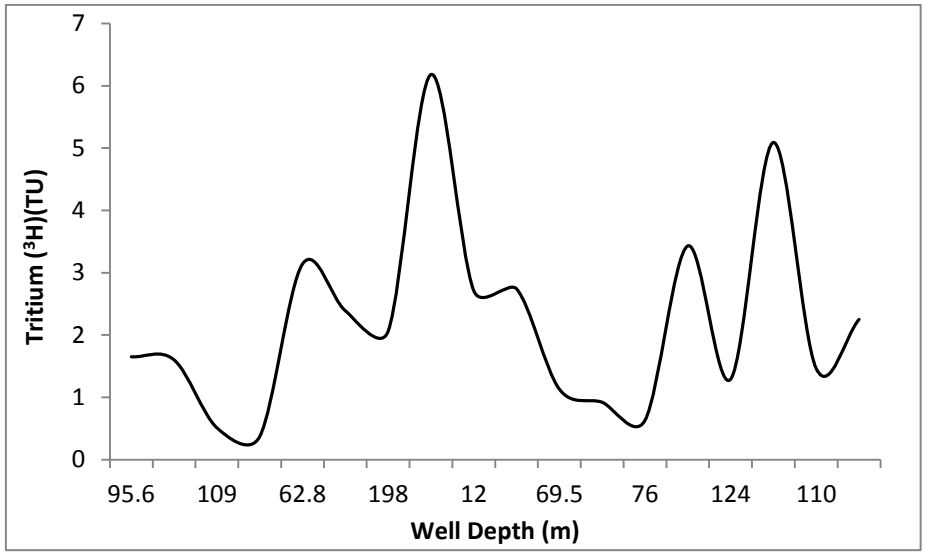

Figure 35: Plot of Tritium data and well depth for boreholes, dug wells and spring in the study area.

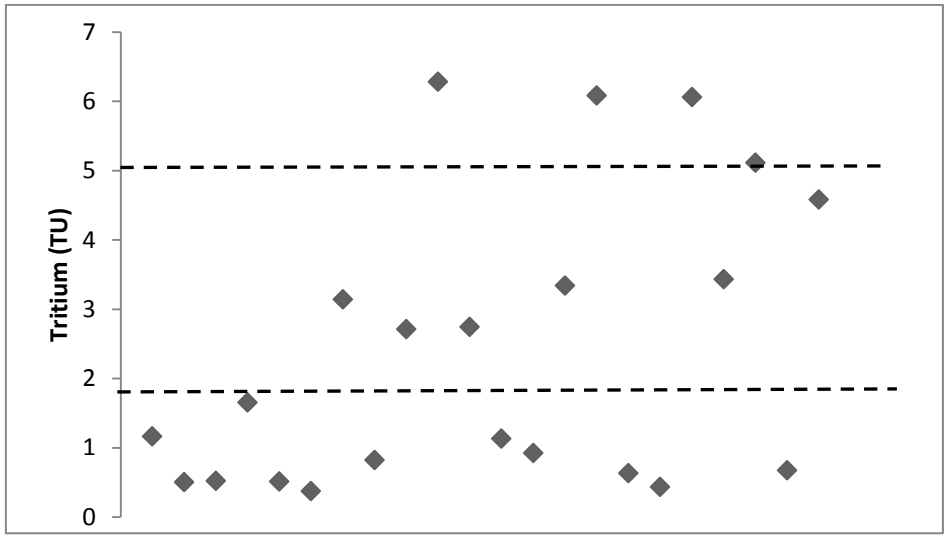

Figure 36: Plot of tritium data of 22 water points in the study area, the categories from Clark and Fritz (1997).

6. CONCLUSION AND RECOMMENDATION

The groundwater in the study area is mainly influenced by the occurrence of basic and acidic volcanic rocks, combined with the effect of major tectonic structures, the geomorphological setup and soil type as well as agricultural and anthropogenic effects. Based on the results and findings the following concluding remarks and recommendations can be made.

6.1. Summary and conclusions

- Shallow groundwater plays an important role as water supply source of drinking, irrigation and livestock development. Most of private owned wells are used for irrigation whereas community owned wells are used for drinking water purpose. The drinking water quality problems were identified by using Deininger for the National Sanitation Foundation (1975) water quality index (WQI). The computed WQI out of 81 groundwater samples excluding surface water, 59 samples represent "Excellent"(72.25%), 12 samples shows "Good water" (13.75%) , three boreholes and two dug wells indicate "Poor water"(5%), 2 dug wells represent "Very poor" (2.5%) and the rest 3 dug wells show "Unfit for drinking purpose"(3.75%).

- Different irrigation water quality constraints were examined and the result indicates that all surface water shows moderate to excellent water quality for irrigation purpose. However, some wells, particularly in the lower of Megech River basin have a high salinity and are not suitable for irrigation. The permeability index (PI) calculation of these wells also indicated their unsuitability.

- Volcanic glass and ferromagnesian were presented minerals from the source rock deduction analysis. In addition to that, weathering processes such as silicate weathering, limestone-dolomite weathering, and plagioclase and carbonate weathering or brine halite-albite and ion exchange were observed from the source rocks deduction analysis.

- The groundwater quality in the study area is mainly influenced by dissolution of salt through the process of evaporation leaching of carbonate rocks, but also agricultural activities such as improper use of fertilizer and pesticide and other anthropogenic effects. Three example as proof (a) High saline shallow wells as revealed by the isotope plot of δ18O versus chlorine (fig.32) the result of from dissolution of salt and leaching of carbonate rocks. (b) The inverse geochemical modelling and the Gibbs plot (fig.33) revealed that evaporation is one the factor that controls the ground water. (c) The high concentration of nitrate in boreholes in Gonder town and lower of the Megech river basin, which are clear indications of the anthropogenic creation pollution and the leaching of fertilizer effect respectively.

- The Aquachem package version 2014.1 was used to classify different water types. In this classification fifteen major chemical facies were identified from the Piper diagram. The number of water types has increased compared to previous studies which resulted from different hydrogeochemical processes or due to interactions between natural environments. Multi cation's water types such as Ca-Mg-HCO_3-NO_3-Cl, Ca-Mg-HCO_3-NO_3 and Ca-Na-Mg-HCO_3-SO_4 are distinct water types with high electrical conductivity. The most dominant hydrochemical types are Ca-Mg-HCO_3, Na-Ca –HCO_3, Ca-HCO_3, Ca-Na-HCO_3, Ca-Mg-Na-HCO_3 and Na-HCO_3 in the

study area. Carbonate weathering and silicate minerals contribute ions to the groundwater. Most dominant ions are Ca^{+2}, Mg^{+2}, Na^{+}, HCO_3^{-}, Cl, SO_4^{-2}, NO_3^{-} and with low-level K^{+},F^{-}, NO_2^{-}, PO_4^{-2}, Fe^{+2} and NH_4^{+}.

- A hierarchical cluster classification elaborately classified the groundwater into three main groups and five subgroups. Among the subgroups, one group GIV is an exceptional group. It contains water samples with high salinity and nitrate concentration (64-128 mg/L). Ca-Mg-SO_4-HCO_3-Cl, Ca-Na-Mg-HCO_3-Cl, Na-Ca-HCO_3, Ca-Mg-HCO_3, Ca-Mg- HCO_3-Cl and Na-Ca-HCO_3-SO_4 are some of the water types with high Electrical Conductivity (1440-2490μS/cm).

- Different mineral species in the water solution and their saturation index were identified by using the PHREEQC hydrochemical model. Six groundwater samples were used for the calculation. The equilibrium with pure solid mineral phases was applied to determine the thermodynamic stability and the solubility of the minerals in water at a given temperature and also as a function of pressure. The used temperature for this calculation was ranging between 25^{0C} -75^{0C}. From water samples, except calcite in water sample CSP-3 the mineral phase in the rest of water samples were not equilibrates. Calcite and Aragonite and Fluorite in sample DW-2 and CO_2 in DW-1 close to zero but, they were not equilibrated completely. The rest minerals phases in all six samples were under saturated and over saturated conditions.

- Inverse hydrogeochemical modelling was applied to determine the groundwater chemistry evolution along the flow path. Three flow phases were selected for the modelling: from Megech, Ribb and Gumara River basins. The result indicates that dissolution and loss of water (through evaporation), dissolution of CO_2, H_2 and O_2 dissolution and precipitation of different mineral phases are the main hydrochemical processes that occurred during groundwater evolution along the flow path.

- This study combined stable isotope proportions of water point's data obtained from secondary with the local meteoric water line (LMWL) for the year of 2002 downloaded from the International Atomic Energy Agency (IAEA) web page. The combination helped to determine the origin of the groundwater and also to determine subsurface hydrologic link.

- The isotope signature in all sampled natural water resources in the basin show a high depletion in of both Oxygen-18 and Deuterium as we as a medium to high Oxygen-18 and Deuterium enrichment. The origin of all water resources is mainly from rainfall. Proof of surface groundwater interaction is only observed between Megech River and boreholes samples and dug wells samples within Megech basin.

- Tritium is one of the trace elements used to determine the age of the groundwater. Based on the tritium concentration of different water points in the basin the groundwater age categorized into three age groups such as groundwater recharged prior to 1952, mixed water classes or recharged before and after 1952 and modern groundwater(recharged after 1987).

6.2. Recommendation

- The disposal of waste material and use of fertilizer should be in more restricted way and according to regulations for protection in order to reduce the level as high nitrate (NO_3) and sulphate (SO_4) concentrations which can now be observed in urban and farm land.

- The water demand is on the increase in the study area. Instead of drilling shallow wells with a limited capacity of poor quality water it is recommended the drill for deep wells which would provide sufficiently fulfil the demand. Another advantage of deep well that these are safe from the pollution; direct evaporation and salt build up.

- A monitoring well should be installed to assess the temporal trends of water parameters near Robit village where the area very high saline shallow dug wells were measured.

- There are hard to very hard ground waters in the study area with TDS values 320-420 mg/l and above. These ground waters are susceptible to incrustation and corrosion so it is better to take care and make care full follow up to the wells and pumping materials and other instruments that can be used for water supply.

- The irrigation project which is currently running in the Megech and Ribb River basins can bring additional recharge to the groundwater this will increase the groundwater level; furthermore, it can cause direct evaporation especially from shallow wells therefore may leads to problems of salinization.

LIST OF REFERENCES

Abreha, A. G. (2014). Hydrogeochemical and water quality investigation on irrigation and drinking water supplies in the Mekelle region, northern Ethiopia (p. 105). Enschede: University of Twente Faculty of Geo-Information and Earth Observation (ITC). Retrieved from http://www.itc.nl/library/papers_2014/msc/wrem/abreha.pdf

Arunprakash, M., Giridharan, L., Krishnamurthy, R. R., & Jayaprakash, M. (2013). Impact of urbanization in groundwater of south Chennai City, Tamil Nadu, India. *Environmental Earth Sciences*, *71*(2), 947–957. doi:10.1007/s12665-013-2496-7

Asmerom, G. H. (2008). Groundwater contribution and recharge estimation in the upper blue nile flows, ethiopia.

Atomic, I., Agency, E., & Educational, U. N. (n.d.). Environmental Isotopes in the Hydrological Cycle Principles and Applications Environmental Isotopes in the Hydrological Cycle Principles and Applications, *1*.

Bereket Fentaw, A. T. (2013). Hydrogeology and hydrochemistry of Debretabore map sheet,Geological Survey of Ethiopia. Addis Ababa.

C.W.FETTER. (1994). *Applied Hydrogeology*.

Chapman, D. (1996). Water Quality Assessments - A Guide to Use of Biota , Sediments and Water in Environmental Monitoring - Second Edition Edited by.

Chowdhury, R. M., Muntasir, S. Y., & Hossain, M. M. (2007). FARIDPUR-BARISAL ROAD IN BANGLADESH, 2–9.

Danbara, T. T. (2014). Deriving Water Quality Indicators of Lake Tana , Ethiopia , from Landsat-8.

Demlie, M., Wohnlich, S., & Ayenew, T. (2008). Major ion hydrochemistry and environmental isotope signatures as a tool in assessing groundwater occurrence and its dynamics in a fractured volcanic aquifer system located within a heavily urbanized catchment, central Ethiopia. *Journal of Hydrology*, *353*(1-2), 175–188. doi:10.1016/j.jhydrol.2008.02.009

Esmaeili, A., Moore, F., & Keshavarzi, B. (2014). Nitrate contamination in irrigation groundwater, Isfahan, Iran. *Environmental Earth Sciences*, *72*(7), 2511–2522. doi:10.1007/s12665-014-3159-z

Federico, C., Pizzino, L., Cinti, D., De Gregorio, S., Favara, R., Galli, G., … Voltattorni, N. (2008). Inverse and forward modelling of groundwater circulation in a seismically active area (Monferrato, Piedmont, NW Italy): Insights into stress-induced variations in water chemistry. *Chemical Geology*, *248*(1-2), 14–39. doi:10.1016/j.chemgeo.2007.10.007

Geyh, M. (2000). Environmental isotopes in the hydrological cycle Volume IV Groundwater.

Glover, E. T., Akiti, T. T., & Osae, S. (2012). Geoscience Major ion chemistry and identification of hydrogeochemical processes of groundwater in the Accra Plains, *50*, 10279–10288.

Haro, W., Hailemariam, D., Getachew, I., Kassahun, T., Ashenafi, S., Burisa, G., & Edris, M. (2010). *Geology,Geochemistry and Gravity Survey of the Debre Tabor Area*.

Hautot, S., Whaler, K., Gebru, W., & Desissa, M. (2006). The structure of a Mesozoic basin beneath the Lake Tana area, Ethiopia, revealed by magnetotelluric imaging. *Journal of African Earth Sciences*, *44*(3), 331–338. doi:10.1016/j.jafrearsci.2005.11.027

Hounslow, A. (1995). *Water Quality Data: Analysis and Interpretation*. Retrieved from http://books.google.nl/books/about/Water_Quality_Data.html?id=scQ9RCHni8kC&pgis=1

Ian D. Clark, P. F. (1997). *Environmental Isotopes in Hydrogeolgy*. United State of America: CRC Press LLC.

Jerome, C., & Pius, A. (2010). Evaluation of water quality index and its impact on the quality of life in an industrial area in Bangalore, South India. *American Journal of Scientific and Industrial Research*, *1*(3), 595–603. doi:10.5251/ajsir.2010.1.3.595.603

Kebede, S., Travi, Y., Alemayehu, T., & Ayenew, T. (2005). Groundwater recharge, circulation and geochemical evolution in the source region of the Blue Nile River, Ethiopia. *Applied Geochemistry*, *20*(9), 1658–1676. doi:10.1016/j.apgeochem.2005.04.016

Kumar, A., Rout, S., Narayanan, U., Mishra, M. K., Tripathi, R. M., Singh, J., … Kushwaha, H. S. (2011). Geochemical modelling of uranium speciation in the subsurface aquatic environment of Punjab State in India, *3*(May), 137–146.

Matthew McCartney, Tadesse Alemayehu, A. S., & Awulachew, and S. B. (2010). *Evaluation of Current and Future Water Resources Development in the Lake Tana Basin, Ethiopia* (p. 39p). Retrieved from http://www.iwmi.cgiar.org/Publications/IWMI_Research_Reports/PDF/PUB134/RR134.pdf

Mazor. (1991). *Geochemical and Hydrodynamic Characterization of the Groundwater System of Puebla Valley, Mexico*.

Mengesh et al. (1996). Geology of Ethiopia.

Nadew, G. A. (2010). Groundwater & Surface Water Interaction in Lake Tana sub-basin using Isotope and Geochemical Approach A Thesis Submitted to the School of Graduate Studies Department of Earth Sciences In partial fulfillment of the requirement for the degree of Master of S. Addis Ababa University.

Panthi, S. R. (2003). Carbonate Chemistry and Calcium Carbonate Saturation State of Rural Water Supply Projects in Nepal, (April), 545–560.

Parkhurst, B. D. L., & Appelo, C. A. J. (n.d.). User ' s Guide to Phreeqc (version 2)— A Computer Program for Speciation , and Inverse Geochemical Calculations, (Version 2).

Parkhurst, D. L., & Appelo, C. a. J. (2013). Description of Input and Examples for PHREEQC Version 3 — A Computer Program for Speciation , Batch-Reaction , One-Dimensional Transport , and Inverse Geochemical Calculations Chapter 43 of. *Modeling Techniques, Book 6*, 1–678.

Pius, A., Jerome, C., & Sharma, N. (2012). Evaluation of groundwater quality in and around Peenya industrial area of Bangalore, South India using GIS techniques. *Environmental Monitoring and Assessment*, *184*(7), 4067–77. doi:10.1007/s10661-011-2244-y

Poonam, T., Tanushree, B., & Sukalyan, C. (2013). Water Quality Indices-Important Tools for Water Quality Assessment:, *1*(1), 15–28.

R.Allan Freeze, J. A. C. (1979). *Groundwater* (illustrate.). Prentice-Hall, 1979.

Rao, G. S., & Nageswararao, G. (2013). Assessment of Groundwater quality using Water Quality Index, 1–5.

Sharif, M. U., Davis, R. K., Steele, K. F., Kim, B., Kresse, T. M., & Fazio, J. a. (2008). Inverse geochemical modeling of groundwater evolution with emphasis on arsenic in the Mississippi River Valley alluvial aquifer, Arkansas (USA). *Journal of Hydrology*, *350*(1-2), 41–55. doi:10.1016/j.jhydrol.2007.11.027

Singh, C. K., Rina, K., Singh, R. P., & Mukherjee, S. (2013). Geochemical characterization and heavy metal contamination of groundwater in Satluj River Basin. *Environmental Earth Sciences*, *71*(1), 201–216. doi:10.1007/s12665-013-2424-x

Srinivasamoorthy, K., Vasanthavigar, M., Chidambaram, S., Anandhan, P., Manivannan, R., & Rajivgandhi, R. (2012). Hydrochemistry of groundwater from Sarabanga Minor Basin , Tamilnadu , *2*(3), 193–203.

Verma, A., Thakur, B., Katiyar, S., Singh, D., & Rai, M. (2013). Evaluation of ground water quality in Lucknow , Uttar Pradesh using remote sensing and geographic information systems (GIS), *5*(2), 67–76. doi:10.5897/IJWREE11.142

Yonas Mulugeta, Aschalew Gurmu, M. A. (2013). Hydrogeological Reoprt of Yifag Map Sheet,Geological Survey of Ethiopia. Addis Ababa.

Zenaw, T. (2009). Ribb Irrigation and Drainage Project Hydrogeology Report (unpublished).

Zewde, G. (2010). School of Graduate Studies Department of Earth Sciences Baseflow Analysis of Rivers in Lake Tana Sub Basin a Thesis Submitted to School of Graduate Studies in Partial Fulfilment of the Requirements for Degree of Master of Science in Hydrogeology by Getach.

Appendix: 1 Interpolation map of EC, PH, NO_3& TDS excluding Serba Mariam spring with EC 10660μS/cm and TDS 6410mg/L

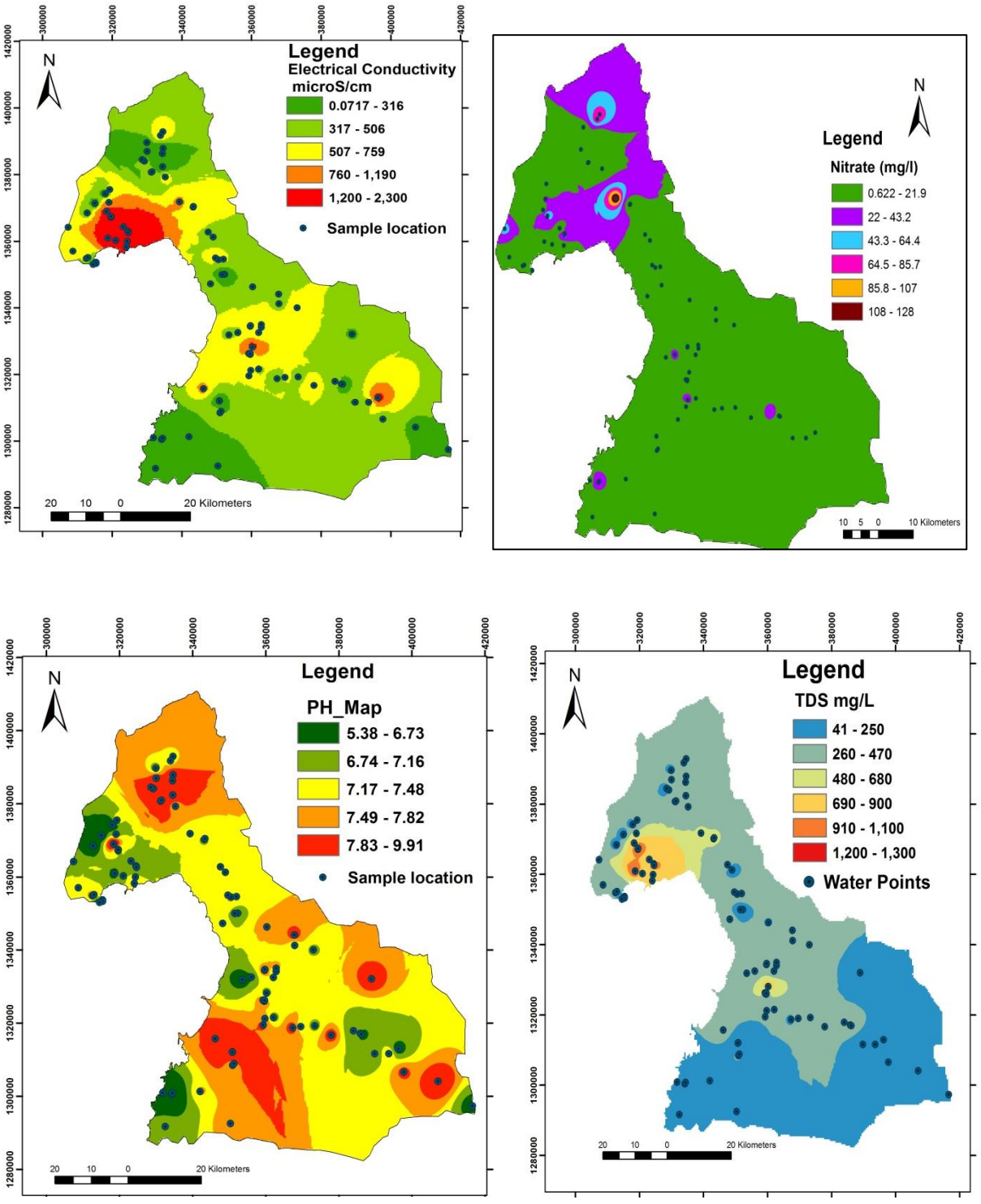

Appendix 2: Ions ratios summary report for the criteria of the Rock Source Deduction (Hounslow, 1995).

Parameter	Attention Value	Conclusion
SiO2 (mmol)	>0.5	Volcanic glass or hydrothermal water possible
HCO3-/SiO2	>10	Carbonate weathering
	>5 and <10	Ambiguous
	<5	Silicate weathering
SiO2/(Na+K-Cl)	<1	Cation exchange
	>1 and <2	Albite weathering
	>2	Ferromagnesian minerals
(Na+K-Cl)/	0.2 - 0.8	Plagioklas weathering possible
(Na+K-Cl+Ca)	<0.2 or >0.8	Plagioklas weathering unlikely
Na/(Na+Cl)	>0.5	Sodium Source other than halite - albite, ion exchange
	0.5	Halite Solution
	<0.5 TDS >500	Reverse Softening, seawater
	<0.5 TDS <500 and >50	Analysis Error
	<0.5 TDS <50	Rainwater
	=0.5 and (HCO3/Si)>10	Dolomite Weathering
Mg/(Ca+Mg)	<0.5	Limestone-Dolomite Weathering
	>0.5	Dolomite Dissolution, calcite precipitation, or seawater
	<0.5 and (HCO3/Si)<5	Ferromagnesian Minerals
	>0.5	Granitic weathering
Ca/(Ca+SO4)	0.5	Gypsum dissolution
	<0.5 and pH<5.5	Pyrite oxidation
	<0.5 and pH neutral	Calcium removal - ion exchange or calcite precipitation
	>0.5	Calcium source other than gypsum - carbonate or silicates
TDS	>500	Carbonate weathering or brine or seawater
	<500	Silicate weathering
Cl/Sum Anions	>0.8 and TDS>500	Seawater or brine or evaporites
	>0.8 and TDS<100	Rainwater
	<0.8	Rock weathering
HCO3/	>0.8	Silicate or carbonate weathering
Sum Anions	>0.8 and SO4 >20meq/L	Gypsum dissolution
	<0.8 and sulfate low	Seawater or brine
Calcite Saturation Index	>0	Oversaturated with respect to Calcite
	0	Saturated with respect to Calcite
	<0	Undersaturated with respect to Calcite

Appendix: 3 Source rocks deduction analysis result

Parameter	CSP-1	Conclusion		
SiO2 (mmol/L)	0.409			
HCO3-/SiO2	5.084	Ambiguous		
SiO2/(Na+K-Cl)	-9.891	Cation exchange		
(Na+K-Cl)/(Na+K-Cl+Ca)	-0.034	Plagioklase weathering unlikely		
(Na/(Na+Cl)	0.412	Analysis Error		
Mg/(Ca+Mg)	5.08	Ambiguous		
TDS	163	Silicate weathering		
Cl-/Sum Anions	0.057	Rock weathering		
HCO3-/Sum Anions	0.813	Silicate or carbonate weathering		
Parameter	DW-2	Conclusion		
SiO2 (mmol/L)	1.331	Volcanic Glass or hydro thermal water possible		
HCO3-/SiO2	11.413	Carbonate weathering		
SiO2/(Na+K-Cl)	1.642	Albite weathering		
(Na+K-Cl)/(Na+K-Cl+Ca)	0.071	Plagioklase weathering		
(Na/(Na+Cl)	0.515	Halite - albite, ion exchange		
Mg/(Ca+Mg)	11.41	Limestone-dolomite weathering		
TDS	1601	Carbonate weathering or brine or seawater		
Cl-/Sum Anions	0.327	Rock weathering		
HCO3-/Sum Anions	0.551	Seawater or brine		
Parameter	CSP-1	Conclusion		
SiO2 (mmol/L)	0.506	Volcanic Glass		
HCO3-/SiO2	6.497	Ambiguous		
SiO2/(Na+K-Cl)	-0.183	Cation exchange		
(Na+K-Cl)/(Na+K-Cl+Ca)	0.594	Plagioklase weathering		
(Na/(Na+Cl)	0.165	Reverse Softening		
Mg/(Ca+Mg)	0.286, 6.50	Ambiguous		
TDS	801	Carbonate weathering or brine or seawater		
Cl-/Sum Anions	0.417	Rock weathering		
HCO3-/Sum Anions	0.396	Seawater or brine		
		Value		
Parameter	CSP-2	CSP-3	BH-1	Coclusion
SiO2 (mmol/L)	0.549	0.669	0.583	Volcanic glass
HCO3-/SiO2	3.28	2.08	2.19	Silicate weathering
SiO2/(Na+K-Cl)	2.657	7.43	2.99	Ferromagnesian Minerals
(Na+K-Cl)/(Na+K-Cl+Ca)	0.152	0.09	0.207	Plagioklase weathering
(Na/(Na+Cl)	0.946	0.69	0.88	halite - albite, ion exchange
Mg/(Ca+Mg)	0.352	0.282	2.19	Ferromagnesian Minerals
TDS	143	115	96	Silicate weathering
Cl-/Sum Anions	0.006	0.041	0.021	Rock weathering
HCO3-/Sum Anions	0.892	0.815	0.948	Silicate or carbonate

Appendix: 4 Chemical data

																							Isotopes	
Sample ID	Name of Location	location	Longitud	Latitude	Elev	EC	PH	NH4	Na	K	Ca	Mg	F	Cl	NO2	NO3	HCO3	SO4	PO4	Temp	TDS	O2	18O	2H
			UTM		m	µs/cm		mg/L	mg/L	mg/L	mg/L	mg/L	mg/L	mg/L	mg/L	mg/L	mg/L	mg/L	mg/L	Celsius	mg/L	mg/L	Permil	permil
G-DW1	Sarmender Hand dug well	Sarmemder	350880	1308449	1795	598	7.12	0.217	44	1.4	73.7	17.48	0.63	7.6	0.005	10.19	401	1.2	0.525	23.3	369	6.24	-2.64	1.59
G-RV1	Gumara river bridge	Gumara	351217	1308882	1792	134	8.03	0.85	6.5	1.7	15.2	6.9	0.77	1.9	0.04	10.2	77	10.2	0.245	23.5	85.6	6.3	-1.78	9.25
G-FW1	Angorbit flood water	Shina Kebele	350776	1312078	1787	138	8.63	0.26	5.8	2.9	16.7	5.98	0.45	2.85	0.015	11.09	79	2.7	0.103	23.1	86	5	8.22	62.44
G-BH1	Woreta w-3 borehole	Wereta	359236	1319518	1745	536	7.95	0.093	84	13.4	30.4	11.96	0.39	13.3	0.01	1.78	336	3.1	0.075	24.2	328	6	-6.81	-27.27
G-RV2	Rib river bridge	Rib	359583	1325967	1791	217	7.95	0.275	10.4	2.7	28.9	8.28	0.33	5.7	0.01	6.98	127	5.7	0.304	23.5	195	6	-0.10	18.57
G-DW2	ShinaTsion Kebele	Shina tsion	359150	1326302	1792	956	7.79	1.32	44	1.6	97.3	52.44	0.41	13.3	0.005	24.35	649	1.4	0.114	25.3	553	5	-1.40	5.32
G-DW3	Awramba	Awramba	367342	1318729	1889	318	8.15	0.093	8.3	1.8	49.4	5.06	0.55	7.6	0.01	18.86	185	1.7	0.217	25.3	191	6	-2.06	0.99
G-DW4	Fogera pain(Twaza kana,r	Tiwaza kana	359731	1321238	1803	562	7.71	0.195	36	6.4	82.1	12.42	0.61	20.9	0.005	36.6	313	0.9	0.032	24.6	315	6	-2.35	-1.43
G-SP2	Tinish Minch spring	Tinish Minch	356959	1316287	1805	350	7.18	0.128	8.6	2.4	59.3	1.84	0.19	23.75	0.015	2.18	188	0.4	0.005	23.8	157	5	-2.64	-0.58
G-DW5	Angorbit hand dug well	Shina	350766	1312020	1790	330	9.04	0.151	23.5	1.3	36.5	10.12	0.26	11.4	0.002	1.48	155	41.9	0.114	25	202	6	0.18	15.77
G-BH2	Hamusit well	hamusit	341996	1301294	1955	123	7.53	0.075	6.1	0.4	15.2	4.6	0.63	1.9	0.1	14.3	74	0.4	0.035	24.3	77	6	-2.15	3.16
G-BH3	Momoshta well	Anbasame	350294	1292522	2066	269	7.79	0.133	17	0.8	29.6	9.66	0.27	0.95	0.12	0.693	169	2.8	0.189	24.1	151	6	-2.29	3.32
G-BH4	Debretabor well-11	Debre tabour =11	389770	1311620	2603	284	6.83	0.119	29.5	1.5	34.2	5.98	0.43	2.85	0.005	21.88	176	0.1	0.39	20.6	173	6	-2.85	-5.69
G-BH5	Gassay well	Gassay	407026	1304114		247	8.43	0.084	23	8.8	22.0	7.36	0.36	6.65	0.54	13.56	139	0.3	0.237	14.6	154	7	-5.56	-25.74
G-BH6	Debretabor(sebara dildy)	Debre tabour	393601	1311601	2570	372	7.57	0.137	80	5.2	8.4	6.44	0.27	3.8	0.02	0.841	243	0.3	0.134	22.1	240	6	-4.44	-16.09
G-DW6	hand dug well	Siraba Mariam	383954	1317915		397	6.95	0.119	18.5	1.1	60.8	6.9	0.53	10.45	0.01	38.7	174	0.2	0.182	23	251		-1.03	7.39
G-DW7	Bura hand dug well	Bura, yifag	362803	1334122	1827	708	6.91	0.275	29	1.1	108.7	16.1	0.45	15.2	0.005	20.15	452	0.2	0.328	25.5	419	5.18	-0.94	7.06
G-DW8	hand dug well(rope pump)	Ansha, yifag	362783	1334971	1927	757	7.78	0.766	27	0.3	138.3	8.28	0.48	8.55	0.005	2.08	517	22.9	0.348	24.1	446	5.3	-0.74	7.39
G-BH7	Yifag dikule deep well	Dikule yifag	359622	1334420	1819	515	7.84	0.106	101	0.7	25.8	3.68	0.27	10.45	0.001	5.98	325	0.5	0.22	25.6	310	5.13	4.55	15.22
G-BH8	Alabo well	Allabu, Addis zmen	367760	1344101	1959	427	8.1	0.112	47	0.7	38.0	11.96	0.33	5.7	0.009	8.71	271	0.1	0.257	27.5	256	5.1	-1.44	5.27
G-DW9	ch. health center hand dug well	Chibchiba (health cl	373010	1340011	1970	621	7.07	0.204	13.5	0.8	83.6	25.76	0.32	10.45	0.005	21.19	394	0.8	0.265	24.1	368	5.07	-0.70	8.79
G-BH9	Sarwuha borehole	Mitra, Enfraz	348183	1347233	1797	513	7.24	0.159	34	2.2	64.6	22.54	0.58	5.7	0.025	1.68	355	0.3	0.498	24.1	314	4.76	-2.37	-2.39
G-DW10	Hand dug well	Enfranz hand	350471	1354457	1921	261	7.78	0.128	19	0.7	34.2	5.98	0.44	4.75	0.014	18.2	162	0.4	0.292	23.8	168.2	5.1	-1.00	5.96
G-BH10	Mina well	Enfranz	349594	1355006	1898	840	7.33	0.137	176	1.1	33.4	5.98	0.71	10.45	0.015	1.58	549	1.9	0.169	21.4	469	5.52	-2.76	-6.59
G-DW11	Ferenge wuha foutain	Ferenge wuha(flow	348924	1361256	2031	298	7.49	0.182	8.9	1.7	42.6	11.04	0.26	3.8	0.041	16.7	176	0.7	0.383	22.9	136.6	5.67	-1.88	1.58
G-RV3	Gumaro river well	MaXegnit	343168	1370231	1918	680	7.01	0.381	30	1	85.9	26.22	0.18	10.45	0.052	6.63	452	0.4	0.39	23.5	493	5.56	-0.97	5.01
G-DW12	B.G. hand dug well	Bahr Gimb	339243	1371808	1906	833	7.22	0.221	23	2.4	104.3	25.76	0.51	68.4	0.01	128.6	239	49.4	0.43	25.3	493	5.62	-0.28	10.34
G-RV4	megech river	Megech	331192	1380758	1863	368	7.07	0.27	11.9	2.3	45.6	16.1	0.32	10.45	0.001	25.2	209	5.7	0.387	23.3	226	5.4	-0.41	10.10
G-BH11	TW-7 well	Gondar TW7	334541	1392929	2066	722	7.4	0.195	104	2	44.1	12.42	0.32	38.95	0.01	81.62	348	19.2	0.284	20.1	432	5.27	0.21	13.35
G-BH12	TW-3 artesian well	Gonder TW3	333851	1391781	2049	859	7.24	0.29	93	2.1	76.0	12.42	0.63	53.2	0.01	82.6	306	23.6	0.162	20.8	506	5.35	-0.18	10.34
G-BH13	st.Rufael Blind school	Gondar ,blind S	329878	1389685	2076	251	6.71	0.168	9.9	1.4	31.9	8.28	0.21	9.5	0.1	10.39	139	11.2	0.098	20.3	157.4	5.18	-0.22	12.53
G-BH14	Wonfela artesian well	Kola Diba	319025	1371679	1810	793	6.92	0.39	31	0.6	108.7	28.98	0.59	19.95	0.005	24.3	458	0.1	0.217	23	489	5.73	0.32	13.63
G-BH15	Tach chanqua	Tach Chanqua	318351	1368918	1809	1440	9.95	1.24	218	0.5	82.1	34.96	0.3	55.1	0.01	2.7	637	184.7	0.237	23.5	822	6.03	0.14	12.93
G-DW13	Guramba hand dug	Guramba band	319520	1367241	1809	1094	6.71	2.1	48	4	123.1	56.58	0.63	29.45	0.01	5.54	719	32.7	0.446	24.1	649	6.08	-1.07	6.15
G-DW14	Robit Hand dug well	Robit hand	324445	1363002	1799	990	6.88	0.49	94	0.2	98.8	28.52	0.71	16.15	0.01	10.24	575	61.5	0.229	24.5	587	5.92	3.07	21.28
G-DW15	Adisgei jara hand dug well	Adisge-Jara Hana	324264	1359992	1807	849	7.28	0.69	138	0.8	45.6	18.4	0.32	37.05	0.01	3.811	471	46.65	0.715	24.6	512	5.86	-2.47	-9.21
G-DW16	Achera Mariam hand dug well	Achera Hana Mariar	320946	1360264	1795	1230	7.18	0.64	240	0.6	38.0	19.78	0.27	12.35	0.01	1.88	761.52	0.95	2.18	24.6	718	5.77	-0.71	5.30
G-DW17	Seraba & Dablo hand dug well	Dablo Seraba	318681	1360964	1793	2210	6.41	1.43	390	2.1	144.4	39.1	0.27	59.85	0.01	6.38	1390.8	14.08	4.2	24.2	1224	5.74	-1.13	3.76
G-DW18	Robit village school hand dug well	Robit school hand	324574	1362610	1812	2490	6.45	4.95	220	1.6	211.3	90.62	0.58	319.2	0.012	64.79	927.2	220.6	0.561	25.3	1398	5.69	0.67	8.39
G-DW19	Arabia diba hand dug well	Arabia Diba	323085	1364310	1804	1032	6.8	0.56	126	0.5	98.8	19.78	0.46	8.55	0.021	5.74	679.17	0.381	0.312	24.6	606	5.99	-0.82	6.01
G-BH16	chalguaye well	Chuahit	307347	1364172	1902	662	6.91	0.312	27	1.5	125.4	6.9	0.32	10.45	0.035	50.9	394.06	0.286	0.099	24.1	397	4.4	-0.53	6.73
G-BH17	Gorgora well	GorGora Mender	312512	1354841	1811	533	7.82	0.244	72	7.3	53.2	6.9	0.87	8.55	0.054	15.34	331.5	0.76	0.158	25.6	330	6.45	-2.32	-5.75
G-RV5	Rib river bridge(chandiba road)	Komni	296613	1370446	1862	245	7.95	0.602	10.4	2.3	32.7	11.5	0.47	5.7	0.015	14.15	148.35	0.47	0.265	25.7	259		2.40	28.60

Appendix: 5 Chemical data

Sample ID	Name of Location	location	Longitude	Latitude	Elev	EC	PH	NH4	Na	K	Ca	Mg	F	Cl	NO2	NO3	HCO3	SO4	PO4	Temp	TDS	O2
			UTM		m	µs/cm		mg/L	mg/L	mg/L	mg/L	mg/L	mg/L	mg/L	mg/L	mg/L	mg/L	mg/L	mg/L	Celsius	mg/L	mg/L
H-BH27			328517	1384497		295	8	0.687	24.37	5.87	41.9	18.23	0.38	3.19	0.01	0.62	295.91	7.2	0.116	23.9	121	4.25
H-BH28			317960	1374260		114.3	5.5	0.65	18.85	5.48	34.3	14.47	0.38	4.25	0.005	0.62	236.12	6.24	0.127	20.5	47.5	4.215
H-BH29			315015	1371379		167.9	6	0.787	5.98	3.91	16.0	5.47	0.38	1.77	0.015	0.62	91.52	4.8	0.187	23.1	67	2.15
H-BH30			312777	1368477		267	6	1.912	9.89	4.3	21.4	8.14	0.38	2.13	0.021	0.62	134.23	5.28	0.265	26.8	110	3.15
H-BH31			315310	1353324		154	6	0.981	34.02	7.04	55.7	24.92	0.38	3.9	0.351	0.62	403.9	8.65	0.1067	21	62	6.25
H-BH32			315310	1353324		147.3	6	0.455	8.74	4.3	20.0	7.42	0.38	1.77	0.015	0.62	123.25	4.8	0.028	21.1	61	5.12
H-BH33			314518	1352983		54.7	5	0.255	8.28	4.3	19.4	7.05	0.38	1.77	0.001	6.2	117.75	4.8	0.049	22.8	220	6.31
H-BH34			416521	1297374		192.2	6.5	0.289	8.05	4.3	19.0	6.93	0.38	1.77	0.065	0.62	114.7	4.8	0.05	23.5	94	5.01
H-SP6			351500	1350000		201.92	7.2	0.2561	9	1.5	21.4	1.5	0.1	2.3	0.084	0.62	103	1.4	0.031	24.8	141	3.12
H-DW39			334563	1387900		440.94	8.2	0.004	40.8	5	25.7	5	0.5	11.3	0.005	0.62	195	23.1	0.018	24.9	309	2.45
H-DW40			334470	1382400		608.97	8.2	0.174	110	0.7	4.8	1	0.12	14	0.006	0.62	293	0.1	0.139	23.6	426	5.21
H-DW41			334400	1386300		496.87	8.2	0.209	43	0.7	32.0	10	0.02	14	0.001	0.62	244	0.1	0.045	20.2	348	6.01
H-DW42			329990	1387000		659.91	8.2	0.181	120	1.2	5.5	1	0.01	14	0.0021	1.24	317	0.1	0.018	24.7	462	4.01
H-DW43			323991	1358237		2320	7.7	0.562	32.8	2.03	137.1	74.45	0.02	134.95	0.01	7.19	281.57	325.17	0.083	22.9	820	3.99
H-DW44			346127	1315692		860	7.9	0.315	80.6	1.96	64.4	22.99	0.01	14.99	0.025	14.26	533.31	7.54	0.129	24	420	2.54
H-RV7			388848	1332071		301	8.2	0.251	12.3	3.75	37.1	4.8	0.01	10	0.015	4.28	130.99	20.85	0.057	23.9	120	2.16
T-DW20	Robit	Gojam	332434	1291707	1077	242	6.96	0.587	3.95	0.71	37.0	5.62	0.12	5.3	0.009	3.1	164.7	7	0.089	26.4	162.14	2.92
T-DW21	15 km from Bhairdar		334154	1300453	1844	110.7	6.17	0.461	3.43	0.37	14.2	3.95	0.32	2.7	0.018	23.1	85.4	1	0.1	25.7	74.169	3.33
T-DW22	Abua	Lebo kemekem	359625	1326216	1805	826	7.04	0.751	29.26	1.47	105.0	37.75	0.02	3.2	0.008	4.4	646.6	17	0.084	25.6	553.42	2.16
T-DW23	Shena Tsion	Lebo kemekem	360188	1328133	1799	1775	6.85	0.573	83.08	5.99	187.8	82.3	0.01	120	0.036	13.3	896.7	120	0.428	25.6	1189.25	2.05
T-DW24	Bura	Lebo kemekem	362031	1332505	1765	457	7.58	0.6	17.31	1.16	84.3	22.06	0.01	15	0.014	5	384.3	1	0.123	23.8	306.19	2.55
T-DW25	Kolo minch	Lebo kemekem	356035	1332555	1805	435	6.6	0.681	19.03	2.67	49.4	16.94	0.21	11.1	0.012	27.2	244	12	0.109	16.7	291.45	2.07
T-DW26	Segnit		353504	1331893	1832	430	6.1	1.833	11.73	1.38	47.6	22.14	0.23	5.7	0.01	14.8	256.2	1	0.129	24.5	288.1	1.66
T-DW27	Kona giorgis		385835	1317161	2338	480	7.22	0.841	18.97	6.01	83.2	8.73	0.16	17.3	0.015	5.8	341.6	2	0.294	25.8	321.6	1.6
T-DW28	Mizu	Fogera	373361	1319243	1946	451	7	0.797	13.55	0.6	59.4	21.79	0.23	7.1	0.018	10.5	286.7	3	0.127	24.8	302.17	2.53
T-DW29	Wej	Fogera	369544	1319065	1902	543	7.2	0.69	32.97	1.04	70.2	15.34	0.15	6.2	0.015	10.9	384.3	3	0.123	24.9	363.81	3.74
T-DW30	Chaina camp	Fogera	362042	1321553	1827	431	6.82	1.019	10.46	1.6	52.1	22.84	0.01	8.1	0.012	10.4	305	2	0.098	24.6	288.77	2.8
T-DW31	Gebreal	Gonder zuria	352285	1350040	1871	254	6.76	0.773	11.55	2.47	35.0	6.16	0.01	3.5	0.009	7.8	427	13	0.182	24.6	170.18	2.34
T-DW32	Enfaraz	Gonder zuria	351899	1354625	1912	601	7.18	0.912	45.32	1.6	66.8	21.36	0.01	12.1	0.013	9.2	427	1	0.16	24.9	402.67	1.72
T-DW33	Ferenge wuha	Gonder zuria	347531	1362756	2012	521	7.18	2.824	28.92	2.99	70.5	18.05	0.01	23.8	0.032	10.2	347.7	6	0.17	24.4	349.07	2.19
T-DW34	Aberja	Gonder zuria	308643	1357028	1848	535	7.5	1.83	36.02	0.8	60.9	21.5	0.31	4.1	0.01	13.1	378.2	1	0.197	22.3	358.45	4.35
T-DW35	Gura Amba	Robit	319614	1367450	1832	2310	7.43	0.721	76.43	12.77	241.3	119.18	0.3	247.5	0.01	105.6	725.9	230	0.342	24.7	1547.7	3.96
T-DW36	Tseda	Maksegnit	335227	1379286	1884	665	7.63	0.781	19.67	1.69	76.8	37.91	0.2	17.7	0.051	5.3	427	13	0.165	20	445.55	2.92
T-DW37	Arno	S.Gonder	360268	1346295	1961	370	7.74	0.65	29.74	2.78	41.6	10.77	0.01	6.3	0.005	7.7	256.2	10	0.167	20.1	247.9	4.16
T-DW38	Korta		331767	1300930	1825	119.2	6.23	0.793	3.53	0.8	12.6	6.06	0.01	11.3	0.009	20.9	128.1	1	0.153	23.1	79.864	2.5
T-BH18	Yifag		359707	1334624	1818	457	7.44	0.15	60.95	1.46	35.4	9.81	0.09	9.8	0.017	23.3	298.9	5	0.038	23.6	306.19	5.28
T-BH19	Debretabore	Farta	397706	1306558	2883.5	351	7.96	0.299	45.52	13.25	12.3	14.32	0.01	5.6	0.004	5.7	225.7	8	0.048	20.2	235.17	4.1
T-BH22	Addis Zemen	Lebo kemekem	367852	1341213	1959	429	7.24	0.274	51.14	0.96	30.1	14.06	0.01	5.5	0.005	10.6	292.8	3	0.05	22	287.43	3.02
T-BH23	Maksegnit	Gonder zuria	343290	1370440	1909	715	7.28	0.052	25.32	1.52	102.0	31.43	0.01	16.1	0.024	14.2	542.9	1	0.041	28.8	479.05	2.22
T-BH24	Gorgora	Gonder zuria	312993	1355113	1805	599	7.49	0.148	56.46	3.59	64.8	13.74	0.61	13.9	0.014	1.2	512.4	8	0.031	25.8	401.33	2.85
T-BH25	Kola Diba		319274	1375494	1843	567	7.63	0.089	31.47	1.51	75.2	20.03	0.01	7.6	0.013	18	366	1	0.028	24.1	379.89	5.96
T-BH26	Azezo		329191	1384094	1960	447	7.78	0.181	56.34	0.73	38.9	10.19	0.19	6.9	0.007	8.6	335.5	7	0.109	22.9	299.49	4.68
T-SP4	Gult	Dera	334415	1300800	1825	169.2	5.97	0.205	6.12	0.35	19.9	6.58	0.01	11	0.011	24.5	79.3	1	0.035	26.4	113.364	2.05
T-SP5	Kona giorgis	Farta	386124	1317013	2329	111.5	6.15	0.279	9.41	1.71	12.7	2.04	0.01	5.9	0.081	2.8	549	1	0.08	24	74.705	4.74
T-Lake Tana	Gorgora		315293	1353699	1802	140	8.69	0.415	6.75	1.88	16.1	5.56	0.24	3.3	0.09	6	91.5	1	0.028	27.4	93.8	6.79

Appendix: 6 Tritium data

Site	Type	X	Y	Well depth	^{3}H (TU)
Gorgora town supply/Kes Mender	borehole	312606	1355049	121	0.5
Dashen brewery borehole 1B/Lashka	borehole	328564	1383745	301	0.52
Tseda town	dug well	334446	1380606		
Arb gebeya town supply	borehole	363781	1285984	95.6	1.65
Jib Asra town supply	borehole	386114	1282962	90	
Debretabore town supply/Gafat No.10	borehole	396407	1313342	109	0.51
Gasay town supply	borehole	407117	1304322	42	0.37
Anbesame town supply	borehole	350291	1292521	62.8	3.14
Yifag town supply	borehole	359714	1334645	60	
Wonzaye	hot spring	355780	1303277		0.82
Wagtera school	dug well	342822	1316411	12	2.71
Mesno cllinic	dug well	354487	1312034		
Tanku Gebriel/Medehaniealem tsebel	cold spring	355164	1309272		6.28
Zarak/Showble school	dug well	347199	1306740	12	
Angereb 6/NW5	borehole	334578	1392871	173	2.74
Kola diba town borehole/Wonfela	borehole	319108	1371888	70.5	1.13
Robit village supply	dug well	324386	1362994	10	
Robit Medihanealem tsebel	dug well	324540	1362647	10	0.92
Cewayit supply	dug well	307771	1364312	4	
Shaga/Gguaye mender/Amlak tadese	dug well	352450	1323310		3.34
Rike well	dug well	349070	1326168		6.08
Woreta town supply/Jicaa borehole	borehole	359326	1319721	76	0.63
Infranz town	dug well	350405	1355601		
Alem Ber/Gala terara	dug well	382592	1317900		
Serba Maryiam/Amora gedel tsebel	cold spring	382171	1317731		0.43
Maksegne village supply	borehole	369675	1319117	63	
Shinasim/Rib	borehole	359629	1326220		
Ager Kirigna Maryam	dug well	349582	1339614		6.06
Ambo Meda/Gaja bahir	borehole	378623	1339111		
Addis Zemen town supply/Alabo No.1	borehole	367852	1341230	137	3.43
Hamusit town supply	borehole	342182	1301222		5.11
Huzet/Gerarge	cold spring	407710	1301117		
Guramba Kidanemheret hot spring	hot spring	367474	1296586		0.67
Zenzelma	borehole	336244	1287877		4.58